INFORMATION TO USERS

This dissertation was produced from a microfilm copy of the original document. While the most advanced technological means to photograph and reproduce this document have been used, the quality is heavily dependent upon the quality of the original submitted.

The following explanation of techniques is provided to help you understand markings or patterns which may appear on this reproduction.

1. The sign or "target" for pages apparently lacking from the document photographed is "Missing Page(s)". If it was possible to obtain the missing page(s) or section, they are spliced into the film along with adjacent pages. This may have necessitated cutting thru an image and duplicating adjacent pages to insure you complete continuity.

2. When an image on the film is obliterated with a large round black mark, it is an indication that the photographer suspected that the copy may have moved during exposure and thus cause a blurred image. You will find a good image of the page in the adjacent frame.

3. When a map, drawing or chart, etc., was part of the material being photographed the photographer followed a definite method in "sectioning" the material. It is customary to begin photoing at the upper left hand corner of a large sheet and to continue photoing from left to right in equal sections with a small overlap. If necessary, sectioning is continued again – beginning below the first row and continuing on until complete.

4. The majority of users indicate that the textual content is of greatest value, however, a somewhat higher quality reproduction could be made from "photographs" if essential to the understanding of the dissertation. Silver prints of "photographs" may be ordered at additional charge by writing the Order Department, giving the catalog number, title, author and specific pages you wish reproduced.

University Microfilms

300 North Zeeb Road
Ann Arbor, Michigan 48106

A Xerox Education Company

THE UNIVERSITY OF OKLAHOMA

GRADUATE COLLEGE

THE PILOTED IGNITION OF THIN MATERIALS

A DISSERTATION

SUBMITTED TO THE GRADUATE FACULTY

in partial fulfillment of the requirements for the

degree of

DOCTOR OF PHILOSOPHY

BY

NARASIMHAN RANGAPRASAD

Norman, Oklahoma

1972

THE PILOTED IGNITION OF THIN MATERIALS

APPROVED BY

C. M. Sliepcevich

Sherrill D. Christian

K. E. Starling

Curtis Wm. Phillips

J. Reed Welker

DISSERTATION COMMITTEE

ABSTRACT

An extensive literature survey revealed that not much work had been done on the piloted ignition of thin materials. The present study was undertaken to investigate the important variables involved in the piloted ignition of thin materials and to develop a generalized mathematical expression to predict ignition time.

The ignition tests were conducted in a chamber of constant induced draft. The samples were subjected to radiation from benzene flames and 2500°K tungsten lamps. The use of different radiant sources provided a means of studying the ignition of materials using radiation of two different spectral qualities. Uniform irradiances of up to about 3.5 cal/cm^2-sec were obtained using tungsten lamps and about 3 cal/cm^2-sec using benzene flames. The pilot light consisted of a perforated stainless steel tube placed above the sample, with propane gas under pressure emerging through the holes and burning as the pilot flame. It was arranged so that the pyrolysis gases flowed over the pilot after they left the sample surface.

The thin materials that were subjected to piloted ignition tests were cotton, cellulose, filter paper, white acrylics, black wool and rayon. Their weight per unit area ranged

from 0.006 gm/cm^2 to 0.04 gm/cm^2 and thicknesses from 0.05 mm to 0.8 mm. All samples were oven-dried before testing.

The parameters on which ignition time depended were incident irradiance, average absorptance for the incident radiation, ignition temperature, weight per unit area of the sample and the sample thickness. The analysis of the ignition time data yielded the following conclusions:

1. A plot of incident irradiance versus reciprocal of ignition time gives a straight line, by extrapolating the line to y-axis where $1/t = 0$ (i.e., $t = \infty$) the minimum incident irradiance below which ignition will not occur can be found.
2. For fabrics of the same density, the ignition time increases for a particular incident irradiance as fabric weight per unit area increases. The ignition time can be correlated as a function of incident irradiance and fabric weight per unit area.
3. The ignition time depends on the spectral distribution of the incident radiant energy.
4. The ignition data can be correlated through the use of a model based on an inert, opaque solid with constant and uniform properties. The final regression analysis of the data gave the equation for predicting ignition time as

$$t_{ig} = 1.11 \times 10^{-8} \frac{w^{1.4} \Delta T_s^{4.2}}{H_a [\text{erf } (1/\sqrt{F})]^{0.9}}$$

ACKNOWLEDGMENTS

I would like to express my gratitude and appreciation to many people who have contributed to this research effort.

Dr. C. M. Sliepcevich, George Lynn Cross Research Professor of Engineering, for his direction and support.

Dr. J. R. Welker, Associate Director of the Flame Dynamics Laboratory, for his invaluable guidance throughout the program.

Dr. K. E. Starling, Associate Professor of Chemical Engineering, Dr. A. W. Aldag, Assistant Professor of Chemical Engineering and Dr. J. E. Francis, Associate Professor of the School of Aerospace and Mechanical Engineering for their service on my graduate committee.

Mr. W. M. Woodard for getting me the TGA, DTG and DSC data.

Dr. C. M. Garrison for helping me with the regression analysis program.

Dr. H. Nouri and Mr. S. Duvvuri for assisting me in the performance of the ignition tests and giving valuable suggestions.

Mrs. Barbara Everidge and Miss Becky Austell for their assistance in the preparation of the manuscript and Mr. Greg Puckett for drawing the figures.

I am grateful to the University of Oklahoma Research Institute for providing financial support.

Finally, I wish to express my deep gratitude to my parents without whose sacrifice this work would not have been possible, and I dedicate this research topic to them.

Narasimhan Rangaprasad

TABLE OF CONTENTS

LIST OF TABLES

LIST OF ILLUSTRATIONS

CHAPTER I

INTRODUCTION

In fire research the phenomena of ignition and damage of cellulosic materials and polymers by external heating has been a subject of extensive investigations. The objectives of these investigations has been to study building fires, forest fires and the thermal radiation effects of nuclear weapons.

The ignition and combustion of these materials involve complex combinations of physical and chemical processes. The ignition studies consist of exposing a solid sample to external heating in the form of radiation of various intensities and of measuring the time required for ignition to take place. The results of these experiments have been interpreted by mathematical analysis of energy transfer within the material.

Welker (38) refers to ignition as the appearance of a flame in the volatile gas stream evolved from a material undergoing pyrolysis. If the volatile gases are ignited with the aid of an external source, such as a nearby open flame or hot wire, it is called "piloted ignition." If the volatile gases are ignited without the aid of an external source, it is called

"spontaneous ignition." If the solid surface simply glows but no flame appears, then it is called "glowing ignition."

In the present work the piloted ignition characteristics of thin materials such as cotton, α-cellulose, rayon and filter paper were studied. Simms (32) points out the importance and usefulness of piloted ignition:

> Piloted ignition is of great practical importance; volatiles are often ignited either by the source of heat itself or by an extraneous source, while the heat is transferred to a combustible in any of a number of ways, e.g., from flames, hot gases, sparks or radiation from a distant source. Examples of this type of ignition include the hem of a skirt or other flammable clothing brushing past an unguarded fire, spread of flame within a room or other compartment, and spread of fire from one burning (hence radiating) building or timber stack to another, the volatiles being ignited by burning brands.

Different investigators have used different techniques and mathematical approaches in order to arrive at some ignition criteria to explain their data. So far such attempts have been unsuccessful. Neither have efforts to generalize mathematical models for ignition of similar materials under different conditions been too successful. Mathematical analyses have led to fairly reliable empirical correlations, however. The different techniques and methods used by various investigators for radiative heating of the material are presented in the form of a table in Chapter II.

Two different radiant sources, benzene flames and tungsten lamps, were used in the present study to obtain the ignition data in order to compare both types of radiant

heating and to study the effects of spectral distribution of the incident radiation. A detailed description of equipment and experimental procedure are given in Chapter III. The ignition data are tabulated in Appendix A and discussed in Chapter IV. Ignition tests were carried out for cotton and α-cellulose with different weights per unit area in order to study the effects of weight on ignition data. The different ignition models available in the literature for thin materials are given in Chapter II; comparison of the present data with these models is made in Chapter IV. Finally a generalized correlation is developed in Chapter IV to predict the piloted ignition time of the materials tested in this work.

Kinetic analyses for some of the fabrics used in the present work were obtained by means of Thermo Gravimetric Analysis (TGA) and Differential Thermal Analysis (DTA) plots as described in Appendix C. The heat of pyrolysis of each fabric was obtained from Differential Scanning Calorimeter (DSC) plots. The results of these analyses were used to predict the temperature profiles of fabrics subjected to radiant heating as discussed in Appendix C. The physical properties of the materials are given in Appendix B and the nomenclature in Appendix D.

CHAPTER II

REVIEW OF LITERATURE SURVEY AND PREVIOUS WORK

The ignition of cellulosic materials by external heating has been a subject of investigation for many years. Extensive literature is available on ignition of cellulosic materials. In this chapter the ignition process, the different criteria proposed for ignition, the different mathematical models developed for the ignition process and the effects of other variables on ignition will be reviewed.

Ignition Process

One of the earliest works on the ignition of materials is that of Brown (6). When a combustible material is heated in the presence of air its temperature increases; as the temperature increases a reaction between the material and oxygen starts. The reaction produces heat that again increases the temperature of the material, thereby increasing the rate of reaction. At the same time there is heat loss from the material through radiation, reflection and convection. At a certain temperature the rate of reaction is sufficiently rapid so that the resulting rate of heat production exceeds that of heat loss. Consequently, the temperature of the material rises

faster than it would because of the external heating alone, and so more rapid heating soon follows. When this process continues, then visible evidences of ignition, such as flow and flame, occur. Brown lists the following requirements for ignition process to take place.

1. A combustible must be present.
2. A source of oxygen, such as air, must be available within certain concentrations relative to the combustible.
3. Heat must be evolved as a result of the reactions producing combustion.
4. The reaction must proceed more or less rapidly over a certain temperature range.
5. The reaction must be accelerated by a rise in temperature.
6. A supply of energy, sufficient to raise the temperature of the reacting substances to the point where the reaction becomes autogenous is necessary.

Wesson (40) points out that the mechanism of thermal decomposition and the composition of the products are different for the two extreme cases of very low and very high thermal radiation. For very slow heating the specimen may be completely charred without flaming; whereas at a high rate of heating glowing or flaming ignition occurs. Wesson lists the following two separate and distinct processes for ignition of flammable solids: (1) the thermal decomposition of a solid phase into volatile products and a residue, and (2) gas phase oxidation reactions of volatiles near the surface.

Alvares, et al. (3) separate the factors influencing the ignition process of materials into two categories--the external and internal. The external factors are those such as the irradiance, time of exposure, area of uniform energy flux, the type of ignition, draft and specimen preheating. The internal factors are mainly the properties of the solid. These can be listed as the absorptivity of the irradiated surface, diathermacy, size of the irradiated area, thermal properties and moisture content of the solid, thickness, homogeneity, pyrolysis characteristics, etc.

Kanury (15) gives the processes governing ignition of a cellulosic solid in a fixed atmosphere. They are: transient thermal conduction in the solid, resultant pyrolysis and pyrolysate outflow, and finally, the ignition of gaseous pyrolysates mixed with air.

Martin (21) divides the ignition behavior of organic solids heated by a remote radiant energy source into three areas which depend upon the level of incident irradiance and the thickness of the exposed solid. In progression from low to high irradiance levels (holding thickness constant), the first is governed by convective heat loss and turbulent mixing, the second by diffusion of heat into solid and the third by the ablation of the irradiated surface. Most of the studies have been directed towards the diffusion controlled ignition of cellulosic materials.

Ignition Criteria

Hallman (13) described the ignition phenomena as a function of many variables. He defines ignition criteria as

$$IG = f(T_z, \bar{T}, T_s, T_o, T_g, R, \Delta H_f, \Delta H_z, E_s, C_p, K, t, L, h, \rho, M, A, \varepsilon_\lambda, \gamma_\lambda, \alpha_\lambda, H_i, \ldots) \quad \text{(II-1)}$$

where IG = ignition criteria

T_g = gas film temperature

$\bar{T}$ = source temperature

T_z = pyrolysis temperature

T_s = surface temperature of the material

T_o = ambient temperature

R = universal gas constant

E_s = activation energy of the material (it may be a cumulative energy factor)

C_p = specific heat

K = thermal conductivity

t = time

L = thickness of the materials

h = convective heat transfer coefficient

M = molecular weight

A = area of the material under tests

ε_λ = emittance of surface for each wavelength involved

γ_λ = attenuation factor for each wavelength involved

α_λ = surface absorptance for each wavelength involved

λ = wavelength

ρ = density

H_i = incident irradiance

ΔH_f = heat of fusion

ΔH_z = heat of pyrolysis

The complexities of ignition phenomena can be realized from Equation II-1.

Martin (22) gives the necessary and sufficient conditions for the ignition of solid fuels subjected to intense thermal radiation. They are:

1. The gaseous fuel escaping from the solid must have a high degree of reactivity either because of its chemical composition or its kinetic energy.
2. The relative concentration of fuel to oxygen must lie between two well defined limits.

Each of these conditions commonly exist at different levels above a decomposing solid, but until they occur simultaneously at the same location, ignition is impossible.

Akita (1) gives the ignition criterion for spontaneous and piloted ignition. For piloted ignition since an external heat source at high temperature already exists, ignition lag was interpreted as the time required for sufficient combustible gases to be generated by decomposition of the solid and for these gases to achieve a proper mixture with air. For spontaneous ignition the evolution of combustible gases is a necessary but not a sufficient condition. The surface temperature

of the solid should attain the ignition temperature. For woods Akita gives 500°C as the approximate surface ignition temperature.

Kanury (15) in his review lists the following conditions for ignition to take place:

1. Attainment of a fixed critical temperature T* by the exposed surface is an adequate criterion to predict transient flaming ignition for radiative as well as convective heating. If the ignition is spontaneous, the concept of critical exposed surface temperature is expected to be associated with some sort of a critical thermal phenomenon. If the ignition is piloted, attainment of the critical temperature by the exposed surface is expected to be a passive indication of attainment of a critical pyrolysis rate.
2. If the enthalpy content of the solid at the instant of termination of the external heating exceeds a critical lower limit enthalpy, persistent flaming is assured. The critical lower limit enthalpy is roughly $2L\rho c(T_p-T_o)$ where ρc is the volumetric heat capacity of the solid, 2L is the thickness of the slab, T_p is a temperature relating to the pyrolysis kinetics (may be taken as approximately 320°C for cellulosic solids) and T_o is the initial temperature.
3. As the slab thickness becomes small, the thin slab limit is approached. In this limit, once ignition occurs, it is persistent. Therefore, for thin bodies, fulfillment

of the T* criterion automatically fulfills the critical enthalpy content criterion.

Simms (30, 31, 32) also supports the hypothesis of the solid reaching a certain fixed temperature for ignition criteria. He correlates his results in terms of simple heat transfer theory using a fixed surface temperature criterion. For spontaneous ignition of wood and other cellulosic materials he reports a correlating temperature of 525°C. In the case of piloted ignition of wood he reports that the correlating temperature depends upon the position of the pilot flame. For piloted ignition of wood he gives correlating temperatures between 300°C and 410°C depending on the position of the pilot flame. Alvares (2) measured the surface temperature of thermally irradiated α-cellulose. He reports a surface ignition temperature of 600°C for spontaneous ignition of α-cellulose.

Bamford, Crank and Malan (5) studied the convective heating of wood by direct contact with gas flames. They postulated a criterion of a critical rate of evolution of volatiles for ignition. Accordingly, sustained ignition is possible when the weight loss at ignition is equal to or greater than 2.5×10^{-4} gm/cm^2-sec.

Deverall and Lai (11) have predicted a criterion for ignition of cellulosic materials. The derived threshold criterion, which does not depend upon detailed information on gas phase kinetics, states that the radiant heat flux applied to the fuel must be twice the heat flux required for pyrolysis

of the fuel less the heat conducted into the solid phase. Written mathematically

$$H_i\Big|_{x=0} = 2\Delta H_f \dot{m}_f\Big|_{x=0} - K \frac{\partial T}{\partial x}\Big|_{x=0} \qquad \text{(II-2)}$$

where H_i = incident irradiance

ΔH_f = heat required for pyrolysis

$\dot{m}_f$ = fuel flux through the exposed surface

K = thermal conductivity of the fuel

T = temperature of the fuel

Equation II-2 provides a necessary condition but not a sufficient condition for ignition. From Equation II-2, Deverall and Lai have calculated the heat of pyrolysis using the ignition data available in the literature.

Ignition Tests

Welker (38), in his literature review on the pyrolysis and ignition of cellulosic materials has given an account of different techniques developed by different people investigating the ignition Phenomena. Table II-1 presents the different methods used by different people for radiative heating of the material.

Ignition Models

Since the piloted ignition of thin materials like cotton, filter paper and cellulose has been studied in this work, the ignition models pertaining only to the thin bodies

TABLE II-1

DIFFERENT METHODS USED FOR RADIATIVE HEATING OF MATERIAL

Investigator	Radiant Source	Material Tested	Other Details
Lawson and Simms (17)	A surface combustion heater, burning a coal gas/air mixture	wood	Specimen, 5 cm square Radiating Temp, 1000°K Range, 0 to 1.5 cal/cm^2-sec
Varma and Steward (37)	A gas fired panel	wood shavings	Specimen, circular with 2 cm diameter
Buschmann (8)	A vertical gas fired refractory panel	wood	Specimen, 6 cm square Radiating Temp, 670°C
Alvares (2) and Martin (21)	Carbon arc image furnace	pure α-cellulose	Range, up to 100 cal/cm^2-sec
Simms (33)	Carbon arc-ellipsoidal mirror	wood, cotton, filter paper, etc.	Area covered, 3 cm^2 Radiating Temp, 4000°K Range, 1.5 to 12 cal/cm^2-sec
Simms (33)	Tungsten filament lamp	wood, cotton, filter paper, etc.	Area covered, 0.5 cm^2 Radiating Temp, 3000°K Range, 1 to 5 cal/cm^2-sec
Smith (34)	15 quartz tube lamps	wood, cardboard, marine uniform, etc.	Radiating Temp, 2500°K

TABLE II-1--Continued.

Investigator	Radiant Source	Material Tested	Other Details
Koohyar (16)	Vertical liquid hydrocarbon diffusion flames	wood	Range, 0 to 0.85 cal/cm^2-sec Specimen area, 100 cm^2
Wesson (40)	Vertical liquid hydrocarbon diffusion flames	wood	Range, 0.to 3.5 cal/cm^2-sec Specimen area, 100 cm^2
Wesson (40)	Tungsten filament lamps	wood	Range, 0 to 3.5 cal/cm^2-sec Specimen area, 100 cm^2

are discussed in this section. Several simplifying assumptions have been made by different authors to derive a reasonably general equation defining the process of thermal damage to cellulosic materials. Koohyar (16) lists the assumptions made. Some of them are given below.

1. Only one-dimensional heat transfer is considered.
2. The process is diffusion controlled. In other words, it is controlled by diffusion of heat and not by rate of reaction.
3. An overall first order reaction with a constant heat of reaction for the weight loss is applicable.
4. The incident irradiance is constant and uniform over the sample.
5. The material is isotropic and its properties are independent of temperature.
6. Average constant values can be used for optical properties of the sample.
7. Lambert's law for semi-transparent material is applicable.
8. The dimensions of the solid remain constant.

On the basis of these assumptions the energy balance for a one-dimensional, diathermanous, porous solid undergoing thermal decomposition has been given by Koohyar (16):

$$K \frac{\partial^2 T}{\partial x^2} + \gamma H_i e^{-\gamma x} - mC_g \frac{\partial T}{\partial x} = \rho c \frac{\partial T}{\partial t} + Q \frac{\partial \omega}{\partial t} \qquad \text{(II-3)}$$

$$-\frac{\partial \omega}{\partial t} = f\omega e^{-E/RT} \qquad \text{(II-4)}$$

where K = thermal conductivity, cal/cm^2-sec-°C/cm

γ = Lambert's law attenuation factor, cm^{-1}

H_i = incident flux at the surface, cal/cm^2-sec

m = rate of mass flow of decomposition gases per unit area, gm/cm^2-sec

C_g = average heat capacity of volatile products, cal/gm-°C

ρ = density, gm/cm^3

c = heat capacity of solid, cal/gm-°C

Q = overall heat of decomposition reaction, cal/gm

ω = weight loss, gm/cm^3

E = activation energy, cal/gm mole

R = gas constant, cal/gm mole-°K

T = absolute temperature, °K

t = time, sec

x = distance, cm

f = frequency factor, sec^{-1}

Simms (30) did a dimensional analysis of the above equations. He neglected the effect of mass convection through the solid. Clearly, while this convective term may be of considerable importance in discussing the combustion of wood, it is effectively zero prior to charring. If ignition is not long delayed after the decomposition becomes rapid, it may be neglected as in the case of piloted ignition. Simms also

included the general case of a radiation pulse which has a peak flux of H_p' at time t_p so that

$$H_i = \lambda H_p'(t/t_p) \qquad \text{(II-5)}$$

where λ is a shape function which is unity for a constant intensity. Equations II-3, II-4 and II-5 are combined to yield

$$K \frac{\partial^2 T}{\partial x^2} = \rho c \frac{\partial T}{\partial t} - \gamma H_p' \lambda (t/t_p) e^{-\gamma x} - Q f \omega e^{-E/RT} \qquad \text{(II-6)}$$

The initial condition is given as $T = T_o$ and $\omega = \omega_o$ and boundary conditions are described by Newtonian cooling, $h(T - T_o)$. The result of the dimensional analysis of the above equation with the conditions given, for the case of an inert, opaque material is

$$\frac{H_p' \, t_p}{\rho c L (T - T_o)} = f \left[\frac{hL}{k}, \frac{x}{L}, \frac{\alpha t}{L^2}, \frac{\alpha t_p}{L^2}\right] \qquad \text{(II-7)}$$

where h = heat transfer coefficient

α = thermal diffusivity of the material

Simms considers two cases, thin and thick materials. The Fourier number, $\alpha t/L^2$, is a measure of the "age" of a problem. If the Fourier number is small, the conducted heat will not have penetrated far as in the case of a thick material. If the Fourier number is large, then the rate of retention of heat is relatively small and the material is approaching conditions where conductivity is no longer a relevant factor, which holds for thin materials. There are two approximations,

the semi-infinite solid and the slab with the linear temperature gradient (corresponding to thin materials). For a slab in which Fourier number is large enough for a quasi-stationary state to exist, the thermal conductivity must not appear in the parameter containing time. By eliminating K from the product of Fourier number and Biot number (hL/K) the working parameter becomes Ht/ρcL. Therefore for thin slabs Equation II-7 becomes

$$\frac{H_i t}{\rho c L \Delta T_m} = f[ht/\rho cL] \qquad \text{(II-8)}$$

where ΔT_m is the mean temperature rise of the slab. Simms (28) gives an analytical solution for Equation II-8:

$$\frac{H_i t}{\rho c L \Delta T_m} = \frac{2ht/\rho cL}{1-\exp(-2ht/\rho cL)} \qquad \text{(II-9)}$$

Simms then plotted $H_i t/\rho c L \Delta T_m$ versus $ht/\rho cL$ and applied a constant ignition temperature such that the theoretical curve gave the best fit through the experimental data. The characteristic ignition temperature for the spontaneous ignition of thin materials was found to be 525°C.

Butler, et al. (9) worked on the ignition behavior of blackened α-cellulose. They considered only radiative heating at x = 0 of a finite body with no losses at x = 0 and x = L. They have correlated their results on the basis of incomplete energy modulus, ht/ρcL, neglecting temperature rise and Fourier number. They give the following reasons for neglecting temperature rise:

1. One would be forced, otherwise, to select an arbitrary value of ΔT.
2. Recognizing the existence of more than one type of ignition phenomenon, the existence of a single value of ΔT for the entire ignition behavior pattern would be highly improbable.

Kanury (15) has given three models for thin bodies:

1. Radiative heating at $x = 0$ of a thin body with Newtonian losses at both $x = 0$ and $x = 2L$ into a fluid at $T_\infty = T_o$. If the body is thin, the spatial gradients may be neglected so that

$$\rho c 2L \frac{dT}{dt} = K \left.\frac{\partial T}{\partial x}\right|_{2L} - K \left.\frac{\partial T}{\partial x}\right|_{0} = H_i - 2h(T - T_o) \qquad \text{(II-10)}$$

$$T = T_o \text{ at } t = 0$$

Equation II-10 has been solved and written in the following manner by Kanury:

$$\frac{H_i^2 \alpha t}{K^2 (T-T_o)^2} = \frac{hL}{K} \left(\frac{H_i}{h(T-T_o)}\right)^2 \ln \left[\frac{1}{1-2h(T-T_o)/H_i}\right] \qquad \text{(II-11)}$$

The appearance of thermal conductivity, K, in Equation II-11 is contradictory as thermal conductivity is considered unimportant according to Equation II-10. Assuming that the critical exposed surface temperature criterion holds, Equation II-11 has been plotted. Kanury says that for spontaneous ignition Equation II-11 holds good for the following range of conditions, $1 \leq H_i \leq 14$ cal/cm^2-sec,

$0.02 \leq 2L \leq 0.065$ cm, $1 \leq t \leq 20$ sec and $T \simeq 525°C$. Equation II-11 shows that as $H_i \to 2h(T-T_o)$, the time to ignition tends to infinity, suggesting the existence of a lower critical irradiance for ignition. In general for thin materials

$$\frac{H_i t}{\rho c L (T-T_o)} = f\left[\frac{K(T-T_o)}{H_i L}, \frac{hL}{k}\right] \qquad \text{(II-12)}$$

2. Radiative heating as $x = 0$ of a finite body with no losses at $x = 0$ and $x = 2L$. Carslaw and Jaeger (10) give the solution to the above problem.

$$\frac{K(T-T_o)}{IL} = \frac{1}{2}\frac{t\alpha}{L^2} + \left(1 - \frac{x}{2L}\right)^2 - \frac{1}{3} - \frac{4}{\pi^2}\sum_{n=1}^{\infty}\frac{(-1)^n}{n^2} \cdot \exp\left(-n^2\pi^2\alpha t/4L^2\right) \cdot \cos n\pi\left(1 - \frac{x}{2L}\right) \qquad \text{(II-13)}$$

Kanury hypothesizes that persistent flaming ignition occurs if the specimen thickness and its volumetric heat capacity are small enough to yield at the termination of exposure a temperature profile in the slab, which when averaged over the entire slab, results in an average temperature greater than some characteristic pyrolysis temperature T_p. That is, the flames persist after the exposure time beyond which the enthalpy contained in the solid is greater than a critical constant enthalpy. In mathematical terms this condition may be stated as

$$\int_0^{2L} \rho c(T-T_o)\, dx \geq \int_0^{2L} \rho c(T_p - T_o)\, dx = 2L\rho c(T_p - T_o) \qquad \text{(II-14)}$$

Integrating the temperature profile given by the solution of radiative heating at x = 0 of a finite body with no losses, the following condition is obtained:

$$\frac{\alpha t}{L^2} \geq \frac{2K(T_p - T_o)}{H_i L} \qquad \text{(II-15)}$$

The persistent flaming ignition time can be obtained from Equation II-15 by using the equality sign. The critical enthalpy content criterion for persistent flaming ignition may also be expressed in terms of char depth d. The char depth is defined as the depth in which the temperature is equal to or greater than T_p. Kanury arrives at the following condition for persistent flaming ignition by substituting Equation II-15 in Equation II-13 and neglecting the summation term.

$$d/2L \geq 0.423 \qquad \text{(II-16)}$$

3. Radiative heating of a finite body at x = 0, irradiance = H_i, Newtonian losses at x = 0, no losses at x = 2L, $T_\infty = T_o$. Carslaw and Jaeger give the solution to the above problem. Kanury approximates the summation series by neglecting all but the first root of the equation and arrives at the following equation for persistent flaming ignition

$$\frac{\alpha t}{L^2} = \frac{2K}{hL}\left[\frac{h(T_p - T_o)}{H_i} + \frac{1}{2}\left[\frac{h(T_p - T_o)}{H_i}\right]^2 + \ldots\right] \qquad \text{(II-17)}$$

Kanury plotted $\alpha t/L^2$ against hL/K for constant $h(T_p - T_o)/H_i$ values. From the figure for a Biot number smaller than one, Kanury gives the minimum required heating time to produce persistent flaming ignition as

$$\frac{\alpha t}{L^2} \propto \left(\frac{h(T_p - T_o)}{H_i}\right)^{1.5} \cdot \left(\frac{K}{hL}\right) \qquad \text{(II-18)}$$

That is $t \propto \rho c L h^{0.5} (T_p - T_o)^{1.5}/H_i^{1.5}$.

Andersen, et al. (4) present a model for predicting the ignition time by combining the heat transfer solution and the kinetic equation, assuming first order kinetics. For the heating of an inert material, neglecting the terms containing the effective extinction coefficient, the heat transfer equation can be written as

$$T = T_o + \frac{2H_a t^{1/2}}{(\pi \rho c K)^{1/2}} \qquad \text{(II-19)}$$

Though Equation II-19 is the solution for an infinitely thick substance, Andersen, et al. used it to arrive at an ignition model of a thin material like cloth. If a substance undergoing exothermic chemical reaction is heated instantaneously to some specified temperature T and held there, reaction would commence at a specific rate that is determined by the temperature. In this case only the reaction term is considered. The reaction time t_r is given by

$$t_r = \frac{cRT^2}{fQE} \exp\,(E/RT) \qquad \text{(II-20)}$$

During the surface heating of the material, any surface temperature T_c given by Equation II-19 at any arbitrary time t_c will have a corresponding reaction time given by Equation II-20. The ignition time will be

$$t_{ig} = t_c + t_r \tag{II-21}$$

Since T_c (and hence t_c) increases monotonically with increase in time, whereas t_r decreases with increase in T_c, and hence with increase in time, it can be seen that the total ignition time should go through a minimum with increase in time. The ignition reaction should commence at this minimum, and hence the criterion for the initiation of the reaction is

$$\left(\frac{dt_{ig}}{dt}\right)_{T=T_c} = \left[\frac{dt_c}{dt} + \frac{dt_r}{dt}\right]_{T=T_c} = 0 \tag{II-22}$$

The evaluation of Equation II-22 using Equations II-19 and II-20 gives

$$T_c = \frac{E/R}{\ln\left(\frac{2R(T_c - T_o)}{k_1^2 k_2 H_a^2 (E-2RT_c)}\right)} \tag{II-23}$$

$$k_1^2 = 4/\pi K\rho c \tag{II-24}$$

$$k_2 = cR/ZQE \tag{II-25}$$

From the kinetic data and physical properties of white and black cloth Andersen, et al. solved Equation II-23 for T_c at different values of absorbed irradiance H_a. Substituting the value of T_c in Equations II-19 and II-20, they got t_c and t_r, and hence t_{ig}, from Equation II-21.

Surface Temperature Studies

The surface temperature and temperature profile histories of a sample subjected to ignition have been of interest to previous investigators because of their importance in determining the course of pyrolysis. Brown (6) defines the ignition temperature as the temperature in the combustible at which the rate of heat developed by the reactions inducing ignition just exceeds the rate at which heat is dissipated by all causes, under the given conditions.

Wesson (40) discusses the different techniques that have been used to determine the irradiated surface temperatures.

1. The most common procedure is to attach a thermocouple to the surface of the sample. The shortcomings of this method are:
   a. An unknown portion of the recorded signal is due to the direct absorption of radiant energy by the thermocouple.
   b. The thermocouple bead may lose its intimate contact with the surface when charring starts.
2. A second method is to place thermocouple junctions at various depths in the sample and to extrapolate the measurements to the surface. The results of this method are also questionable, due to the nature of contact, depth of energy penetration for extremely short exposure periods, the distance from the surface and the extrapolating technique.

3. The third method is by means of radiation pyrometers which allow remote measurements of the surface temperature. This method is classified into two groups,
   a. Optical pyrometers.
   b. Radiation pyrometers.

Martin (21) measured the surface temperature of cellulose samples using an infrared pyrometer. He also measured the temperature at various depths using thermocouples. Alvares (2) used a radiation device to measure the surface temperature of α-cellulose at ignition. Smith and Schilberg (35) used a radiometer sensitive to radiation in a narrow band. The wavelengths used for temperature measurements were longer than the wavelengths of the radiation incident on the sample surface in order to preclude effects of reflection of incident radiation to the temperature detector. They measured the piloted ignition temperature and spontaneous ignition temperatures for several materials. MacHattie (20) measured the surface temperature of textile fabrics under intense thermal radiation using an infrared radiation pyrometer comprised of an optical system and a radiation detector.

Simms (31) did not measure the ignition temperature; he calculated it based on a simple heat transfer model. He estimated spontaneous ignition temperature for thin materials like cotton and filter paper to be about 525°C. Andersen, et al. (4) predicted the ignition temperature by combining a

simple heat transfer model and a kinetic equation, assuming first order kinetics to hold good as given by Equation II-23.

Reaction Kinetics

The composition and the yield of gases, vapors and char, and the relative proportion of flammable and non-flammable gases that are produced, will vary according to the conditions of temperature, pressure, time, etc., under which pyrolysis of an organic material occurs. The decomposition into different products depends on whether pyrolysis is slow or rapid. Slow heating of cellulosic material produces much charcoal, little tar and less flammable gases. On the other hand, rapid heating produces little charcoal, but much tar and highly flammable gases. The rate of evolution of gaseous products is also dependent on the rate of heating.

Most of the analyses of the kinetics of pyrolysis of cellulose have been based on the assumption that an overall first order reaction is valid. The determination of activation energy and frequency factor necessary to determine the assumed first order kinetics of weight loss has received most attention. The methods used to study pyrolysis fall into two broad classes, isothermal environments and increasing temperature environments. The method pertaining to ignition studies is to measure the kinetics of pyrolysis based on determining the weight loss of a specimen exposed to an increasing temperature environment. Welker (38) has reviewed the work done by different investigators on the thermal decomposition of cellulose.

Martin (22) and Sauer (29) discuss the concept of thermal decomposition as a kinetic reaction; they conclude that first order reaction kinetics correlate the weight loss data satisfactorily. The expression for the first order reaction mechanism is

$$-\frac{d\omega}{dt} = k\omega = f\omega e^{-E/RT} \qquad \text{(II-26)}$$

where k = reaction rate constant. The values of activation energies and frequency factors given by different investigators are not comparable since they are only for a certain range of temperatures and heating conditions. Martin (22) has tabulated the values of activation energy and frequency factor of cellulosic materials. These values range from 25 kcals/gm mole and 1.9×10^{9} sec^{-1} for temperature limits of 110°-220°C for α-cellulose to 32.1 kcals/gm mole and 1.3×10^{12} sec^{-1} for temperature limits of 165°-265°C for cotton. Lipska and Parker (19) found the value of E to be 42 kcals/gm mole for α-cellulose in the temperature range of 250°-300°C. They studied the pyrolysis of α-cellulose under isothermal conditions. Murty and Blackshear (26) studied the reaction kinetics of α-cellulose cylinders. They studied the following relation.

$$\frac{d\rho}{dt} = -f(\rho - \rho_{char})^{n} e^{-E/RT} \qquad \text{(II-27)}$$

where n = order of reaction. They found out that a first order equation (n = 1) fitted the experimental data well. Plotting activation energy E as a function of temperature they

arrived at the following equation

$$E \text{ (kcals/mole)} = 5.08 + 0.0214\ T\ (°K) \qquad \text{(II-28)}$$

They have given the apparent values of the parameters as E = 13 to 22 kcals/gm mole and f = 10^4 to 10^7 per second.

The heat of decomposition or heat of pyrolysis, Q, depends on sample temperature and particular stage of pyrolysis. The measurements of the heat of decomposition fall into two broad classes. In the first, the solution of a transient heat balance is used to estimate the heat effects. Values of the heat of decomposition reported by various investigators using this technique range from about 30 cals/gm to 300 cals/gm, all exothermic. The second technique used to measure heat effects is based on differential thermal analysis (DTA). Tang and Neill (36) used DTA to measure heat of decomposition of α-cellulose and found an endothermic heat of decomposition of about 88 cals/gm in a helium atmosphere. The value of Q would not be the same for different experiments that are carried out under different heating rates and experimental conditions. Brown (7) reports heat of pyrolysis values of 43.2 cal/gm for white pine and 27 cal/gm for oak, both endothermic.

Absorptivity

Welker, et al. (39) compared their white cotton ignition data using flame radiation with the data of Lee and Alvares (17), who used a tungsten filament lamp source operating

at 2500°K. Welker, et al. observed that the flame source caused ignition in about 1/3 the time that was required for the tungsten source. They concluded that the ignition behavior of flammable materials is also dependent upon the spectral distribution of the incident radiation and the absorptance characteristics of the material being irradiated. Welker, et al. therefore reasoned that a single correlation could be developed for relating the ignition behavior as a function of the net energy absorbed which they defined as follows:

$$H_a = H_i - \text{energy loss} \qquad \text{(II-29)}$$

where H_a = absorbed energy

H_i = measured incident irradiance

The energy losses term includes integrated reflected energy losses, integrated transmitted energy losses, both over the applicable range of wavelengths, convective and reradiated energy losses from both front and rear surfaces of the target. The transmitted, reradiated and convective losses are neglected compared to the absorbed and reflected energies. Welker also decided to neglect these effects in attempting to compare the two sets of data as a function of absorbed energy. The fraction of energy absorbed by white or black cotton for both flame radiation and tungsten source was found from the absorptance data of the fabrics. For the emissive power of the flame source Welker used the data of Ryan, Penzias and Tourin (26). An average total absorptance for a given sample-radiation

source configuration was defined as

$$\alpha_{av} = \frac{\int_{\lambda_1}^{\lambda_2} \alpha_\lambda e_\lambda \, d\lambda}{\int_{\lambda_1}^{\lambda_2} e_\lambda \, d\lambda} \qquad \text{(II-30)}$$

where α_{av} = average total absorptance for the sample-irradiation source configuration under consideration

α_λ = absorptance of sample at wavelength λ

e_λ = emissive power of radiation source at wavelength λ

The integration limits λ_1 and λ_2 are those wavelengths that include all of the energy in the spectrum for the given radiation source. Equation II-30 is approximated as

$$\alpha_{av} = \frac{\Sigma \, \alpha_\lambda e_\lambda \Delta\lambda}{\Sigma \, e_\lambda \Delta\lambda} \qquad \text{(II-31)}$$

Equation II-31 was used by Welker to obtain the values of α_{av}. The absorbed irradiance was calculated as

$$H_a = \alpha_{av} H_i \qquad \text{(II-32)}$$

Welker plotted the ignition time versus absorbed irradiance to prove the agreement between the different data. Monahan, et al. (24) have given the spectral absorptance data for different fabrics.

Pilot Position

Simms (32) studied the effect of pilot position on the piloted ignition of woods. He noted that the time for piloted ignition to occur increased as the pilot flame was moved outward from the face of the sample in the perpendicular direction. Piloted ignition ceased altogether if the pilot was just beyond 2 cm from the surface, which was about the visible thickness of the volatile stream. The flow of volatiles past the sample face was laminar. Simms concluded that because of the laminar conditions, gradients in the concentration of the combustible volatiles would exist in the flow field which he thought would account for the variation in ignition time with pilot flame position. Muir (25) found that piloted ignition continued to occur even with the pilot at a relatively large distance above the sample. Wesson (40) overcame the problem by having a heated coil as a pilot light and the coil was large enough to prevent its location from being an important parameter in ignition time measurements.

CHAPTER III

DESCRIPTION OF APPARATUS AND EXPERIMENTAL PROCEDURE

In the present work the ignition cabinet used previously by Koohyar (16), Wesson (40) and Hallman (13) was utilized to study piloted ignition characteristics.

Experimental Apparatus

Figures III-1 and III-2 show the front and back sides of the ignition cabinet. The cabinet is made up of galvanized sheet steel. The overall dimensions are 1.5 meters wide, 1 meter deep and 2 meters high. The windows are made of Herculite tempered plate glass. Herculite is used since it can withstand a working temperature of up to about 290°C. Figure III-3 is a schematic cross section diagram of the front view of the cabinet. The sample is mounted on the vertical ceramic panel. A liquid fuel channel burner is mounted on the right side of the sample. The galvanized steel burner is mounted on a worm gear at the front and back sides of the cabinet; it is 50 cm long and 5 cm wide. Figure III-4 shows the cross section of the burner. In order to develop higher heat fluxes, pressure regulated oxygen is supplied along the flame base by means of the tube which is mounted on the channel burner as

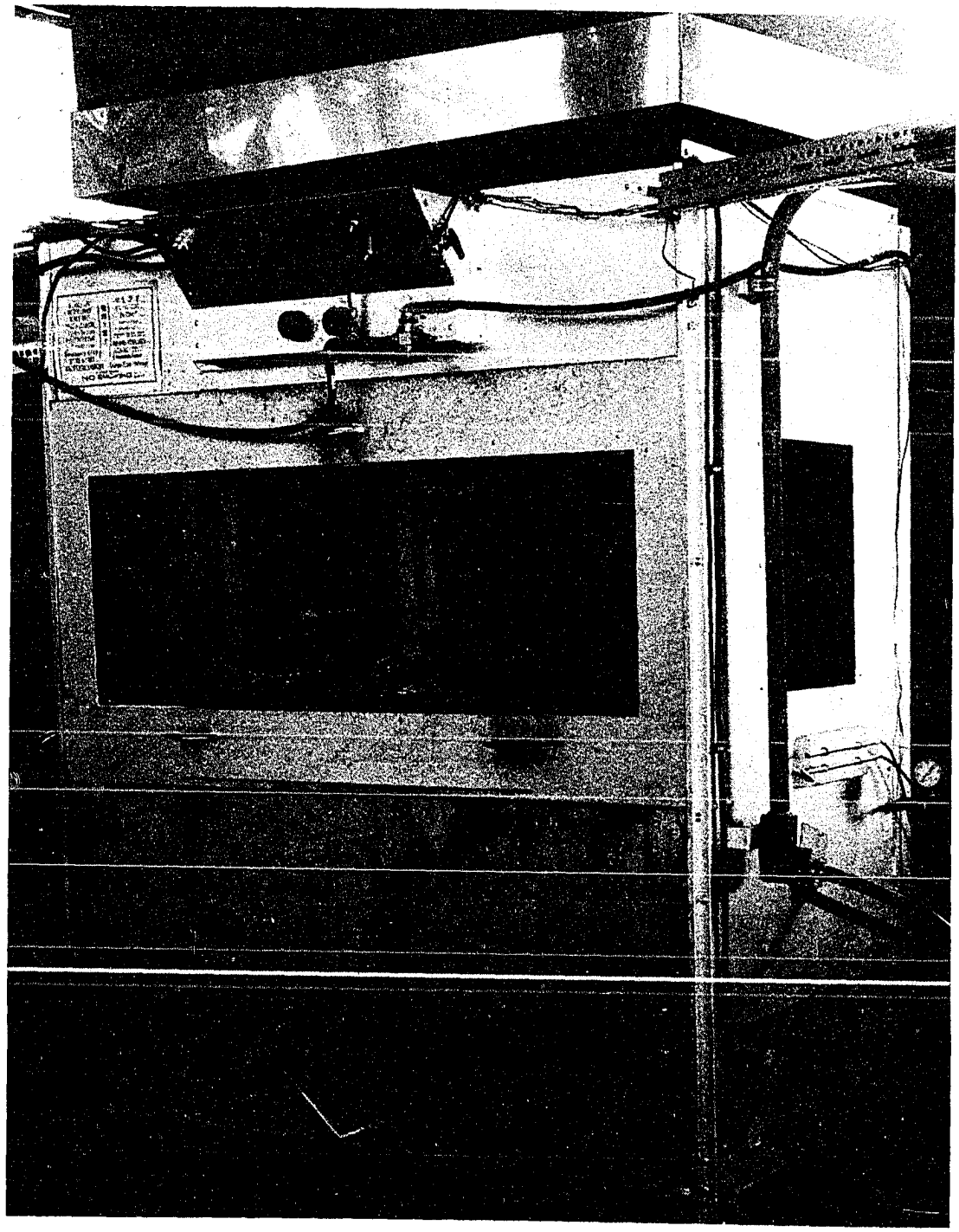

Figure III-1. Front View of the Ignition Cabinet.

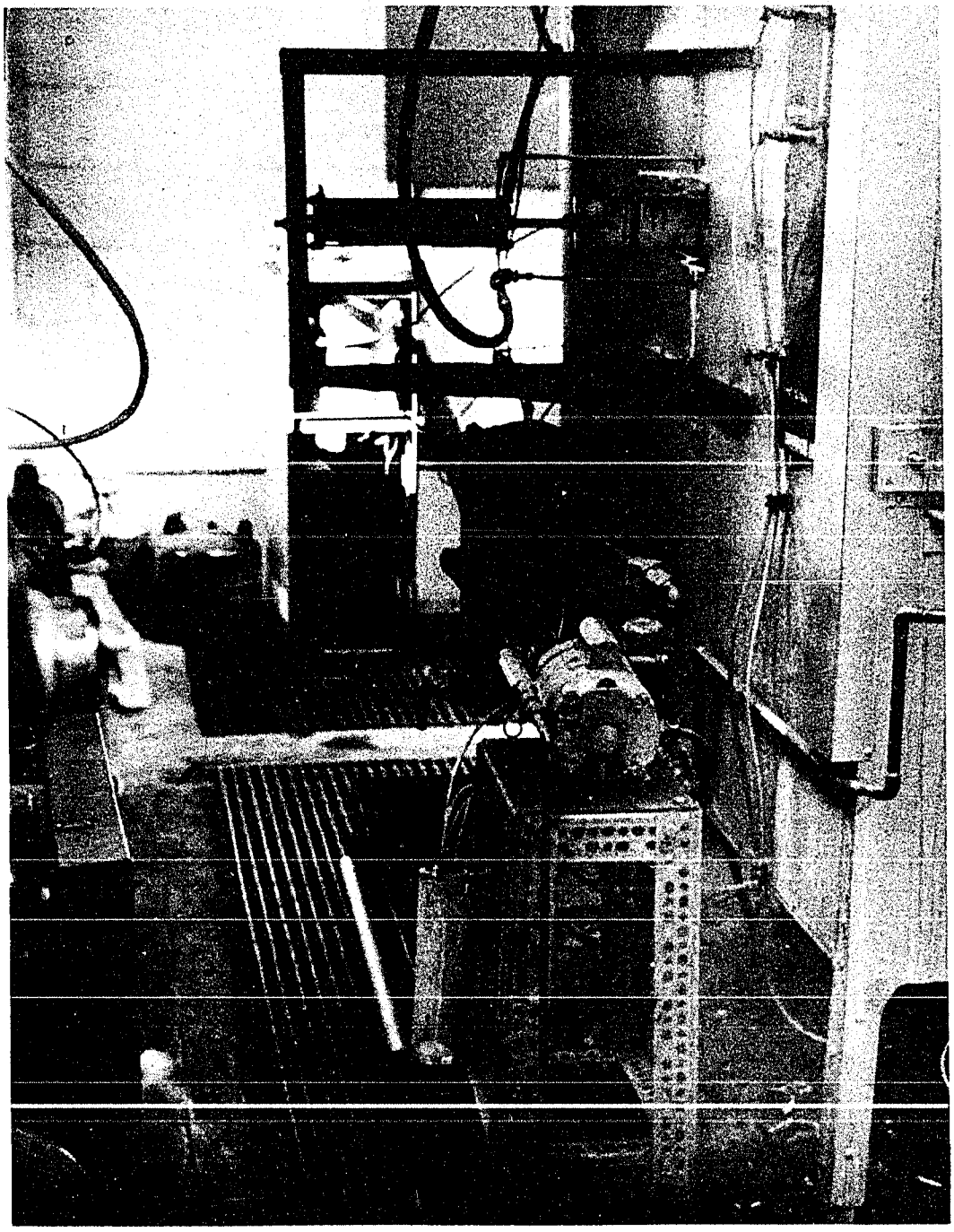

Figure III-2. Rear View of the Ignition Cabinet.

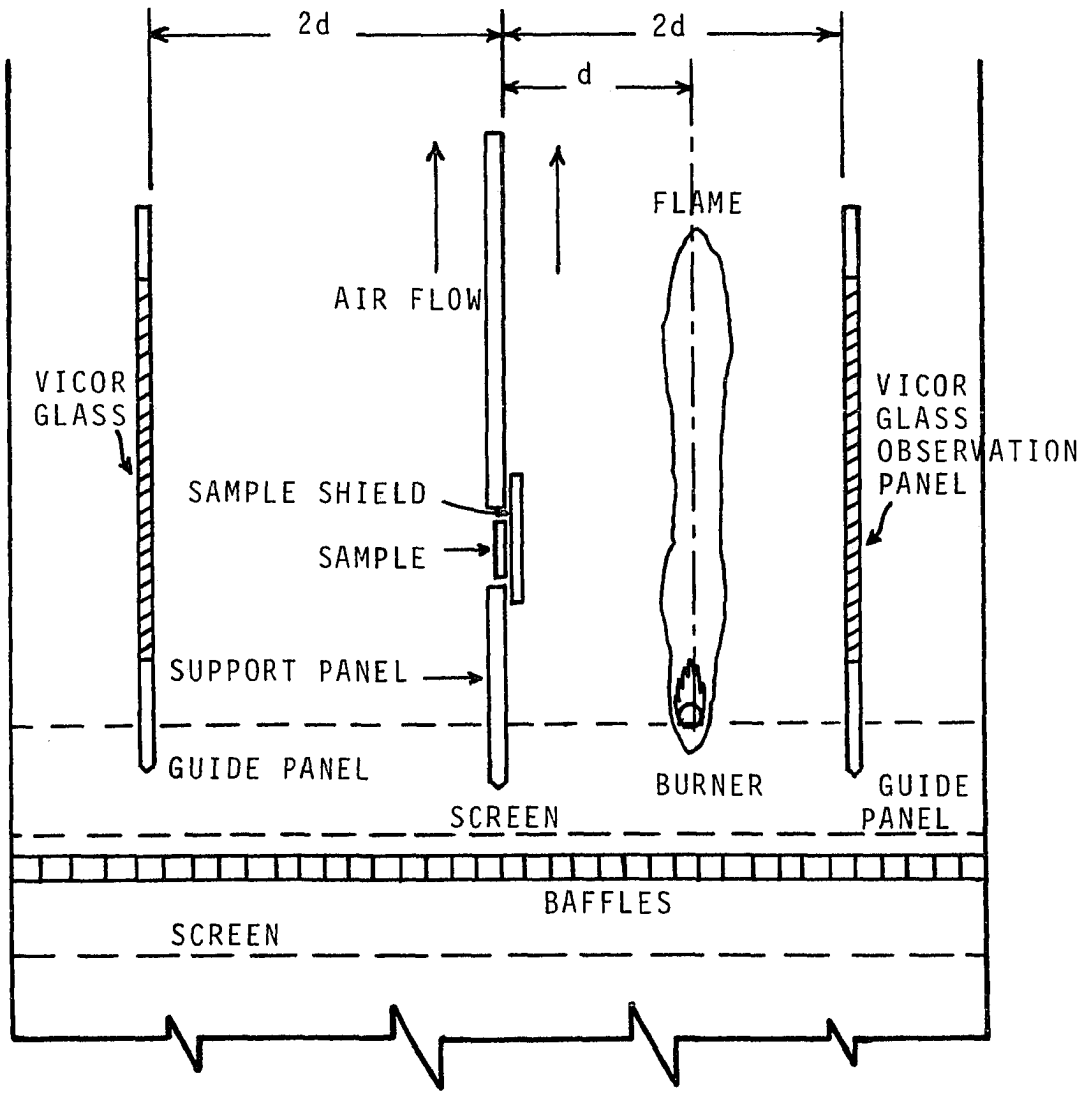

Figure III-3. Schematic Diagram of Single Burner Ignition Cabinet Tests.

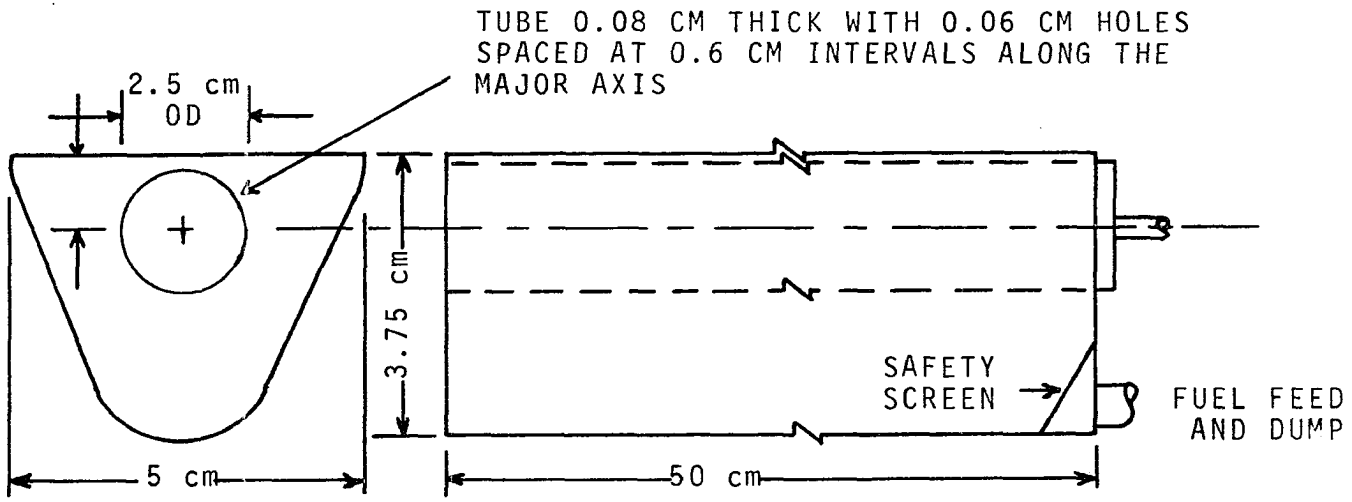

Figure III-4. Diagram of Burner Channel with O_2 Feed Tube.

shown in Figure III-4. This tube is made of stainless steel with an outside diameter of 1.27 cm. On the top of the tube holes 0.0635 cm in diameter, 0.635 cm apart, are drilled to distribute the oxygen along the flame base. In the case of the tungsten filament radiation tests the burner is used as a support base for the tungsten lamp holder. The tungsten filament panel is 15 cm high, 30 cm wide, and has eight 1000-watt tungsten filament quartz lamps.

It was found by Koohyar (16) that if the flame was brought too close to the wall it leaned towards the wall. In order to avoid that, a guide panel is provided as shown in Figure III-3. To observe the sample from the end of the cabinet, the guide panel has a "Vicor" glass window. The distance of the guide panel from the sample panel is always maintained at twice the distance of the burner from the sample panel, as shown in Figure III-3.

The irradiance level at the sample position can be varied by altering the distance between the sample and the radiation source. This adjustment is done by a worm gear drive arrangement which moves the burner as well as the guide panel towards or away from the sample. The burner and the guide panel are simultaneously moved. The gears and the chain sprocket arrangement are connected to an electrically-driven pulley. The power is provided by a 115 V, AC, reversing-type motor. In order to facilitate these movements the burner is

connected to the fuel tank by means of a flexible tube. An exhaust fan is mounted above the cabinet to remove the exhaust gases and smoke from the cabinet and to provide a uniform flow of air across the sample and inside the cabinet. The baffles provided at the bottom of the cabinet (as shown in Figure III-3) also help in providing uniform flow of air through the cabinet. The air velocity inside the cabinet can be varied by changing the position of a damper situated in the stack.

Fuel and Oxygen Supply System

Figure III-5 is a schematic diagram of the liquid fuel and oxygen supply system. The liquid fuel used for the ignition tests is benzene. Benzene is supplied to the burner from a fuel reservoir made of 15 cm diameter aluminum pipe. A liquid level indicator is provided on the fuel reservoir. The capacity of the reservoir is 5 gallons. A fuel pump is provided to pump the fuel into the reservoir. A constant head siphon is used to maintain a constant fuel level in the burner. The fuel in the supply line acts as a seal between the burner and the supply tank. The level of the fuel in the burner can be varied by varying the position of the end of the breather tube. As the fuel level in the burner approaches the breather's level, the head between the burner and the tank balances and the flow of fuel stops. The level of the fuel is maintained even while burning.

As shown in Figure III-5, a vacuum system has been provided for extinguishing the fire once the sample has been

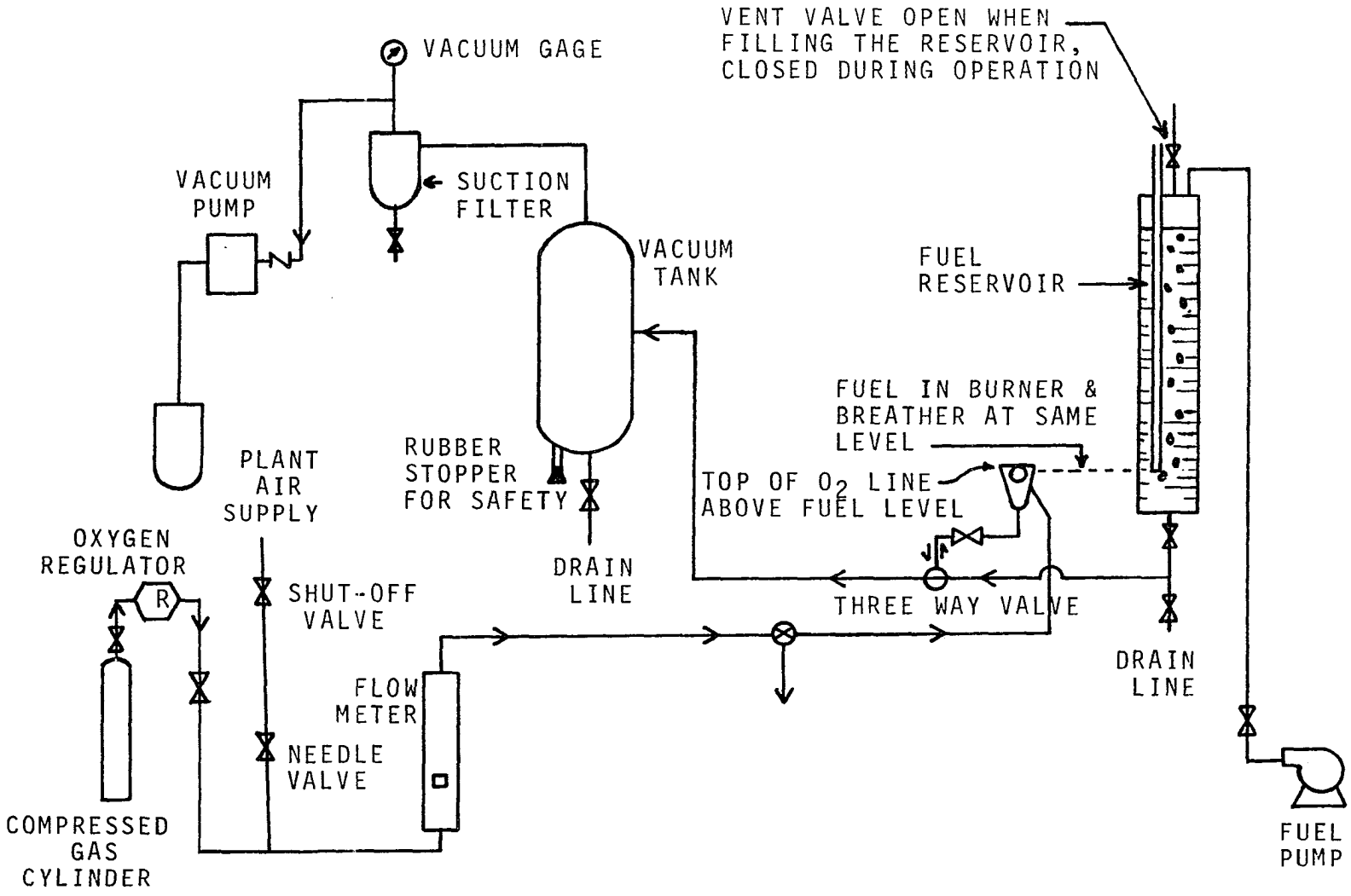

Figure III-5. Schematic Diagram of Fuel and Oxygen Supply and Control Systems.

ignited. The three way valve shown in the figure is operated by a handle which is in front of the cabinet (shown in Figure III-1). When the handle is moved right, the burner is open for benzene to flow from the fuel tank. While the burner is being filled with fuel, the vacuum pump is started. This pump maintains vacuum in the vacuum tank and the fuel outlet line. As soon as the sample ignites, the handle is turned left which actuates the three-way valve to isolate the fuel tank. Now, since the fuel outlet line is under vacuum, the fuel is drawn into the vacuum tank. After each test the fuel in the vacuum tank is emptied into a can. The vacuum pump is run until the fire is extinguished completely. The fire is generally extinguished in about 10-15 seconds. The fuel in the burner is ignited by an electrical spark after the fuel has reached the desired level. The electrical spark is manually initiated from outside the cabinet.

As stated before, to develop higher heat fluxes oxygen is supplied along the flame base. This oxygen is supplied to the system from a compressed gas cylinder. The oxygen pressure is maintained at 45 psig, and its flow is controlled by a needle valve. The oxygen goes through a rotameter to the burner.

Tungsten Lamp System

Figure III-6 shows the Tungsten Lamp System. The heat source consists of a bank of eight 1000-watt lamps mounted on a reflector. As described before the reflector and lamps are

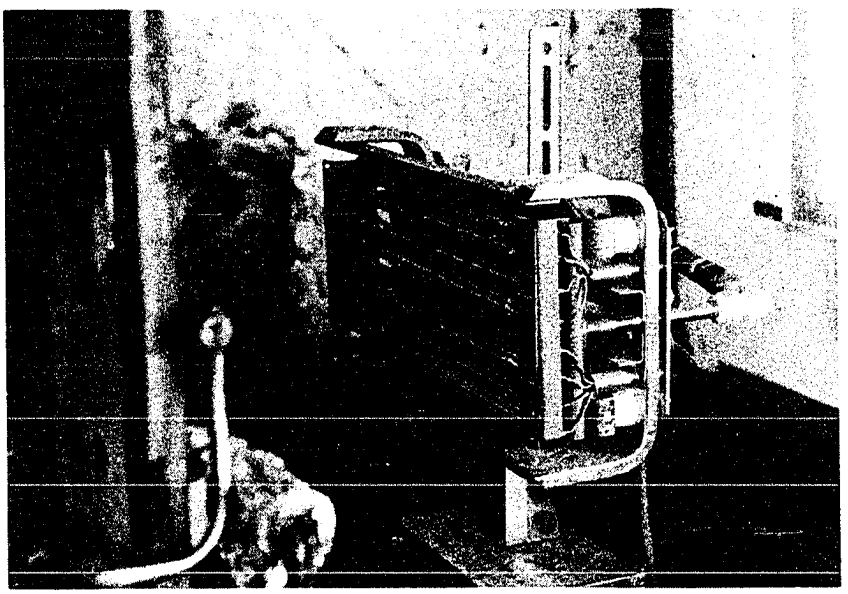

Figure III-6. Tungsten Lamp System.

mounted on the burner channel. The incident irradiance is increased by moving the lamps towards the sample and is decreased by moving the lamps away from the sample. Power to the lamps is supplied by a 230 V, AC, supply. The lamp ends and power leads are cooled by a low velocity air flow, the velocity of which is adjusted by a needle valve.

Sample Protection

The experimental procedure involves measuring the piloted ignition time of various samples of the same material at different incident irradiance levels. This measurement requires that the radiant source be first brought to the desired incident irradiance level before exposing the sample. Also the heating system must reach a steady state flux level. During this period the sample must be protected from the radiant source by a shield as shown in Figure III-7. The shield is made of aluminum with cooling water passageways. The shield can be moved horizontally between the guide rails. In the forward position it protects the sample. The backward movement of the shield, and exposure of the sample, is achieved almost instantaneously by a three-way air valve provided in front of the cabinet. It takes about 0.1 second to expose the entire sample.

Pilot Light System

The pilot light consists of a perforated stainless steel tube located above the sample. One end of the tube is

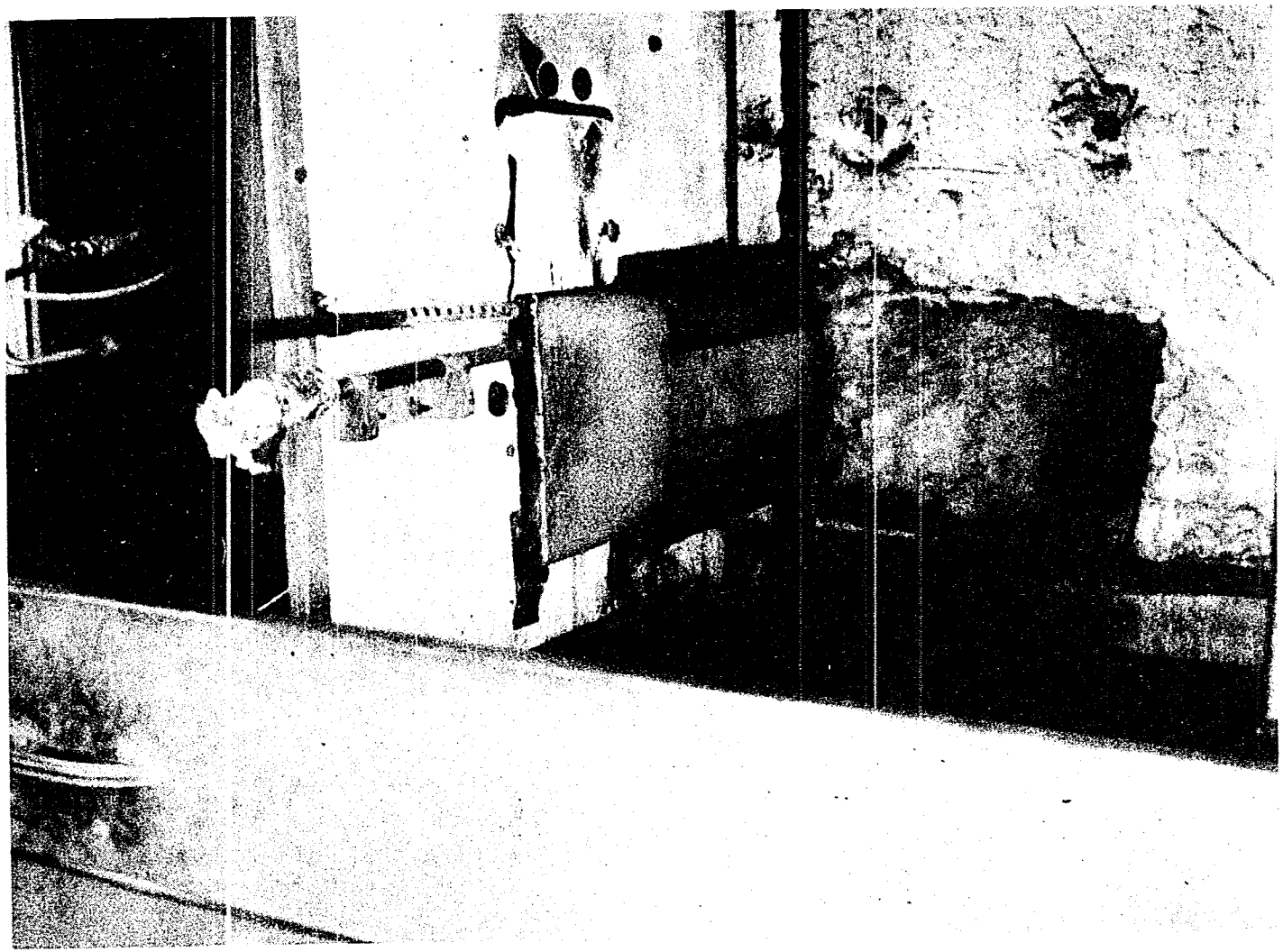

Figure III-7. Heat-Shield in Closed Position.

attached to the shield (as shown in Figure III-7). The diameter of the tube is 1.27 cm. There are two rows of fine holes along the axis of the tube, one in the front and one in the rear. Propane gas under pressure emerges through the holes and burns as the pilot flame. The pilot flame is about 0.635 cm in front and 2.54 cm above the sample. It is arranged so that the pyrolysis gases flow over the pilot after they leave the sample surface.

Instrumentation

During the test runs the following variables were measured: (1) The incident irradiance on the sample; (2) the time required for piloted ignition to occur.

The incident irradiance was measured by a water cooled radiometer, called the "Permanent Radiometer." The range of the radiometer is 0-10 cal/cm^2-sec. It has 150° viewing angle. For the measurement of ignition time a cadmium selenide photo-conductive cell was used. The CdSe changes resistance as it is illuminated. The photo-conductive cell decreases in resistance as the light level increases and increases in resistance as the light level decreases. The photo-conductive cell is water cooled, placed inside a tube, and mounted in such a manner that it sees the upper edge of the sample surface. The photo-conductive cell tube is placed just below the pilot light tube as shown in Figure III-7.

The output from the radiometer and the photo-conductive cell were recorded on a 2-channel Honeywell Electronic 19

recorder. The recorder had an accuracy of ± 0.25 percent. The maximum speed of the recorder was 1 inch/second. Figure III-8 shows the typical output from the recorder for a particular run. Once the shield was opened the radiometer output increased slightly because the shield partially obstructed the radiometer field of view. When the sample ignited there was a sudden drop in the photo-conductive cell output, which defines the ignition point. For each run the chart speed was noted. By measuring the distance on the chart between opening the shield and the ignition point, the ignition time was determined.

Experimental Procedure

As can be seen in Figure III-7, the permanent radiometer is installed adjacent to the sample. It has a sapphire window to protect it from damage. The measured output is not directly the incident irradiance on the sample, but it is calibrated so that it can be translated into the incident irradiance on the sample.

Calibration Procedure

The calibration was done by installing temporarily another radiometer in the place of the sample, called the "test radiometer." Both "permanent" and "test" radiometers were the same type and were factory calibrated. The outputs from both the radiometers were connected to the Honeywell recorder. In the case of tungsten lamps, the incident

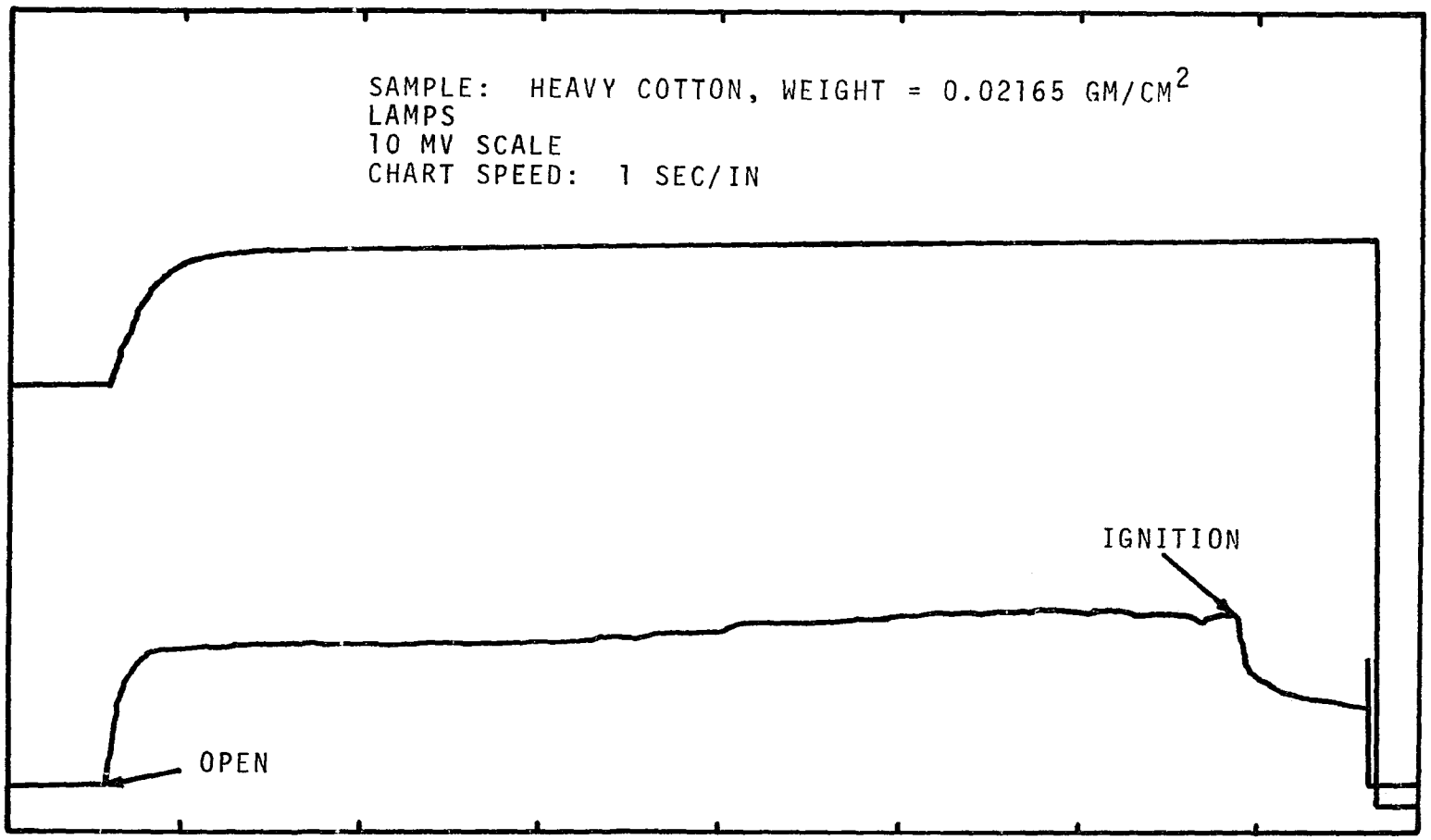

Figure III-8. Typical Recorder Output During Experimental Run.

irradiance on the "test" radiometer was varied by moving the lamps forward or backward. The millivolt outputs from both radiometers were simultaneously recorded on the recorder chart. The same procedure was used in the case of flames. In the case of flames the burner movement and oxygen supply were used to vary the incident irradiance. Figure III-9 is the factory calibration graph for the "test" radiometer from which the incident irradiance could be found. The corresponding millivolt output of the "permanent" radiometer was found from the calibration chart. Figure III-10 shows the calibration graph for tungsten lamps. The entire calibration procedure was carried out whenever the radiant source was changed from lamps to flames or vice versa.

Procedure

In the present work the piloted ignition characteristics of cotton, cellulose, filter paper, wool, acrylics and other thin materials were studied. The individual samples were cut from larger sheets. The cut sample size was 18 cm by 10 cm. The sample holder diagram is shown in Figure III-11. There are two retainer posts with pins on them. One of them is fixed whereas the other can be rotated. The sample surface exposed to radiation was in front of the guide posts. The sample was held tightly by the pins on the retainer post. The sample dimension exposed to radiation was 10 cm by 10 cm. In order to prevent the edge effects, a piece of "Permacel"

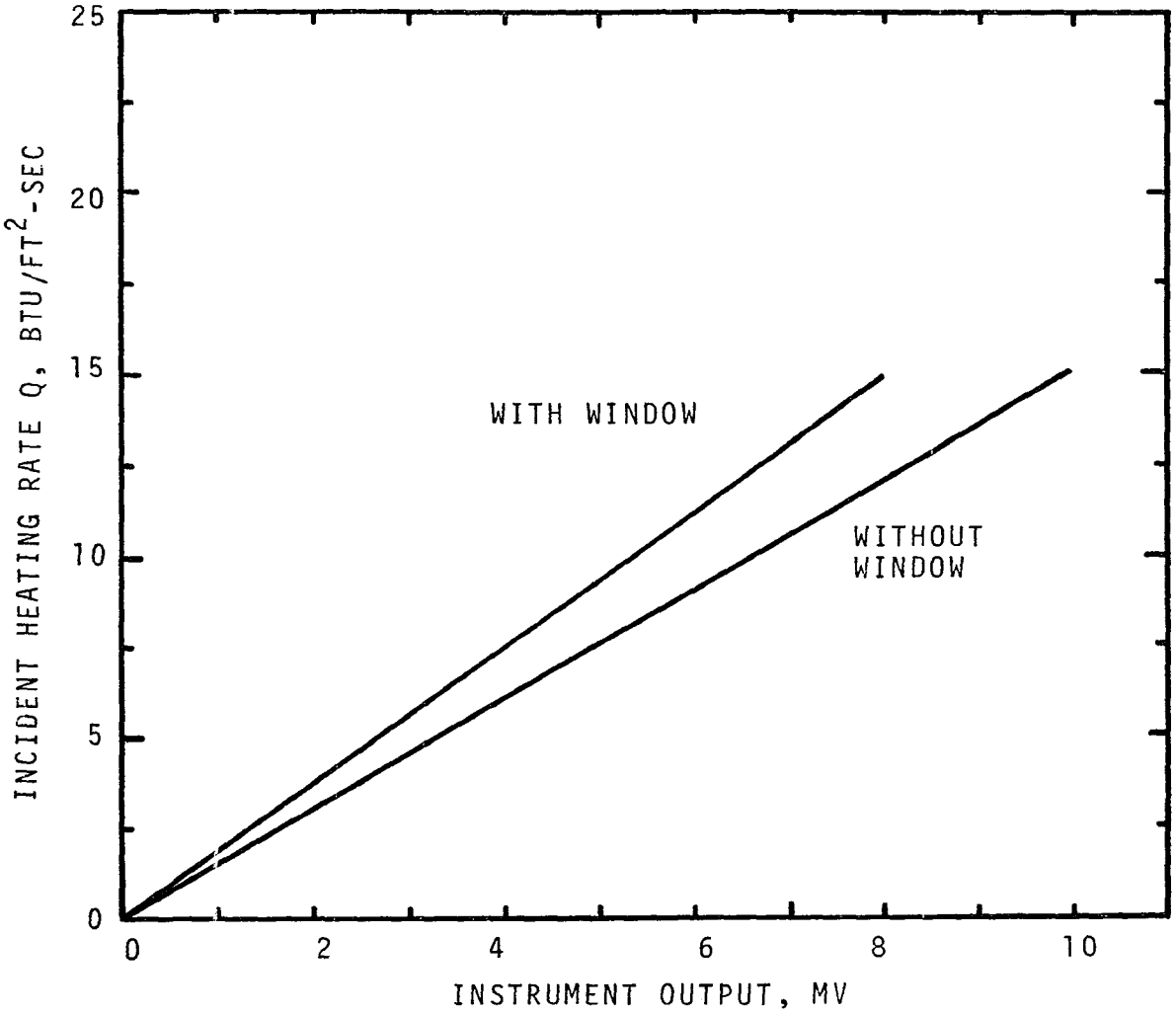

Figure III-9. Factory Calibration Graph for "Test" Radiometer.

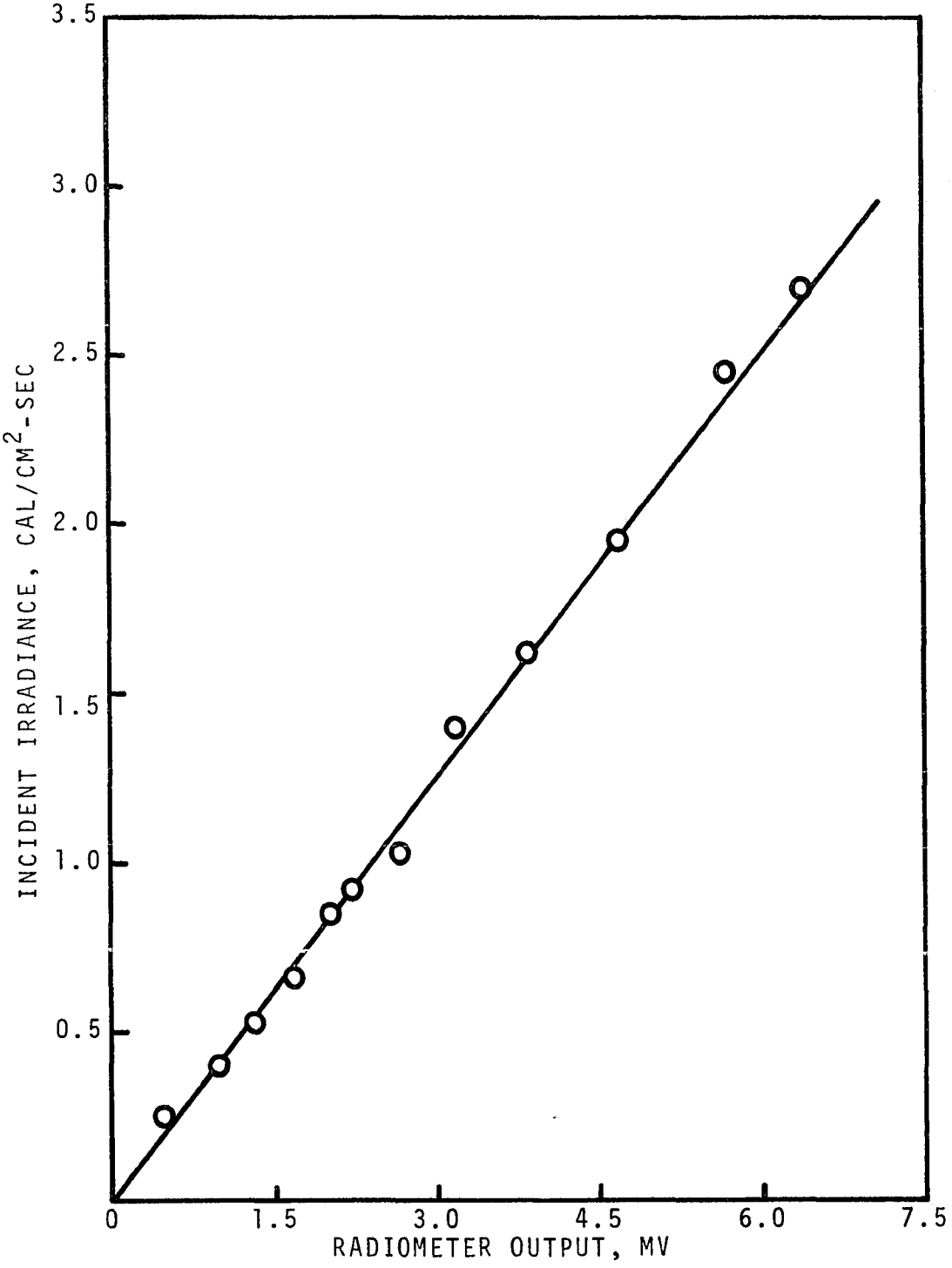

Figure III-10. Calibration Graph for Tungsten Lamps.

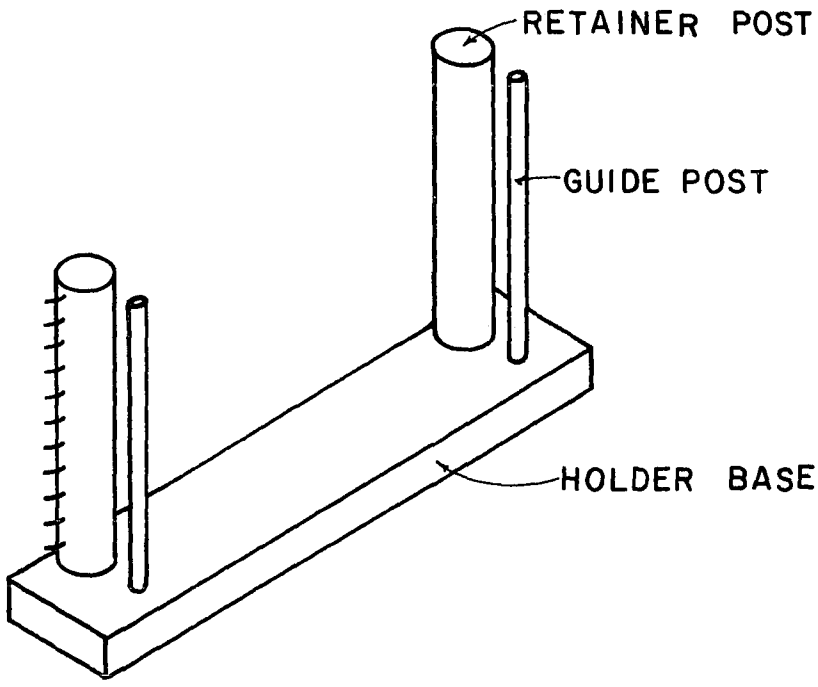

Figure III-11. Fabric Sample Holder

reflecting tape was applied at the top and bottom of the sample. All the samples were oven dried at 70°C for four hours. Then the samples were put in a polyethylene bag while they cooled to maintain the dryness.

There were certain common procedures that were followed whether using tungsten lamps or benzene flames as radiant source. They are listed below:

1. The Honeywell recorder was turned on and allowed to warm up.
2. The exhaust fan and air compressor were turned on.
3. The valve on the water line was opened to supply water to the protective shield, radiometer and the ignition detector.
4. The permanent radiometer window was cleaned.
5. After the Honeywell recorder warmed up, it was calibrated against a potentiometer.
6. The ignition detector switch was turned on.
7. The outputs of the ignition detector and radiometer were checked by holding a lighted match in front of the viewing tube and in front of the window respectively.
8. The propane gas was then supplied to the pilot tube by opening the valve at the top of the propane cylinder. The gas was then lit.
9. The sample was then taken out of the polyethylene bag and "Permacel" tape was put on it. The sample was then installed in the sample holder and mounted on the vertical

ceramic panel inside the ignition cabinet (as shown in Figure III-3).

10. The water cooled shield was then pushed forward to protect the sample.
11. The ignition cabinet door was then closed.
12. At the beginning of each run the recorder speed, the type of material, sample number and the radiant source were noted on the recorder chart.
13. The radiant source was then brought to the desired irradiance level.
14. The recorder speed was then brought to the desired rate.
15. Next the protective shield was operated pneumatically to expose the sample to radiation by operating the three-way valve.
16. As soon as the ignition of the sample took place the irradiation from the radiant source was turned off.
17. Finally, the ignition cabinet door was opened and the burnt sample was taken out.

The cabinet was then ready for the next run and the entire operation was repeated.

Tungsten Lamp System

1. At the beginning of the experiments the lamps were connected to the 230 V AC supply.
2. The needle valve on the air line was opened to supply low velocity air to cool the lamp ends and power leads.

3. After the shield had been pushed forward to protect the sample the tungsten lamps were switched on.
4. The desired irradiance level was obtained by moving the lamps towards or away from the sample.
5. As soon as the ignition occurred the lamps were switched off.

Benzene Flame System

1. The fuel reservoir was filled with benzene using the fuel pump.
2. The valve at the top of oxygen cylinder was opened to supply oxygen to the burner. The oxygen pressure was maintained at 45 psig.
3. At the start of each run the burner was cleaned using compressed air.
4. At the start of each run the spark ignitor was checked.
5. After closing the ignition cabinet door the three way valve in front of the cabinet was opened to allow benzene to flow into the burner. Immediately the vacuum pump was started.
6. When the desired fuel level was reached in the burner, the benzene was ignited using the spark ignitor.
7. The incident irradiance on the sample was varied by increasing or decreasing the oxygen supply as well as by moving the burner towards or away from the sample. The oxygen supply was controlled by a needle valve.

8. As soon as ignition of the sample took place, the needle valve was closed to cut off the oxygen supply, and the three way valve was closed to cut off the benzene supply to the burner in order to extinguish the fire.
9. After the fire was extinguished the vacuum pump was switched off.
10. The fuel in the vacuum tank was drained into a can.
11. As a precaution, the fuel level in the fuel reservoir was checked after each run.
12. At the end of each day the remaining benzene in the fuel reservoir was drained off.

Shutdown of the Cabinet

At the end of the runs the whole ignition cabinet was allowed to cool. For that purpose the exhaust fan and the cooling water supply to the shield and radiometers were not switched off immediately after finishing the runs. They were allowed to continue for about 15 more minutes and then switched off. The photo-conductive cell and the recorder were turned off. The pilot light was extinguished by closing the valve on top of the propane bottle, thereby cutting off the propane supply. The compressor was also switched off. If tungsten lamps had been used, the cooling air supply was cut off by closing the needle valve. If benzene flames had been used, then the oxygen cylinder valve was closed.

CHAPTER IV

RESULTS AND DISCUSSION

The review of previous work on the ignition of thin materials, as discussed in Chapter II, indicated that not much work had been done on the piloted ignition of thin materials. The objectives of this study were:

1. To study the ignition characteristics of thin materials (mostly cellulosic) under radiation from benzene flames and 1000-watt tungsten lamps in order to compare both types of radiant heating.
2. To compare the present data with the ignition models available in the literature for thin materials.
3. To develop a mathematical model that would permit a prediction of piloted ignition time of a thin material when subjected to radiant heating.

During the experiments the incident irradiance and the ignition time were measured for each run as discussed in Chapter III. Both were taken from the output from the recorder as shown in Figure III-8. Also the thickness and weight per unit area of the materials tested were noted. A complete summary of the ignition data is given in Appendix A. The values of the

physical properties of the materials tested are given in Appendix B.

Incident Irradiance and Ignition Time Relationship

A typical relationship between irradiance and ignition time is presented in Figure IV-1. From the figure it can be seen that as irradiance increases, ignition time decreases, and at higher irradiance the ignition time appears asymptotic. At the same time, when irradiance falls below about 0.8 cal/cm^2-sec the ignition time increases rapidly and becomes asymptotic at a particular incident irradiance, suggesting the existence of a minimum incident irradiance below which ignition will not occur. Figure IV-2 presents the relationship between irradiance and ignition time on a log-log plot.

Minimum Incident Irradiance Required for Piloted Ignition

The differential equation for one-dimensional heat conuction through an inert, opaque, slab is given by:*

$$\alpha \frac{\partial^2 \Delta T}{\partial x^2} = \frac{\partial \Delta T}{\partial t} \qquad \text{(IV-1)}$$

The initial condition is $\Delta T = 0$ for $0 < x < L$. The boundary conditions chosen are:

$$t > 0;\ x = L \text{ (front surface)}: \quad -K \frac{\partial \Delta T}{\partial x} = \alpha_{av} H_i \qquad \text{(IV-2)}$$

$$t > 0;\ x = 0 \text{ (back surface)}: \quad \partial \Delta T / \partial x = 0 \qquad \text{(IV-3)}$$

---

*The nomenclature is given in Appendix D.

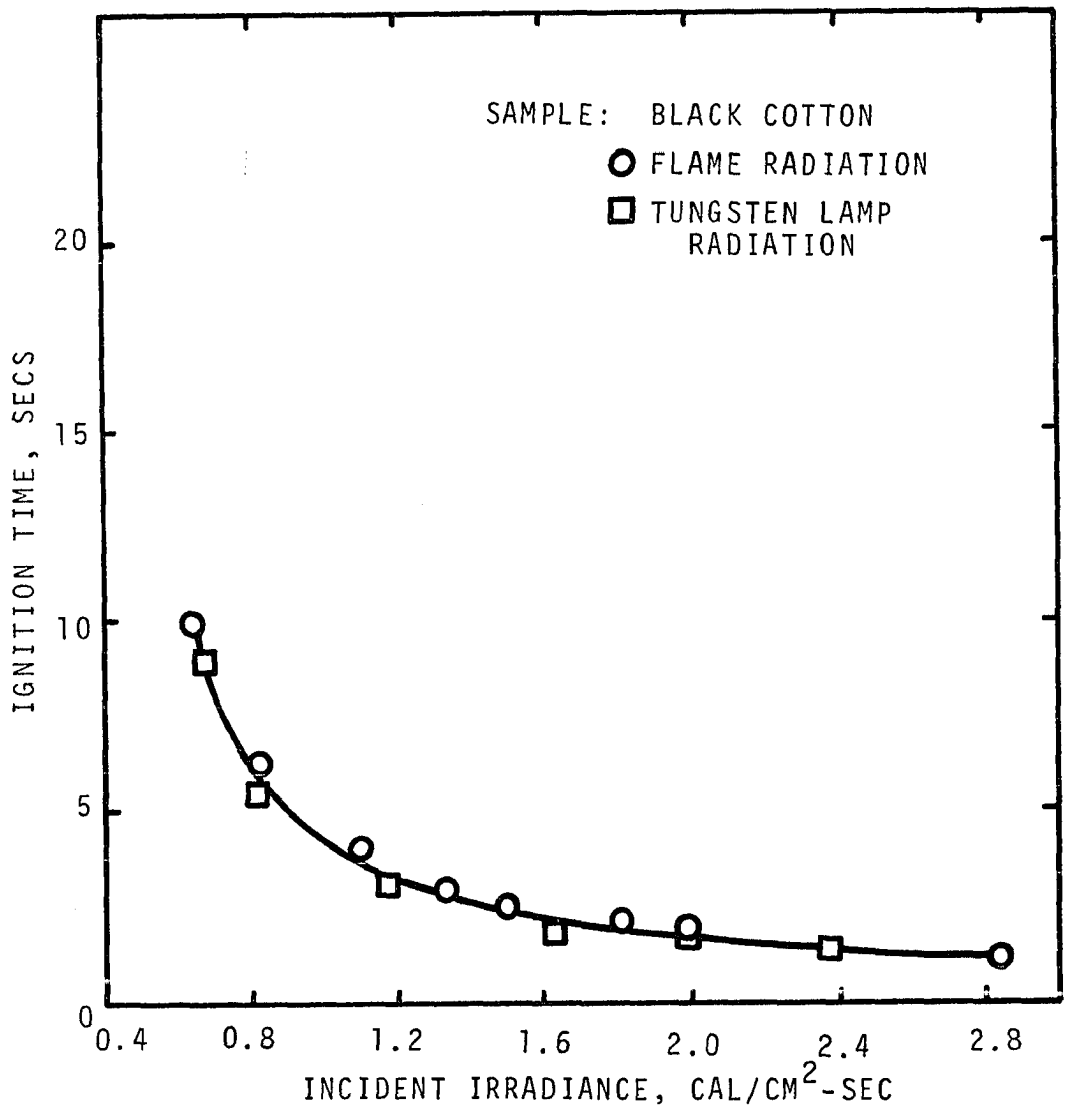

Figure IV-1. Typical Relationship Between Irradiance and Ignition Time.

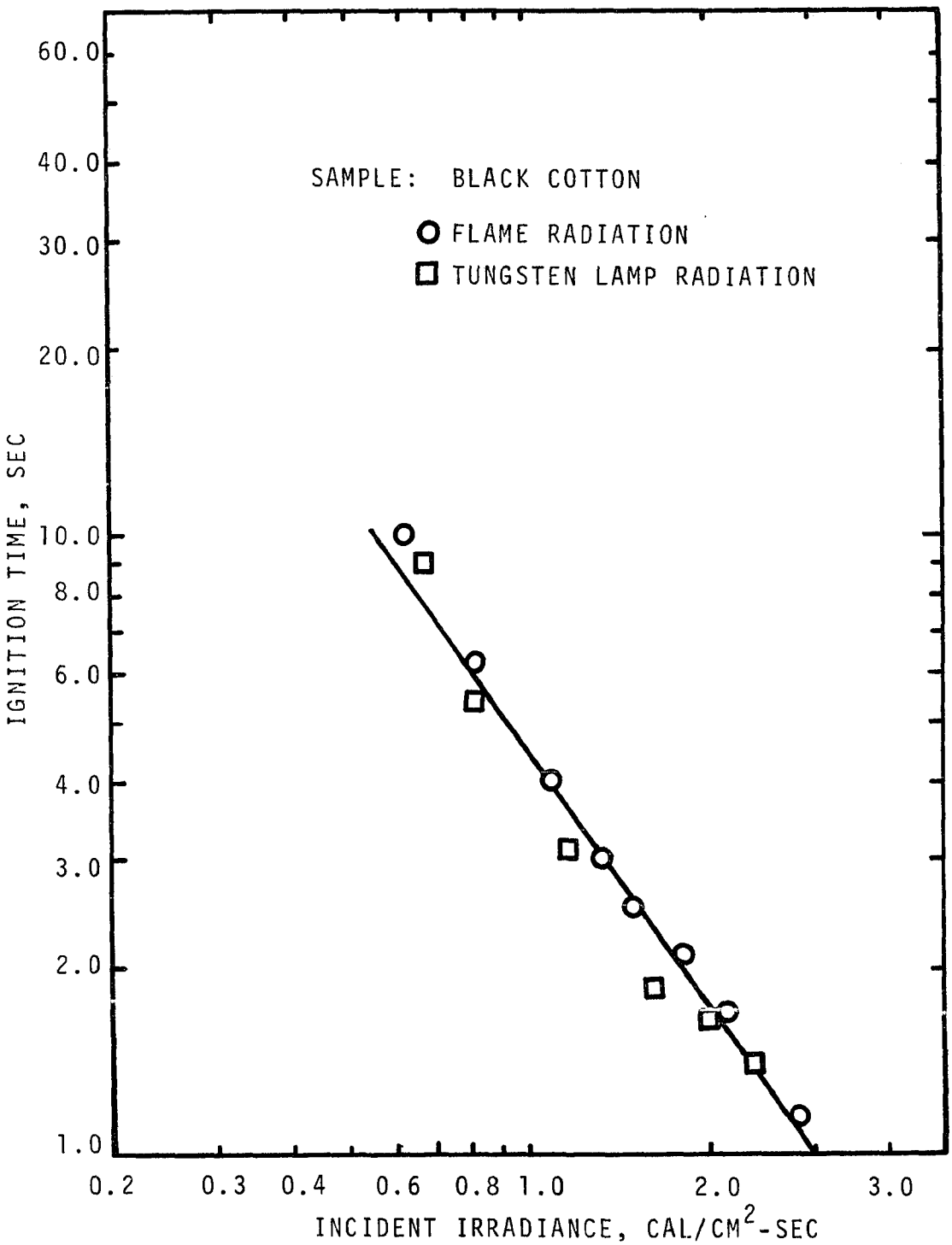

Figure IV-2. Typical Relationship Between Irradiance and Ignition Time.

The solution to Equation IV-1 with the above conditions is given by Carslaw and Jaeger (10) for the surface temperature rise as

$$\Delta T_s = \frac{2\alpha_{av} H_i t^{1/2}}{(K\rho c)^{1/2}} \sum_{n=0}^{\infty} \text{ierfc} \frac{2nL}{2(\alpha t)^{1/2}} + \text{ierfc} \frac{(2n+2)L}{2(\alpha t)^{1/2}} \tag{IV-4}$$

The summation term in Equation IV-4 is now written as f_n, and the Fourier modulus, $\alpha t/L^2$, as F, so the summation can be rewritten as

$$f_n = \sum_{n=0}^{\infty} [\text{ierfc} \frac{n}{\sqrt{F}} + \text{ierfc} \frac{n+1}{\sqrt{F}}] \tag{IV-5}$$

The square root of the Fourier modulus for the thin materials tested in this work ranges from about 0.8 to 6. Plotting f_n versus $\sqrt{F}$ as given by Equation IV-5, a straight line is obtained as shown in Figure IV-3. Therefore, Equation IV-5 can be written as

$$f_n = a + b\sqrt{F} = a + b\sqrt{\alpha t/L} \tag{IV-6}$$

where a and b are constants. The values of a and b are 0.12 and 0.484 respectively. Combining Equations IV-4 and IV-6, the surface temperature rise is given as

$$\Delta T_s = \frac{2\alpha_{av} H_i t^{1/2}}{(K\rho c)^{1/2}} [a + b \frac{\sqrt{\alpha t}}{L}] \tag{IV-7}$$

If the surface temperature at ignition, the thermal and physical properties, and the thickness of the material being

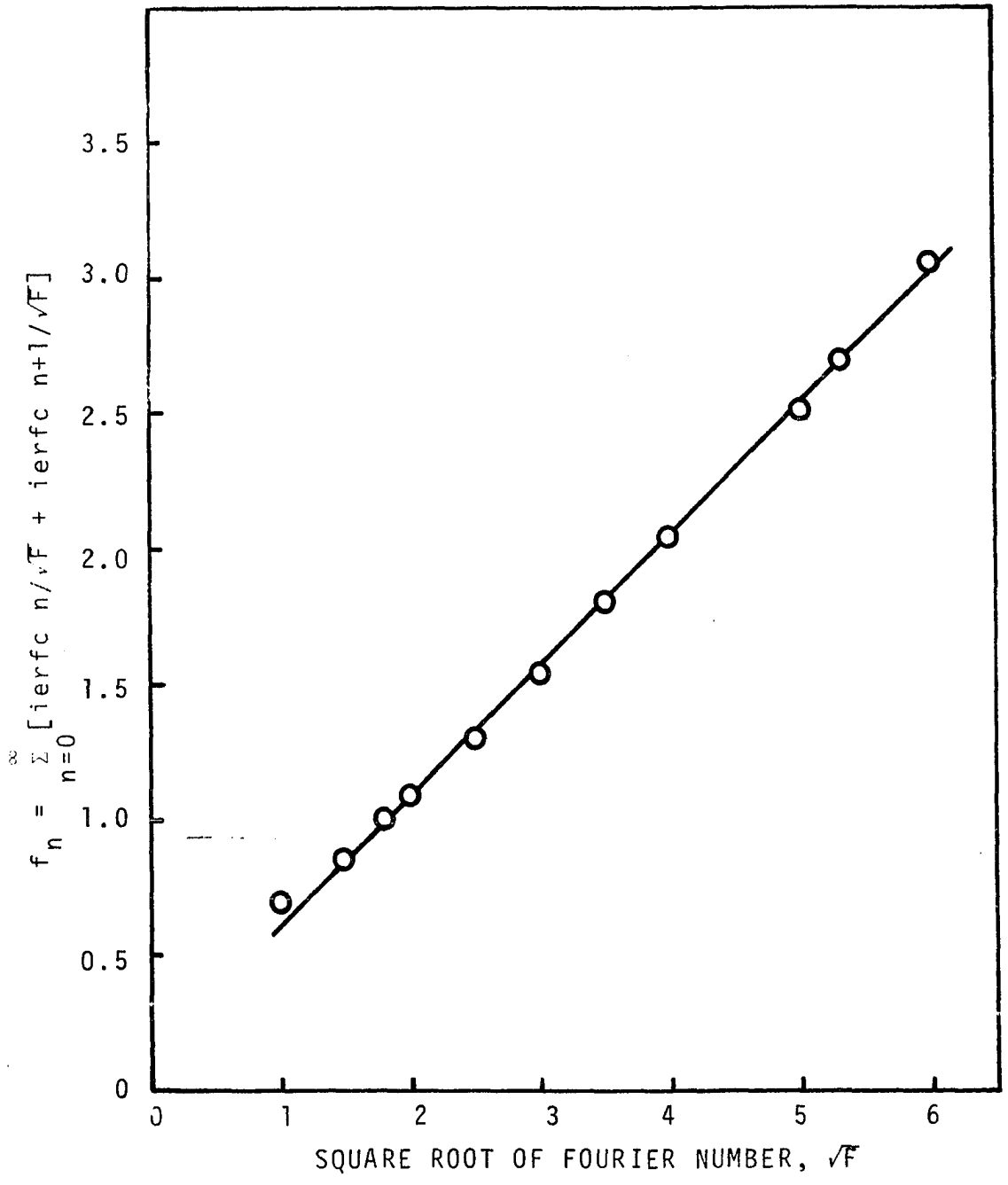

Figure IV-3. Correlation Between f_n and $\sqrt{F}$.

tested are assumed constant for a particular material, Equation IV-7 can be written as

$$H_i = \frac{c}{at^{1/2} + b't} \qquad \text{(IV-8)}$$

where c and b' are again constants. c is $\Delta T_s (k\rho c)^{1/2}/2\alpha_{av}$, and b' is $b\sqrt{\alpha}/L$. For example, in the case of black cotton the value of b' was found to be 1.188. The values of $at^{1/2}$ ranged from 0.13 to 0.38 and that of b't from 1.37 to 11.88 for black cotton. Generally the values of $at^{1/2}$ were found to be 3 to 10 percent of the values of b't and hence $at^{1/2}$ could be neglected compared to b't. Therefore

$$H_i \propto 1/t \qquad \text{(IV-9)}$$

Plotting H_i versus 1/t and extrapolating the line to the y-axis where 1/t = 0 (i.e., $t = \infty$) the minimum incident irradiance for piloted ignition is obtained as shown in Figure IV-4. Table IV-1 lists the minimum incident irradiance for piloted ignition for the materials tested in the present work. The minimum incident irradiance gives the value of incident irradiance below which piloted ignition will not occur.

Fabric Weight as a Parameter and Correlation of Weight Effects

In order to study the effects of fabric weight on ignition, ignition data for heavy cotton with different weights was obtained. The weight of the fabric ranged from 0.0193

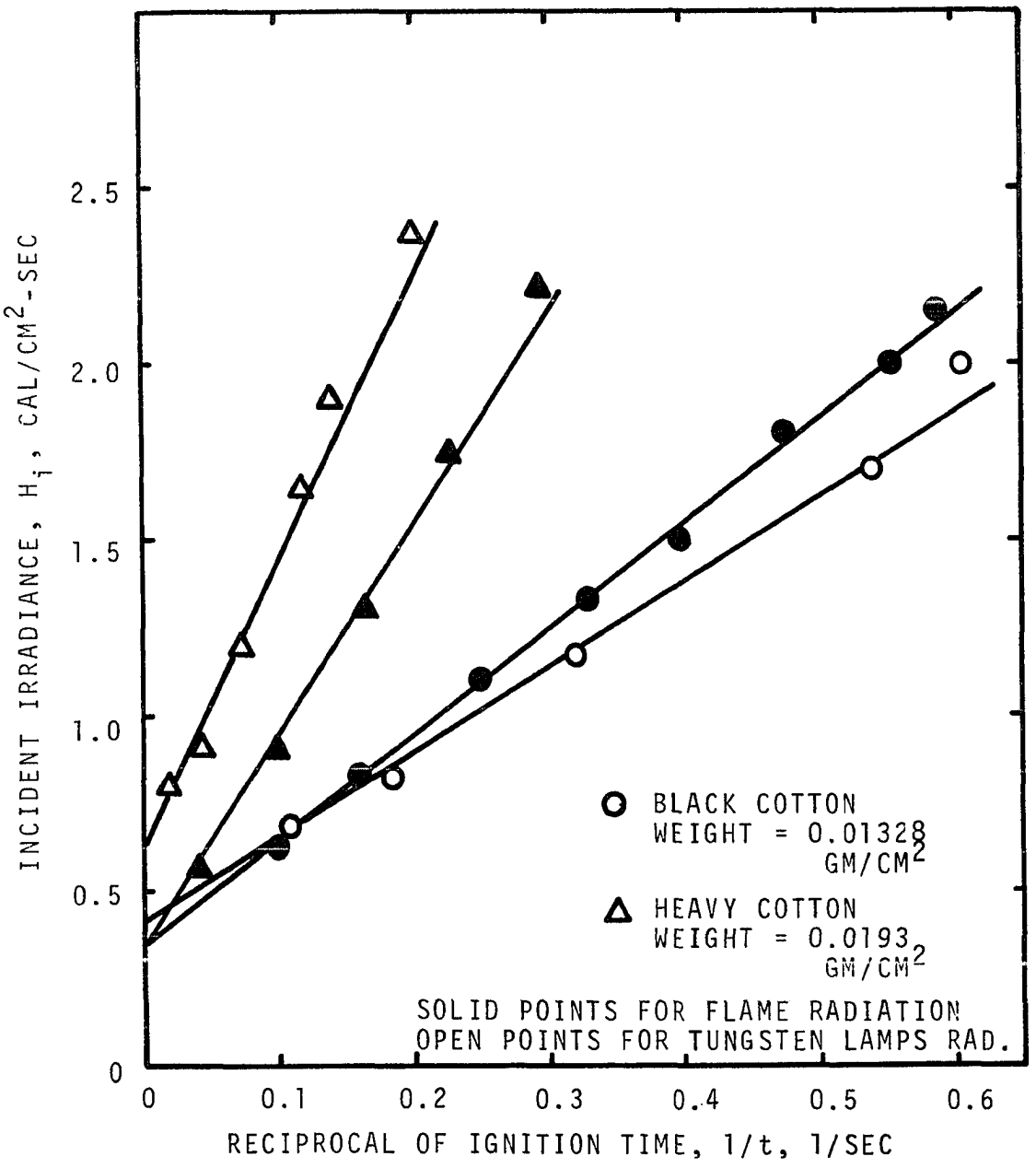

Figure IV-4. Effect of Incident Irradiance on Reciprocal of Ignition Time.

TABLE IV-1

MINIMUM INCIDENT IRRADIANCE FOR PILOTED IGNITION

Material	Minimum Incident Irradiance cal/cm^2-sec
Flames:	
Black cotton	0.32
White cotton	0.50
Black rayon	0.96
White rayon	0.96
Heavy cotton-ecru (average)	0.36
α-cellulose (average)	0.58
Filter paper (average)	0.70
White acrylics	1.16
Lamps:	
Black cotton	0.36
White cotton	0.82
Black rayon	1.42
White rayon	1.42
Heavy cotton-ecru (average)	0.62
α-cellulose (average)	0.74
Filter paper (average)	0.97
White acrylics	0.91

gms/cm^2 to 0.0352 gms/cm^2. The density of the fabric was the same for all the weights. The ignition time versus incident irradiance plots for three different weights of fabric for benzene flame radiation and tungsten lamp radiation are given in Figures IV-5 and IV-6. From the figures it can be seen that the ignition time increases as the weight of the fabric increases for a particular incident irradiance. The ignition time can be written in the following functional manner.

$$t_{ig} = g\, H_i^{\,a}\, w_o^{\,b} \qquad \text{(IV-10)}$$

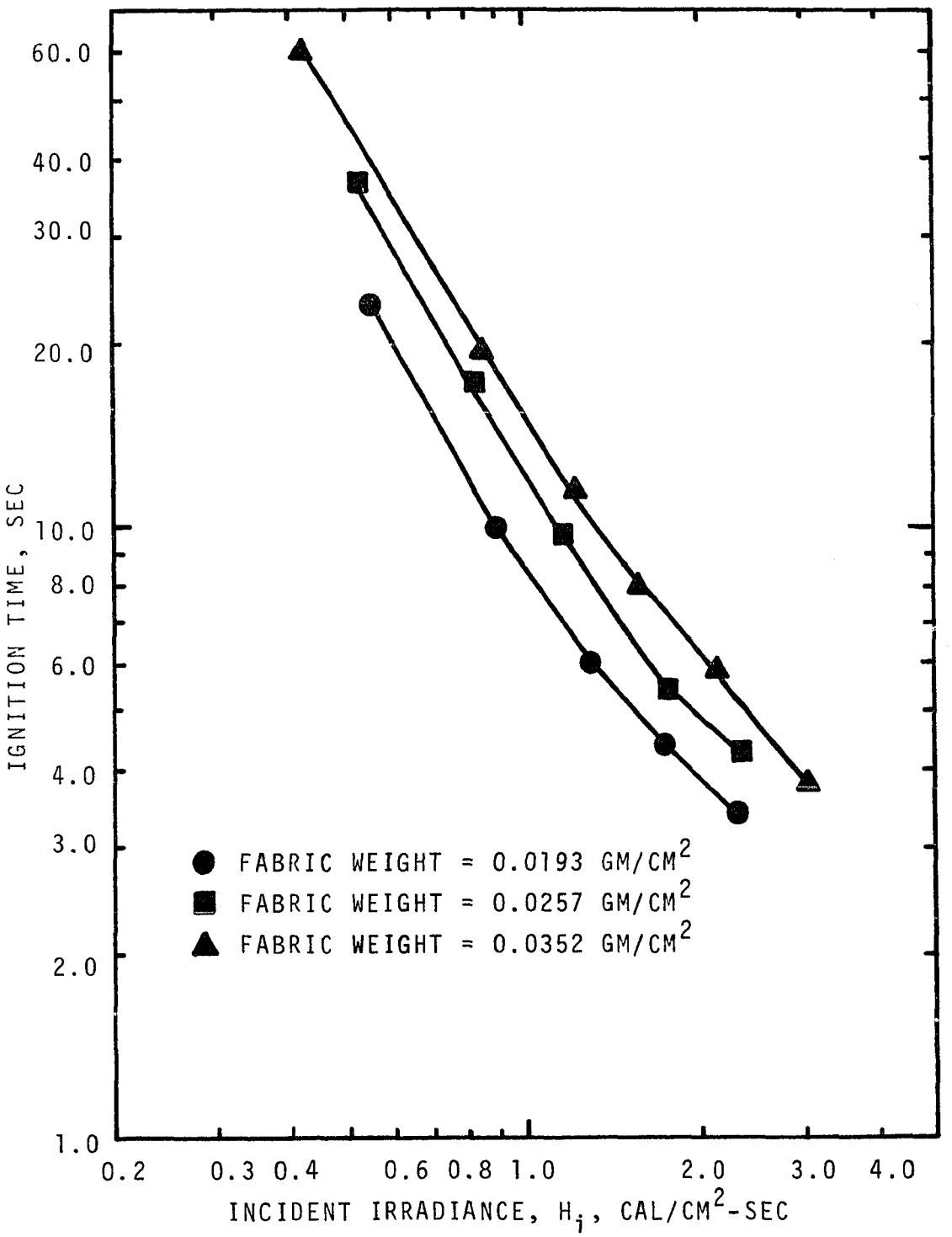

Figure IV-5. Effect of Ignition Time on Incident Irradiance for Heavy Cotton with Different Fabric Weights for Benzene Flame Radiation.

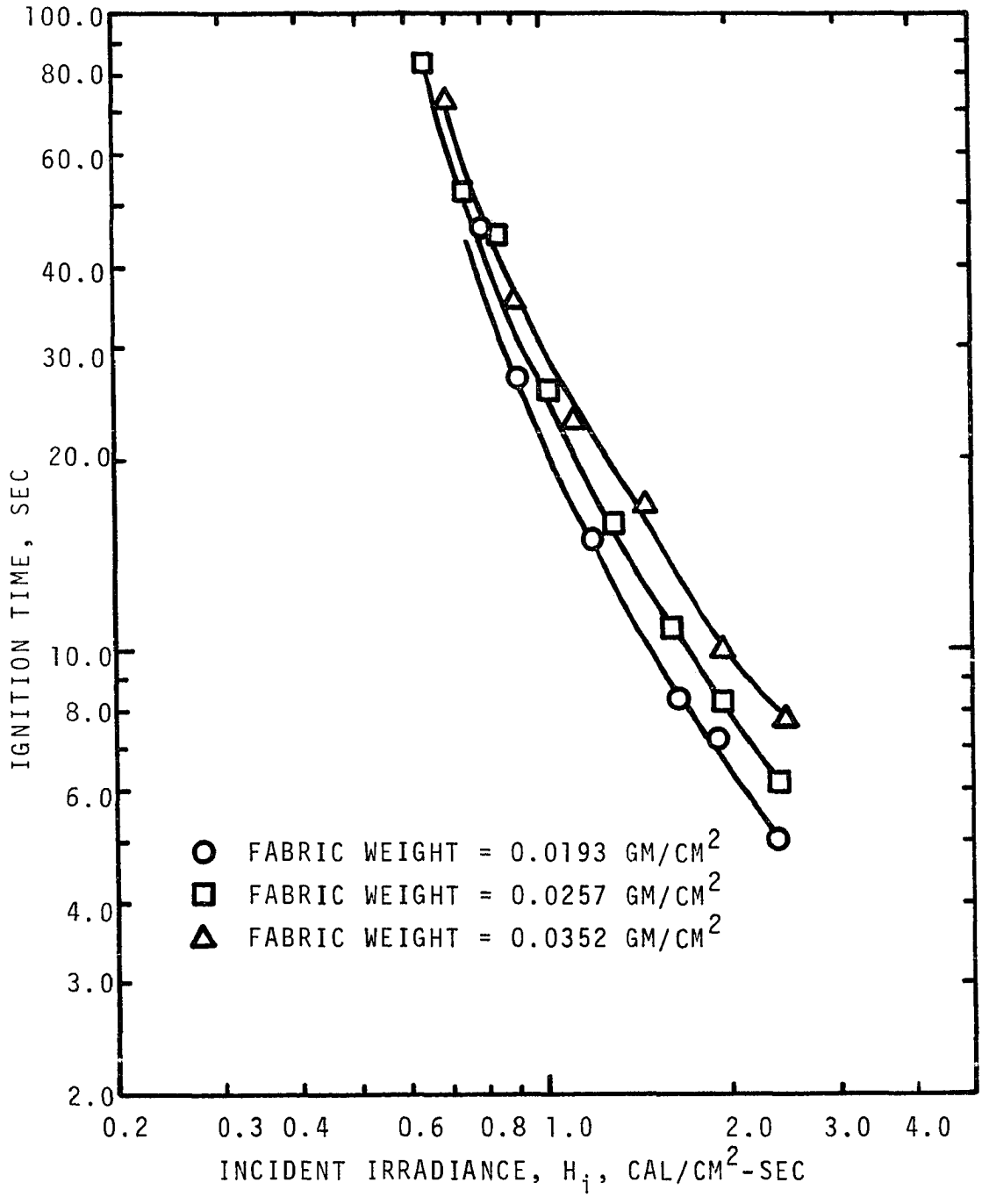

Figure IV-6. Effect of Ignition Time on Incident Irradiance for Heavy Cotton with Different Fabric Weights for Tungsten Lamp Radiation.

where g, a and b are constants. A regression analysis program was run to find out the values of g, a and b for flame radiation and tungsten lamp radiation. For benzene flame radiation the correlation was

$$t_{ig} = 206.0\ H_i^{-1.4}\ w_o^{0.75} \qquad \text{(IV-11)}$$

with a correlation coefficient of 0.984 and an error of estimate of 0.157. The ignition time is plotted against $H_i w_o^{-0.5}$ as incident irradiance, H_i, is the primary independent variable. Figure IV-7 is a plot of t_i versus $H_i w_o^{-0.5}$ for flames data. For tungsten lamp radiation the correlation is

$$t_i = 189\ H_i^{-1.9}\ w_o^{0.5} \qquad \text{(IV-12)}$$

with a correlation coefficient of 0.986 and an error of estimate of 0.15. Figure IV-8 is a plot of t_i versus $H_i w_o^{-0.25}$ for lamps data. Similarly the ignition time correlation for the α-cellulose samples for flame radiation was found to be

$$t_{ig} = 288\ H_i^{-2.2}\ w_o^{0.9} \qquad \text{(IV-13)}$$

with a correlation coefficient of 0.975 and an error of estimate of 0.215, the weight range being 0.02415 gms/cm^2 to 0.03766 gms/cm^2.

Comparing the Figures IV-5 and IV-6 it can be seen that the ignition time for the tungsten source is two or three times that required for the flame source. This difference is caused by the different spectral distribution of the incident

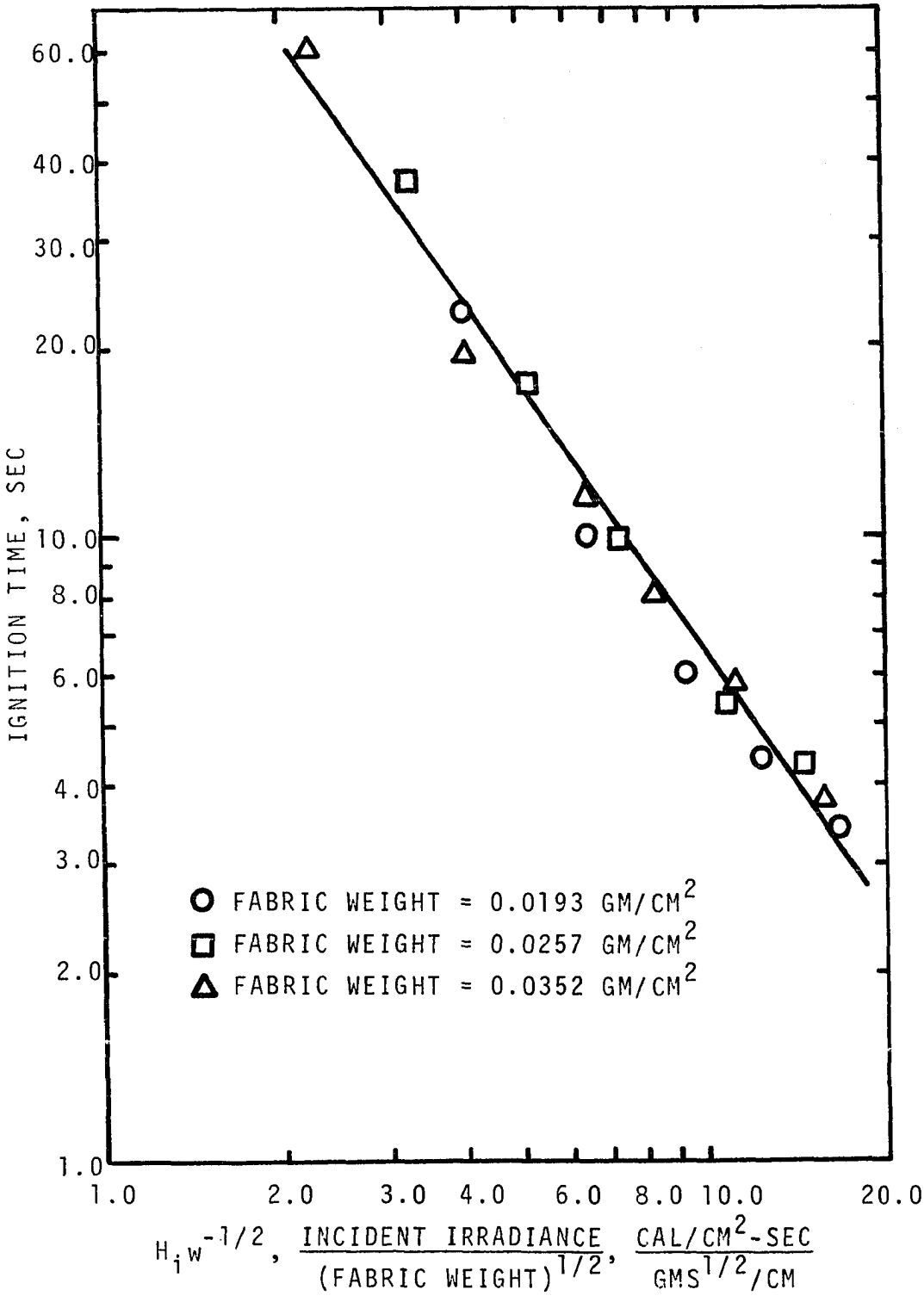

Figure IV-7. Relationship Between Ignition Time, Incident Irradiance and Fabric Weight for Heavy Cotton Samples Using Flame Radiation.

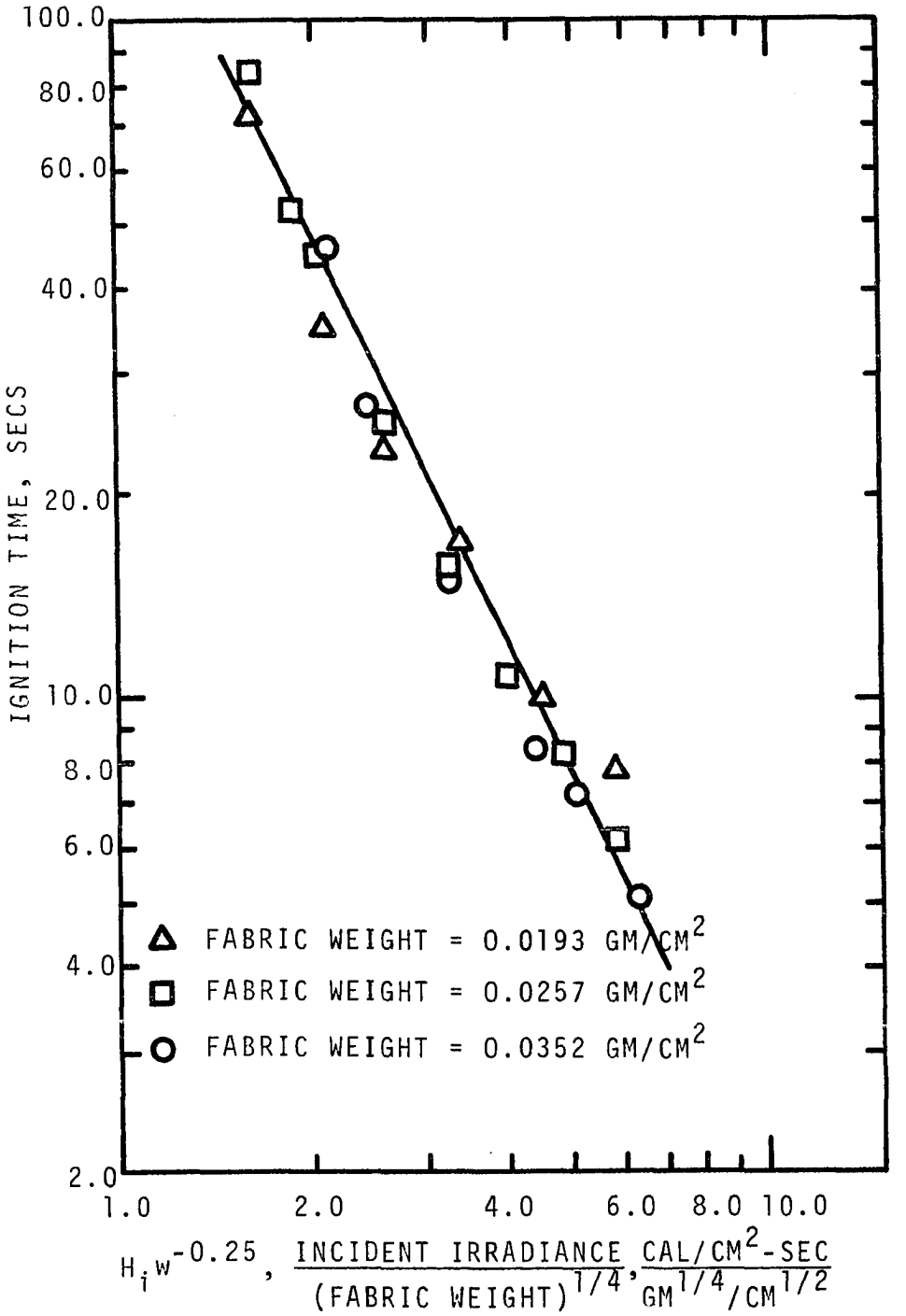

Figure IV-8. Relationship Between Ignition Time, Incident Irradiance and Fabric Weight for Heavy Cotton Samples Using Tungsten Lamp Radiation.

radiation and the spectral absorptance characteristics of the materials being irradiated. The effects of absorptance have been discussed in Chapter II under "Absorptivity." The average absorptance is found from Equation II-31,

$$\alpha_{av} = \frac{\Sigma\ \alpha_\lambda e_\lambda \Delta\lambda}{\Sigma\ \ e_\lambda \Delta\lambda} \qquad \text{(II-31)}$$

Figure IV-9 is the plot of the absorptance used for the fabrics in the present work, and Figure IV-10 is the plot of emissive power versus wavelength for tungsten lamp source and flame source. Both have been reproduced from Wesson's thesis (40). The hexane flames data of Ryan, Penzias and Tourin (28) were used even though benzene was used as the fuel in the tests. Ryan, Penzias and Tourin found out that the spectra of different hydrocarbon flames were so similar that there was little object in studying a great variety of hydrocarbon mixtures. The combustion products, and consequently the gross spectral features, were similar for all. Because of the above mentioned reasons there is little difference in the emissive powers of the two fuels. .

The absorbed irradiance is found from Equation II-32,

$$H_a = \alpha_{av}\ H_i \qquad \text{(II-32)}$$

The average absorptance for heavy cotton was found to be 0.721 for flame radiation and 0.457 for tungsten lamp radiation.

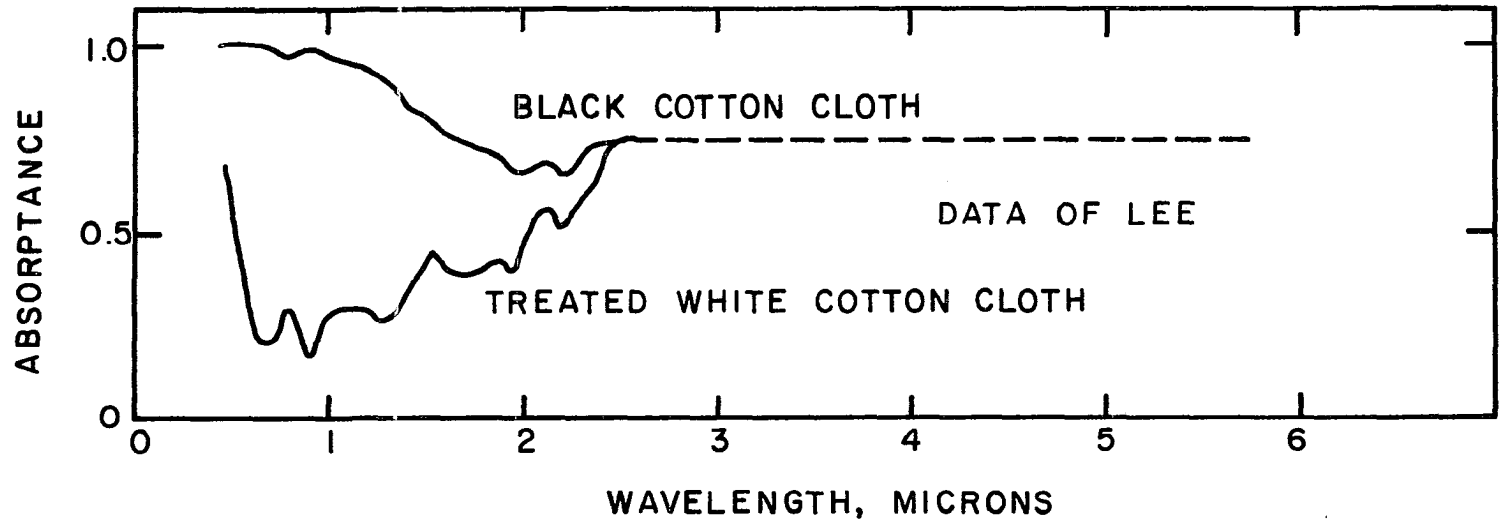

Figure IV-9. Monochromatic Absorptance Characteristics of White and Black Cotton Cloth (40).

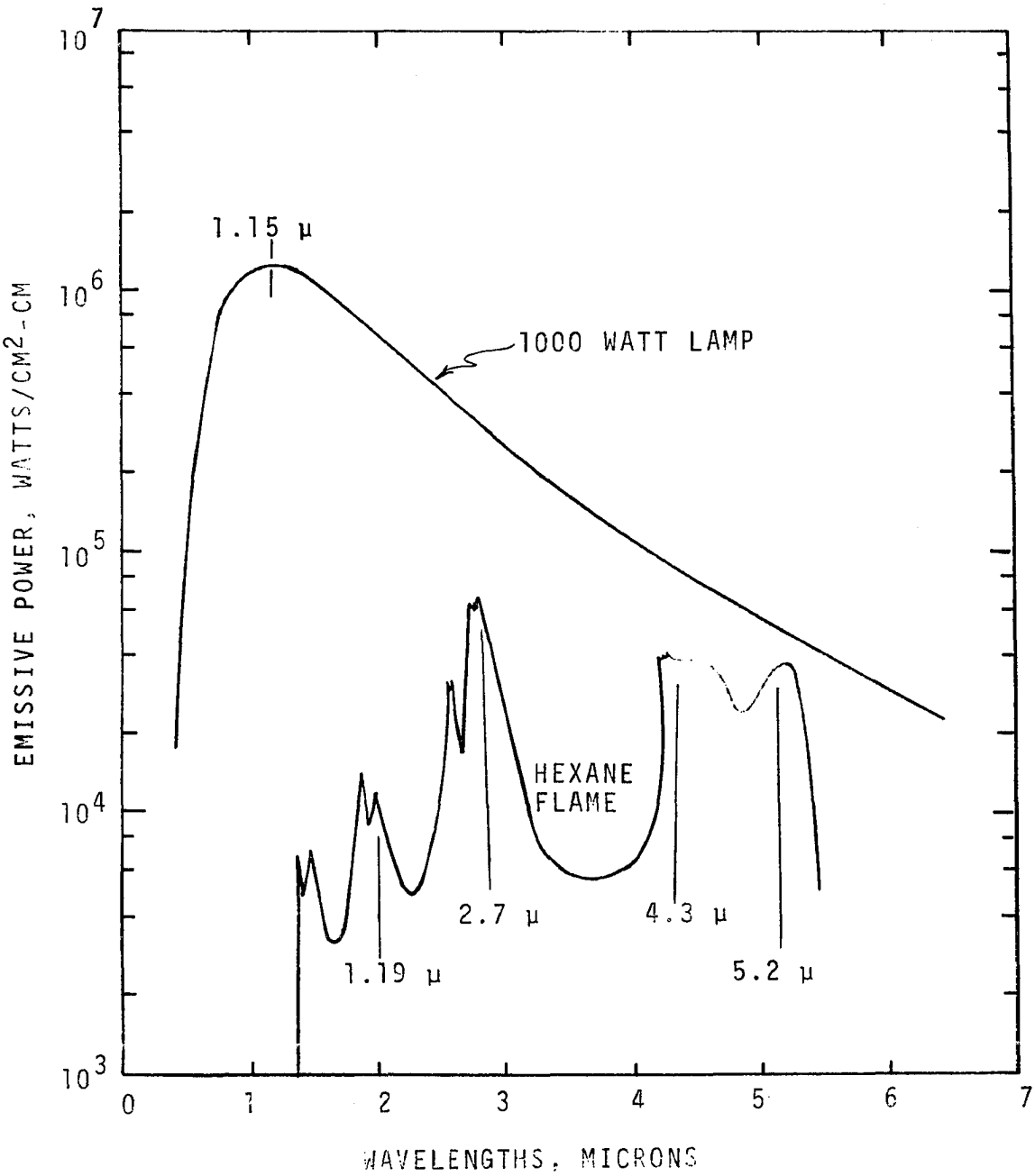

Figure IV-10. Comparison of Emissive Powers of a Blackbody Irradiance Source with a Flames Irradiance Source (40).

The average absorptance of other materials are listed in Table B-1. Figure IV-11 is a plot of ignition times as a function of absorbed irradiance. From Figure IV-11 it can be seen that the ignition data with both the flame source and the tungsten source can be reduced to a single correlation for each weight of the fabric. From the figure it can also be seen that for a particular absorbed irradiance the ignition time of the fabric increases as the fabric weight increases. Therefore, a regression analysis program was run to find the correlation between ignition time, absorbed irradiance and fabric weight. The relation obtained is

$$t_{ig} = 89.8\ H_a^{-1.61}\ w_o^{0.66} \qquad \text{(IV-14)}$$

with a correlation coefficient of 0.984 and an error of estimate of 0.154. Here again the ignition time is plotted against $H_a w_o^{-0.4}$ as absorbed irradiance, H_a, is the primary independent variable. Figure IV-12 is a plot of t_i versus $H_a w_o^{-0.4}$.

Ignition Temperature

Temperature is one of the main parameters in heat transfer problems. In the present study direct surface temperature measurements could not be taken. The ignition temperature was taken from the Differential Thermogravimetric Analysis plot of each material. A typical DTG plot for heavy cotton is given in Figure IV-13. The ignition temperature is taken as the temperature corresponding to the peak, where the

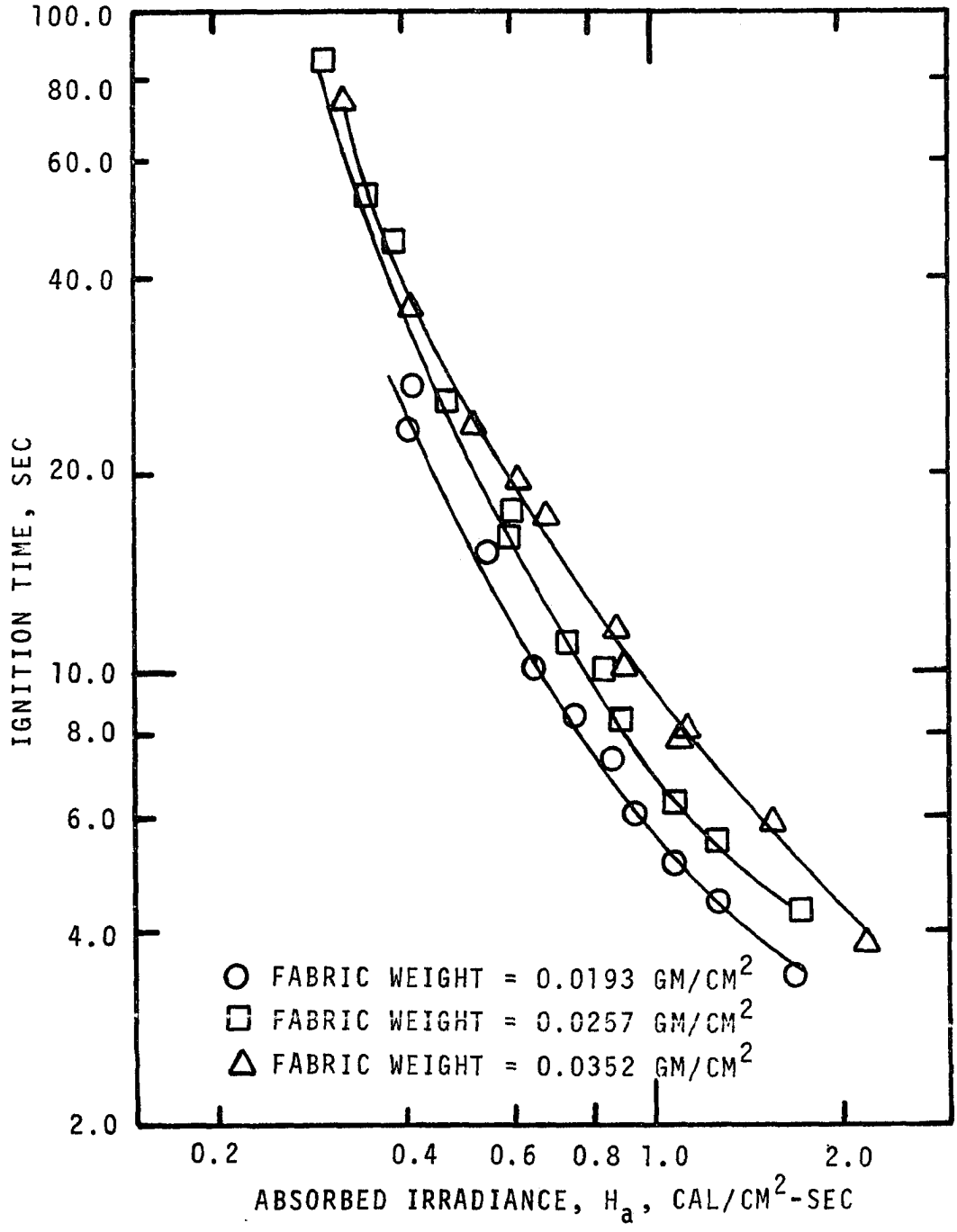

Figure IV-11. Heavy Cotton Ignition Times as a Function of Absorbed Irradiance.

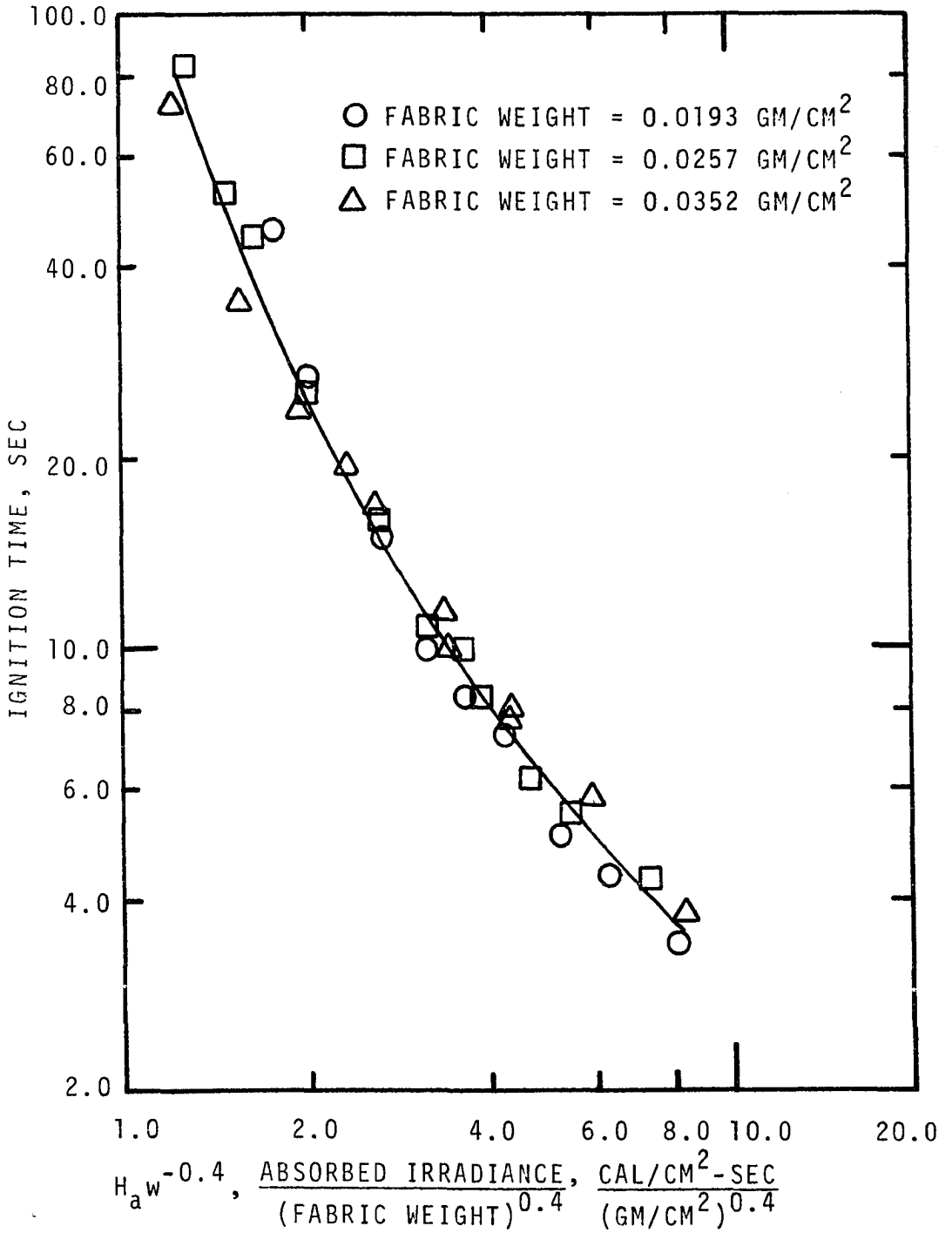

Figure IV-12. Relationship Between Ignition Time, Absorbed Irradiance and Fabric Weight for Heavy Cotton Samples.

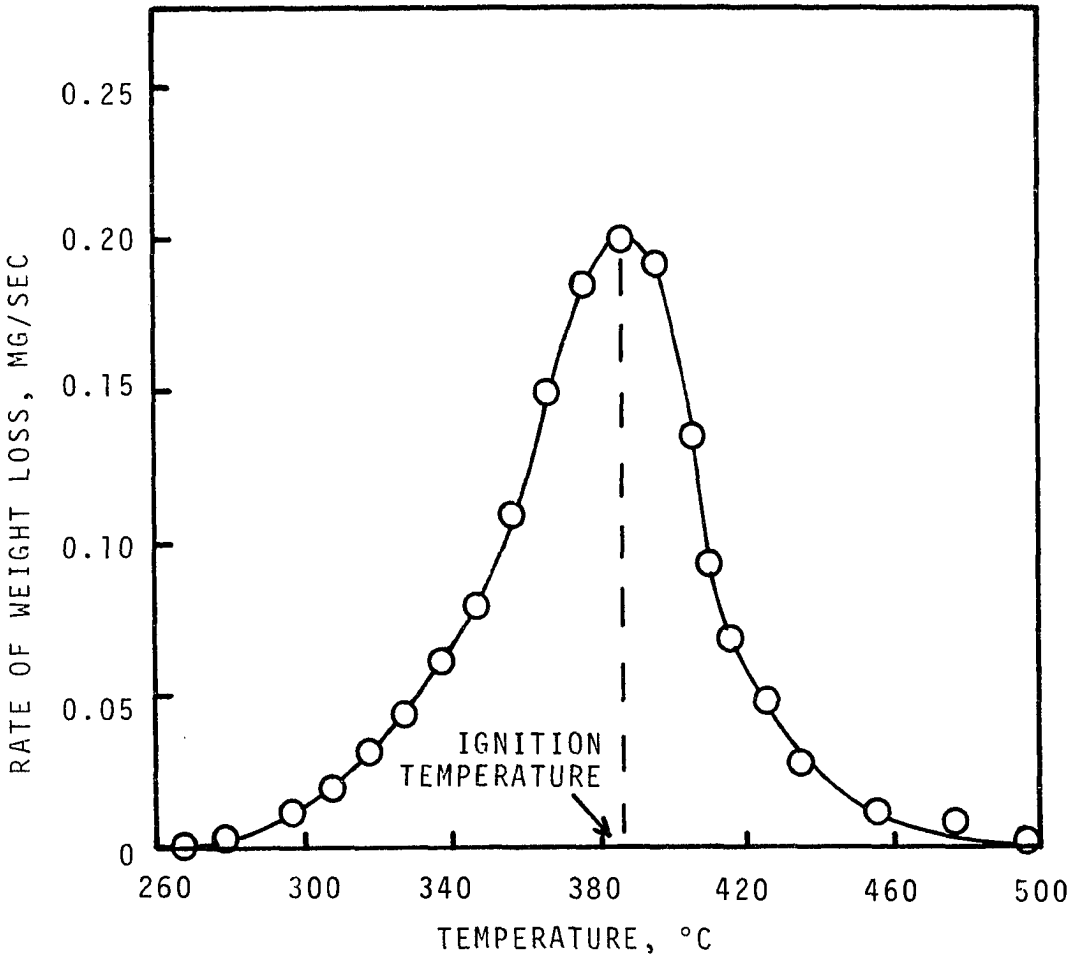

Figure IV-13. Typical DTG Curve for Heavy Cotton.

rate of weight loss is maximum. Table IV-2 gives the ignition temperature of different materials taken from their respective DTG plots.

TABLE IV-2

IGNITION TEMPERATURE OF MATERIALS

Material	Ignition Temperature, °C
Black cotton	360
White cotton	416
Rayon	400
Heavy cotton	386
α-cellulose	440
Filter paper	424
Acrylics	395
Black wool	410

Comparison of Ignition Data with the Ignition Models Available in Literature

The various ignition models available in the literature for thin materials are given in Chapter II. In this section a comparison is made between those models and the present ignition data (given in Appendix A). Equation II-9 gives Simms' (29) analytical solution for thin materials. In terms of absorbed irradiance it is

$$\frac{H_a t}{\rho c L \Delta T_m} = \frac{2ht/\rho cL}{1 - \exp(-2ht/\rho cL)} \qquad \text{(II-9)}$$

Simms assumed an arbitrary value of 8×10^{-4} cal/cm^2-sec-°C for the heat transfer coefficient h. This value is about three times higher than the values estimated by Alvares, et al. (3) and Wesson (40), derived from boundary layer theory. They report an average value of 2.8×10^{-4} cal/cm^2-sec-°C for heat transfer coefficient for the present experimental set-up. Figure IV-14 gives the comparison between the theoretical Equation II-9 and the experimental data. For ΔT_m the ignition temperatures from Table IV-2 have been used. From Figure IV-14 it can be seen that the curve obtained from the experimental data is approximately twice that of the theoretical curve predicted by Equation II-9. Figure IV-14 also has the disadvantage of having the variable t appearing in both ordinates. Any correlation of experimental data with the same major variable appearing in both ordinates is viewed with suspicion.

Next the ignition data is compared with Kanury's (15) model given by Equation II-11. In terms of absorbed irradiance it is

$$\frac{H_a^2 \alpha t}{K^2 (T-T_o)^2} = \frac{hL}{K} \left[\frac{H_a}{h(T-T_o)}\right]^2 \cdot \ln \left[\frac{1}{1-2h(T-T_o)/H_a}\right] \qquad \text{(II-11)}$$

Figure IV-15 gives the comparison of the experimental data with Equation II-11. The correlation of Figure IV-15 is poor and again the group $h(T-T_o)/H_a$ appears in both ordinates.

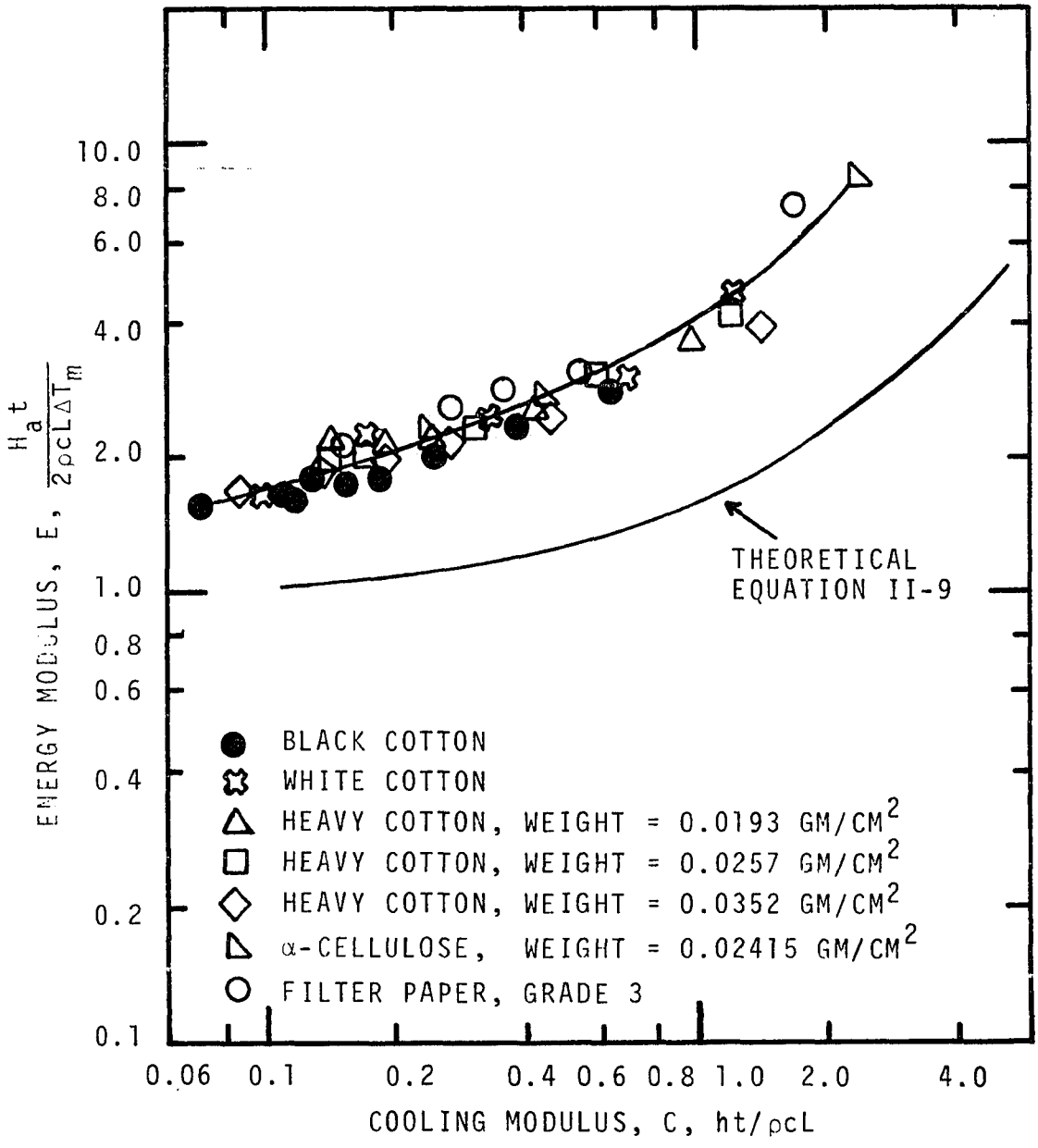

Figure IV-14. Comparison of Ignition Data with Equation II-8.

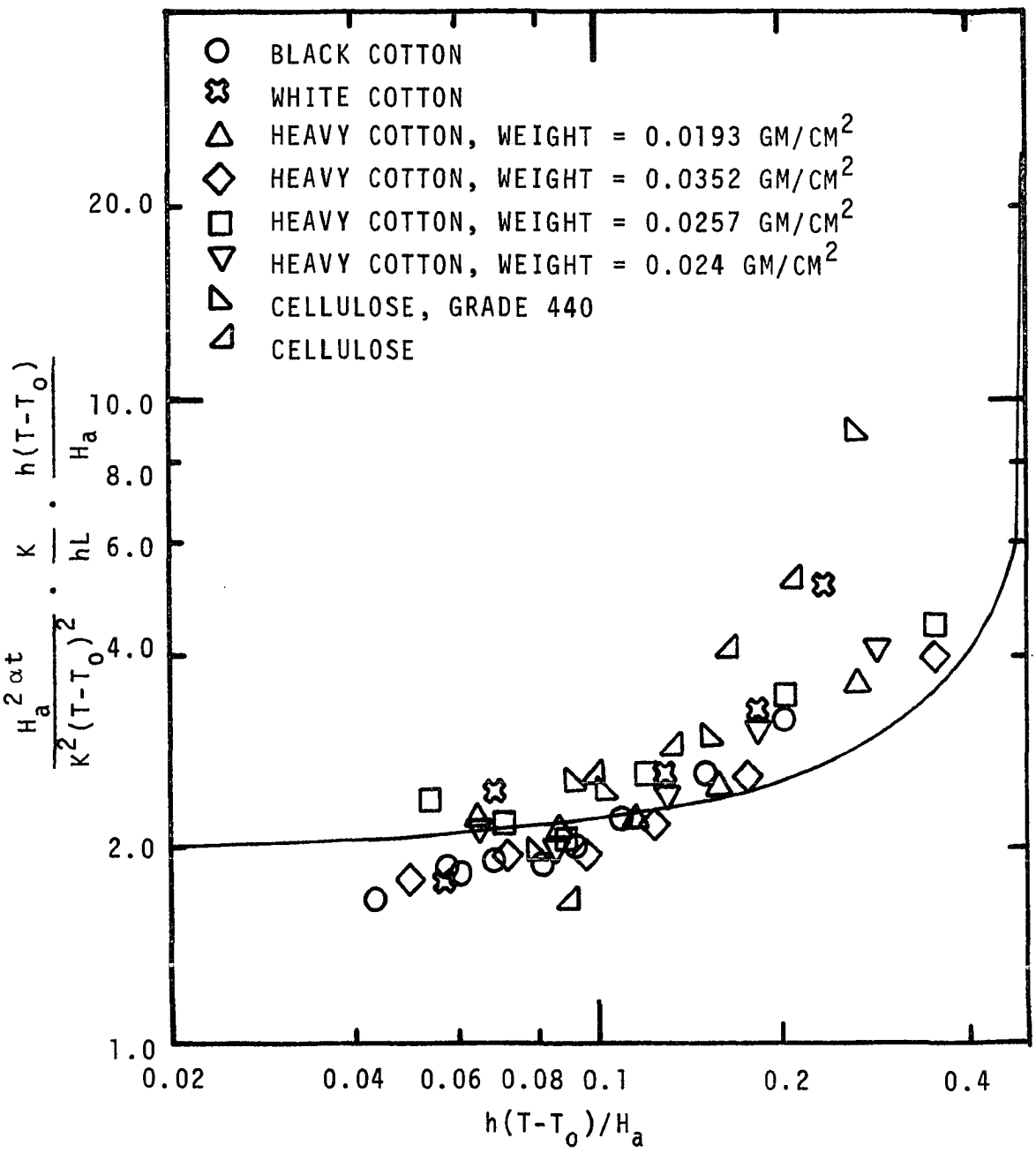

Figure IV-15. Comparison of Ignition Data with Equation II-11.

Andersen's (4) model is given by Equations II-19, II-20, II-21 and II-23. Figure IV-16 gives the comparison of the present data to Andersen's model. The curve in Figure IV-16 is the ignition time versus absorbed irradiance predicted by the model. From the figure it is evident that the model gives a poor correlation for piloted ignition time of cloth. Also Andersen, et al. (4) have assumed very arbitrary values for activation energy, frequency factor and heat of pyrolysis for cotton cloth.

Mathematical Analysis

The energy balance equation governing the ignition model is given by Equations II-3 and II-4. Neglecting the mass flow term in Equation II-3, the equations are given as

$$K \frac{\partial^2 T}{\partial x^2} + \gamma H_a e^{-\gamma x} = \rho c \frac{\partial T}{\partial t} + Q \frac{\partial \omega}{\partial t} \qquad \text{(IV-15)}$$

$$- \frac{\partial \omega}{\partial t} = f\omega \exp(-E/RT) \qquad \text{(II-4)}$$

The initial condition is $T = T_o$ and $\omega = \omega_o$ at $t = 0$. The boundary conditions are

$$x = 0 \text{ (front surface)}: \quad - K \frac{\partial T}{\partial x} = H_a - \varepsilon\sigma T^4 - h(T-T_0) \qquad \text{(IV-16)}$$

$$x = L \text{ (back surface)}: \quad - K \frac{\partial T}{\partial x} = \varepsilon\sigma T^4 + h(T-T_o) \qquad \text{(IV-17)}$$

By introducing the following dimensionless groups

$\bar{x} = x/L$; dimensionless distance

$\bar{t} = ft$; dimensionless time

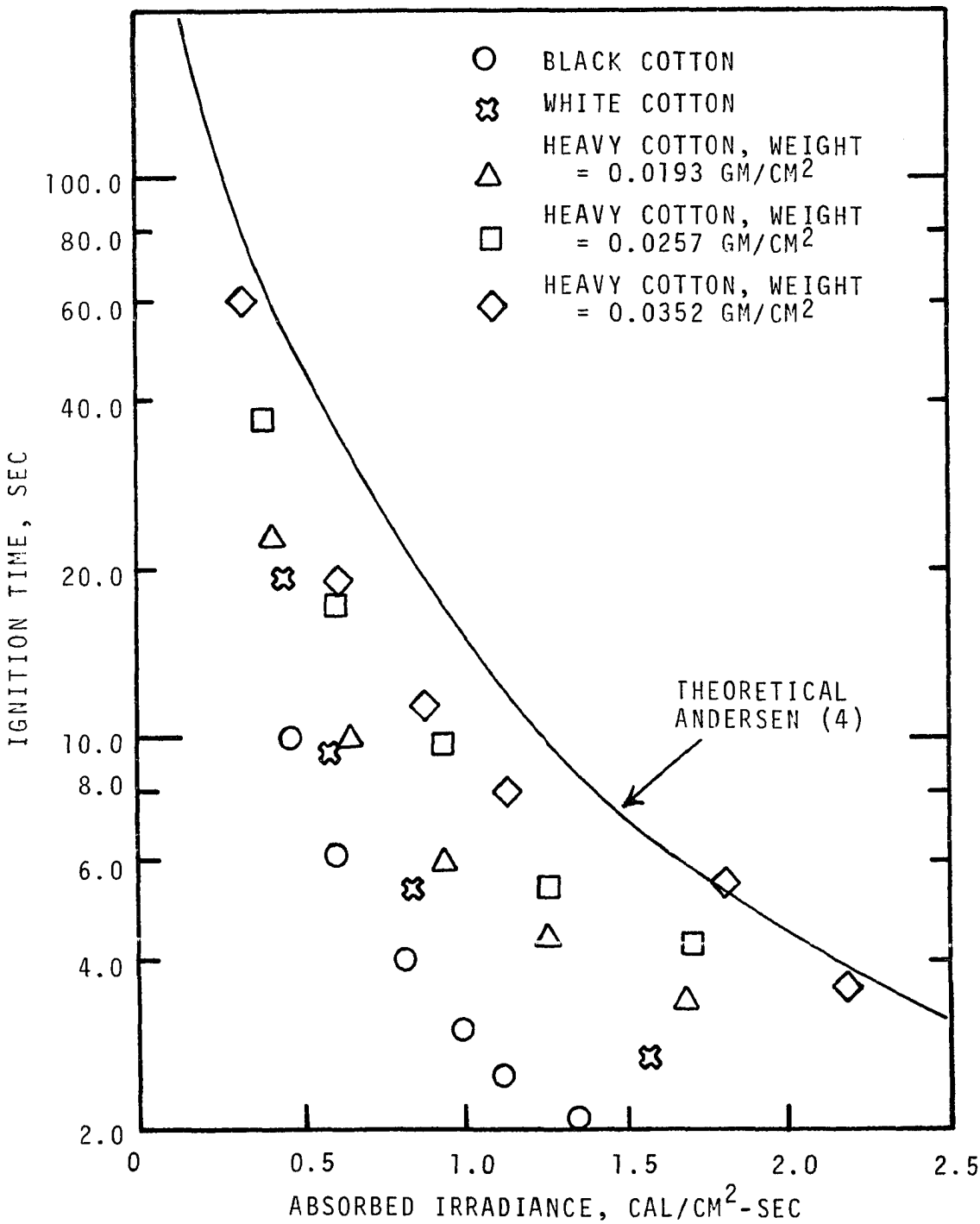

Figure IV-16. Comparison of Ignition Data with Andersen, et al. (4) Model.

$\bar{T} = RT/E$; dimensionless temperature

$\bar{\omega} = \omega/\omega_o$; dimensionless weight

Equations IV-15 and II-4 become

$$\frac{\alpha}{fL^2}\frac{\partial^2\bar{T}}{\partial\bar{x}^2} + \frac{\gamma H_a R}{\rho c f E} e^{-\gamma L\bar{x}} = \frac{\partial\bar{T}}{\partial\bar{t}} + \frac{QR\omega_o}{\rho c E}\frac{\partial\bar{\omega}}{\partial\bar{t}} \qquad \text{(IV-18)}$$

$$\frac{\partial\bar{\omega}}{\partial\bar{t}} = -\bar{\omega}\exp(-1/\bar{T}) \qquad \text{(IV-19)}$$

The initial condition is $\bar{T} = \bar{T}_o = RT_o/E$ and $\bar{\omega} = 1$ at $\bar{t} = 0$.

The boundary conditions become

$$\left.\frac{\partial\bar{T}}{\partial\bar{x}}\right|_{\bar{x}=0} = -\frac{H_a RL}{KE} + \frac{\varepsilon\sigma LT_o^3}{K}\left(\frac{\bar{T}^4}{\bar{T}_o^3}\right) + \frac{hL}{K}(\bar{T}-\bar{T}_o) \qquad \text{(IV-20)}$$

$$\left.\frac{\partial\bar{T}}{\partial\bar{x}}\right|_{\bar{x}=1} = -\frac{\varepsilon\sigma LT_o^3}{K}\left(\frac{\bar{T}^4}{\bar{T}_o^3}\right) - \frac{hL}{K}(\bar{T}-\bar{T}_o) \qquad \text{(IV-21)}$$

Hence the solution will be in the form

$$\frac{RT}{E} = \Phi\left[\frac{RT_o}{E}, \frac{x}{L}, ft, \frac{\alpha}{fL^2}, \frac{\gamma H_a R}{\rho c f E}, \frac{QR\omega_o}{\rho c E}, \frac{H_a RL}{KE}, \gamma L, \frac{hL}{K}, \frac{\varepsilon\sigma LT_o^3}{K}\right] \qquad \text{(IV-22)}$$

$$\bar{\omega} = \Phi\left[\frac{RT}{E}, ft\right]$$

Many simplifications of Equation IV-22 can be made. If the effect of diathermancy is neglected, the terms containing γ are omitted from the above equations. However, any groups that can be formed out of the excluded terms that do

not contain γ must be retained. Thus for opaque materials the terms γL and $\gamma H_a R/\rho cfE$ are excluded, but $H_a R/fE\rho cL$, their ratio is retained. Combining this ratio with the groups ft and RT/E the energy modulus $H_a t/\rho cLT$ is formed. Combining the group $H_a RL/KE$ with RT/E yields the irradiance modulus, $H_a L/KT$. It is the temperature rise, $(T - T_o)$, not the absolute value of T, which is the relevent parameter. Equation IV-22 for an opaque material in terms of energy modulus becomes

$$\frac{H_a t}{\rho cL(T-T_o)} = \Phi \left[\frac{\alpha t}{L^2}, \frac{QR\omega_o}{\rho cE}, \frac{H_a L}{K(T-T_o)}, \frac{hL}{K}, \frac{\varepsilon\sigma T_o^3}{K}\right] \qquad \text{(IV-24)}$$

If the material is inert, the terms containing Q, E, R and f must be deleted. Then Equation IV-24 becomes

$$\frac{Hat}{\rho cL\Delta T} = \Phi \left[\frac{\alpha t}{L^2}, \frac{H_a L}{K\Delta T}, \frac{hL}{K}, \frac{\varepsilon\sigma LT_o^3}{K}\right] \qquad \text{(IV-25)}$$

Equation IV-25 is the general dimensionless form for an inert, opaque material. The equation can further be reduced depending on the stipulated boundary conditions. Also it can be seen that the energy modulus is equal to the product of the irradiance modulus and Fourier modulus, $\alpha t/L^2$. So Equation IV-25 can be rewritten as

$$\frac{H_a L}{K\Delta T} = \Phi \left[\frac{\alpha t}{L^2}, \frac{hL}{K}, \frac{\varepsilon\sigma LT_o^3}{K}\right] \qquad \text{(IV-26)}$$

If the convection and radiation losses are neglected, the boundary conditions given by Equations IV-16 and IV-17 become

$$-K \left.\frac{\partial T}{\partial x}\right|_{x=0} = H_a \qquad \text{(IV-27)}$$

$$\left.\frac{\partial T}{\partial x}\right|_{x=L} = 0 \qquad \text{(IV-28)}$$

The solution will be of the form

$$\frac{H_a L}{K\Delta T} = \Phi\ [\alpha t/L^2] \qquad \text{(IV-29)}$$

The surface temperature rise for the above case is given by Carslaw and Jaeger (9) as

$$\frac{\Delta T_s K}{H_a L} = \frac{\alpha t}{L^2} + \frac{1}{3} - \frac{2}{\pi^2} \sum_{n=1}^{\infty} \frac{1}{n^2}\, e^{-(n^2\pi^2\alpha t)/L^2} \qquad \text{(IV-30)}$$

The solutions given by Equation IV-30 and Equation IV-4 are the same. They have been written in different forms. Figure IV-17 gives the correlations of ignition data based on these moduli. The curve given below the ignition data is predicted by Equation IV-30. The correlation shown in Figure IV-17 does not show any marked tendency to bend as predicted by the theoretical curve. The line drawn through the data plotted in Figure IV-17 was found by regression analysis. It is

$$\left(\frac{\alpha t}{L^2}\right)^{1/2} = 1.464\ \left(\frac{H_a L}{\Delta T_s K}\right)^{-0.781} \qquad \text{(IV-31)}$$

with a correlation coefficient of 0.971 and an error of estimate of 0.172. The data points will approach the theoretical curve more closely if the convective and reradiation losses can be accounted for in the absorbed irradiance term. These

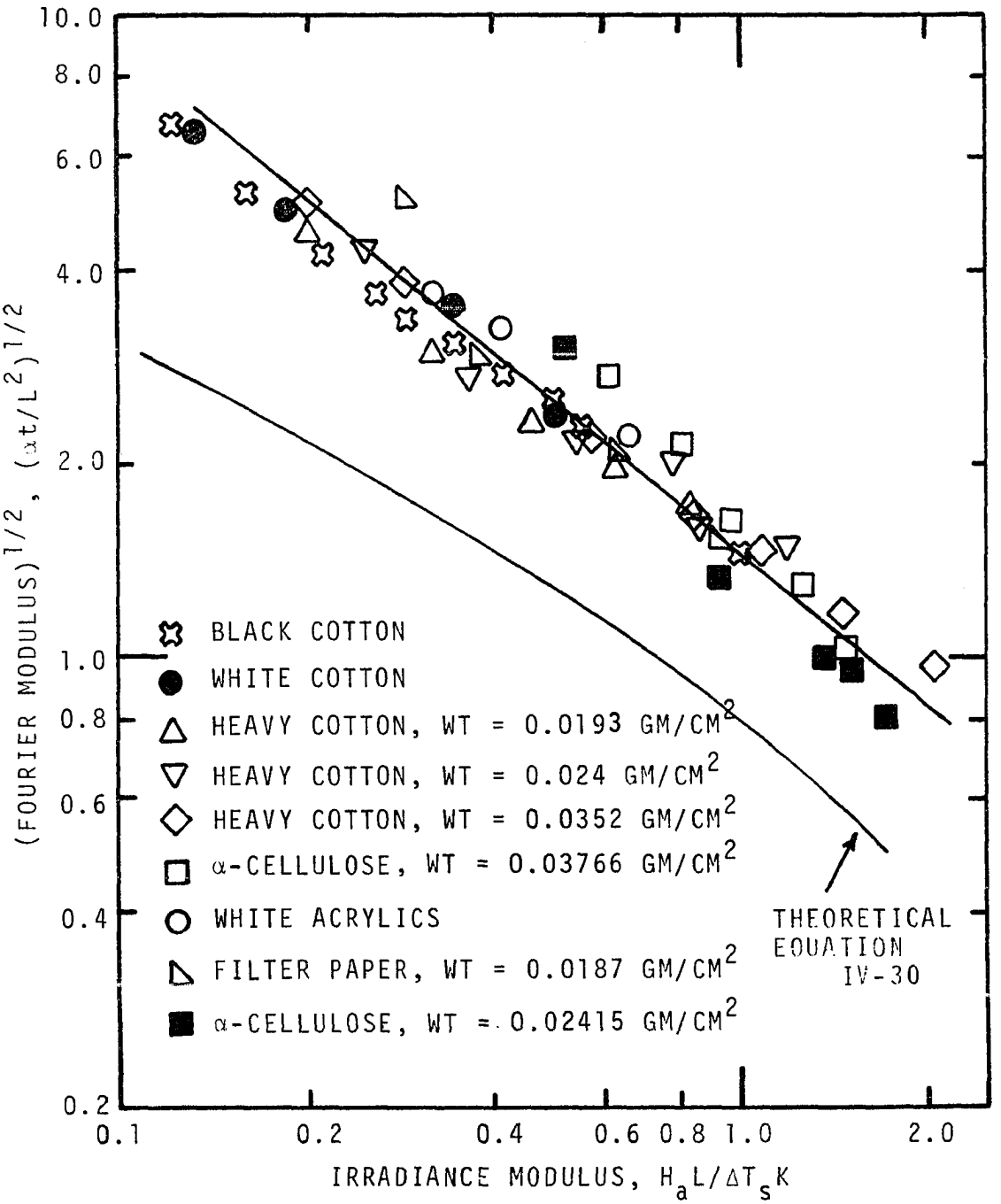

Figure IV-17. Correlation of Ignition Data Based on Equation IV-29.

losses can be obtained by integrating the temperature profiles of the materials subjected to irradiation. Right now such temperature profiles are not available for the materials tested in the present work.

In order to study the effects of Biot number hL/K and radiation number $\varepsilon\sigma T_o^3 L/K$, the functional form of Equation IV-26 was subjected to regression analysis and the following correlation was obtained.

$$\left(\frac{\alpha t}{L^2}\right)^{1/2} = 1.813 \left(\frac{H_a L}{\Delta T_s K}\right)^{-0.788} \left(\frac{hL}{K}\right)^{0.136} \left(\frac{\varepsilon\sigma T_o^3 L}{K}\right)^{-0.05} \qquad \text{(IV-32)}$$

with a correlation coefficient of 0.973 and an error of estimate of 0.126. Figure IV-18 is a plot of $(\alpha t/L^2)^{1/2}$ versus $(H_a L/\Delta T_s K)(hL/K)^{-0.173}(\varepsilon\sigma T_o^3 L/K)^{0.063}$. As the coefficients on hL/K and $\varepsilon\sigma T_o^3 L/K$ are small, the relation given by Equation IV-32 is no better than IV-31. This conclusion is further evident by comparing Figures IV-17 and IV-18. The scatter in data of Figure IV-18 is no better than that of Figure IV-17. Thus, the effects of Biot number hL/K and radiation number $\varepsilon\sigma T_o^3 L/K$ can be neglected.

General Correlation of Ignition Data

From Figure IV-17 it can be seen that though the data points do not follow the theoretical curve, they can be correlated into a single correlation using the one-dimensional model. This conclusion is further validated from the section on the minimum incident irradiance for piloted ignition. So

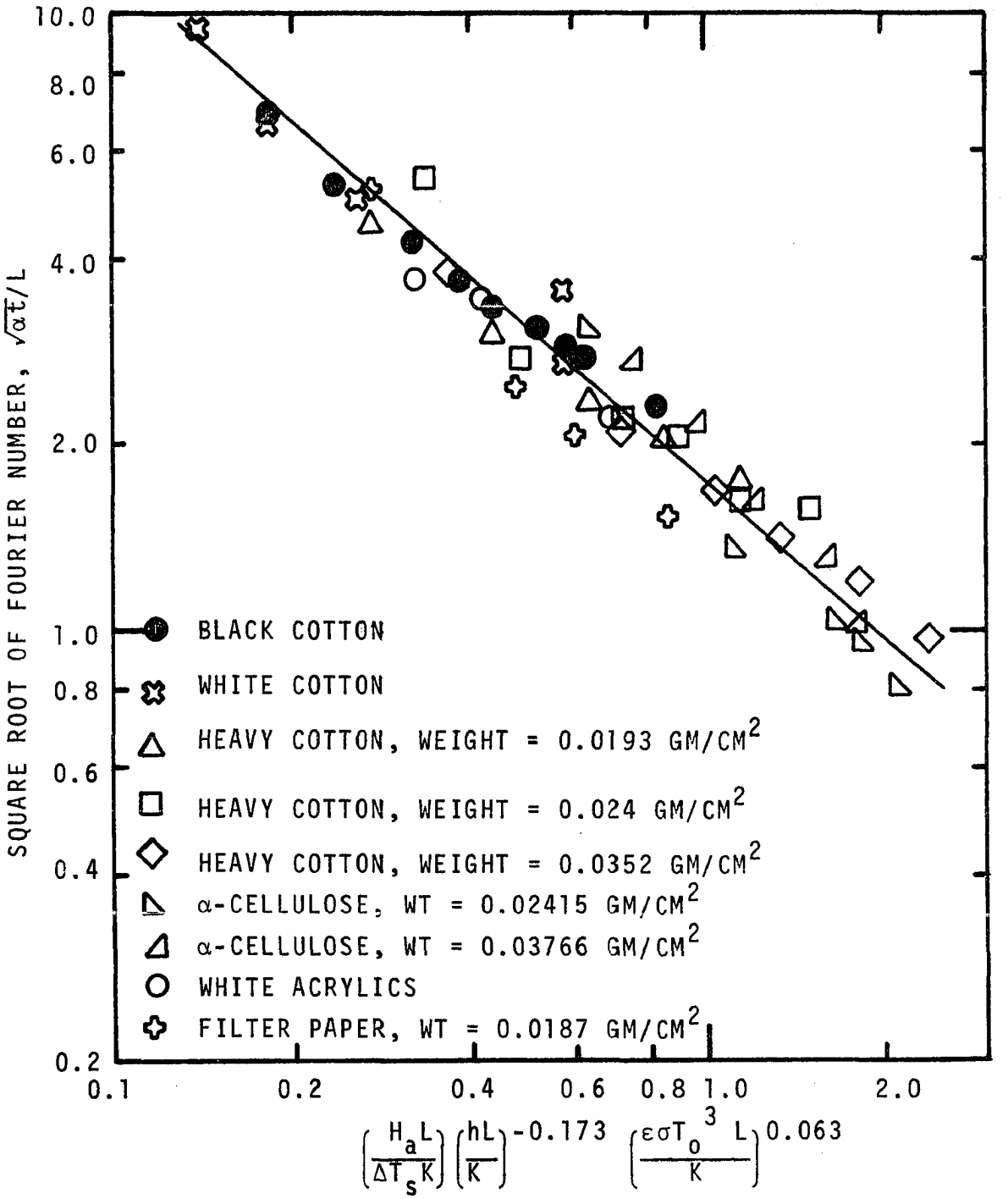

Figure IV-18. Correlation of Ignition Data Based on Equation IV-32.

the one-dimensional model given by Equation IV-1 with boundary conditions given by Equations IV-2 and IV-3 is satisfactory for thin materials. The solution is given by Equation IV-4. It is

$$\Delta T_s = \frac{2\alpha_{av} H_i t^{1/2}}{(K\rho c)^{1/2}} \sum_{n=0}^{\infty} \text{ierfc} \frac{2nL}{2(\alpha t)^{1/2}} + \text{ierfc} \frac{(2n+2)L}{2(\alpha t)^{1/2}} \qquad \text{(IV-4)}$$

Equation IV-4 can be rewritten in the functional form

$$\alpha_{av} H_i \sqrt{t} = \Phi \left[\Delta T_s, (K\rho c)^{1/2}, \text{erf } (L/\sqrt{\alpha t})\right] \qquad \text{(IV-33)}$$

where erf $(L/\sqrt{\alpha t})$ is used for convenience instead of ierf $(L/\sqrt{\alpha t})$. In the present analysis the effect of specific heat c has been neglected, as there is little variation in c for materials tested. As in the case of woods, the thermal conductivity, K, is assumed to be dependent on the density ρ (40). The density in turn is dependent on the weight per unit area, w, of the material. The effect of weight as a parameter has been discussed in a previous section. The function erf $(L/\sqrt{\alpha t})$ takes care of the effects of thickness of the material. So Equation IV-33 can be modified as

$$t_{ig} = \Phi \left[H_a, w, \Delta T_s, \text{erf } (1/\sqrt{F})\right] \qquad \text{(IV-34)}$$

Equation IV-34 relates the ignition time to the absorbed irradiance, weight per unit area of the material, the surface ignition temperature rise, and the Fourier Modulus. Based on Equation IV-34 the ignition data obtained were subjected to a linear regression analysis to yield the expression

$$t_{ig} = 1.11 \times 10^{-8} \frac{w^{1.42} \Delta T_s^{4.2}}{H_a [\text{erf}(1/\sqrt{F})]^{0.92}} \qquad \text{(IV-35)}$$

with a correlation coefficient of 0.981 and an error of estimate of 0.217. Figure IV-19 is the plot of experimental ignition time versus calculated ignition time obtained from Equation IV-35. A "95 percent confidence limits" have been drawn and from the figure it can be seen that most of the data points lie within the 95 percent limits. The ignition time is plotted against $H_a \text{ erf}(1/\sqrt{F})/w^{1.5}\Delta T_s^{4}$ as absorbed irradiance, H_a, is the primary independent variable. Figure IV-20 is the plot of ignition time versus $H_a \text{ erf}(1/\sqrt{F})/w^{1.5}\Delta T_s^{4}$.

From Figures IV-19 and IV-20 it is evident that the correlation given by Equation IV-35 is fairly good. Only the data points of α-cellulose with weight 0.02415 gm/cm^2, some of the filter paper, white acrylics and black wool lie much above the general grouping of data. The reason why the white acrylics and wool data lie far above the line may be because of the fact that the thermal properties were not accurately known.

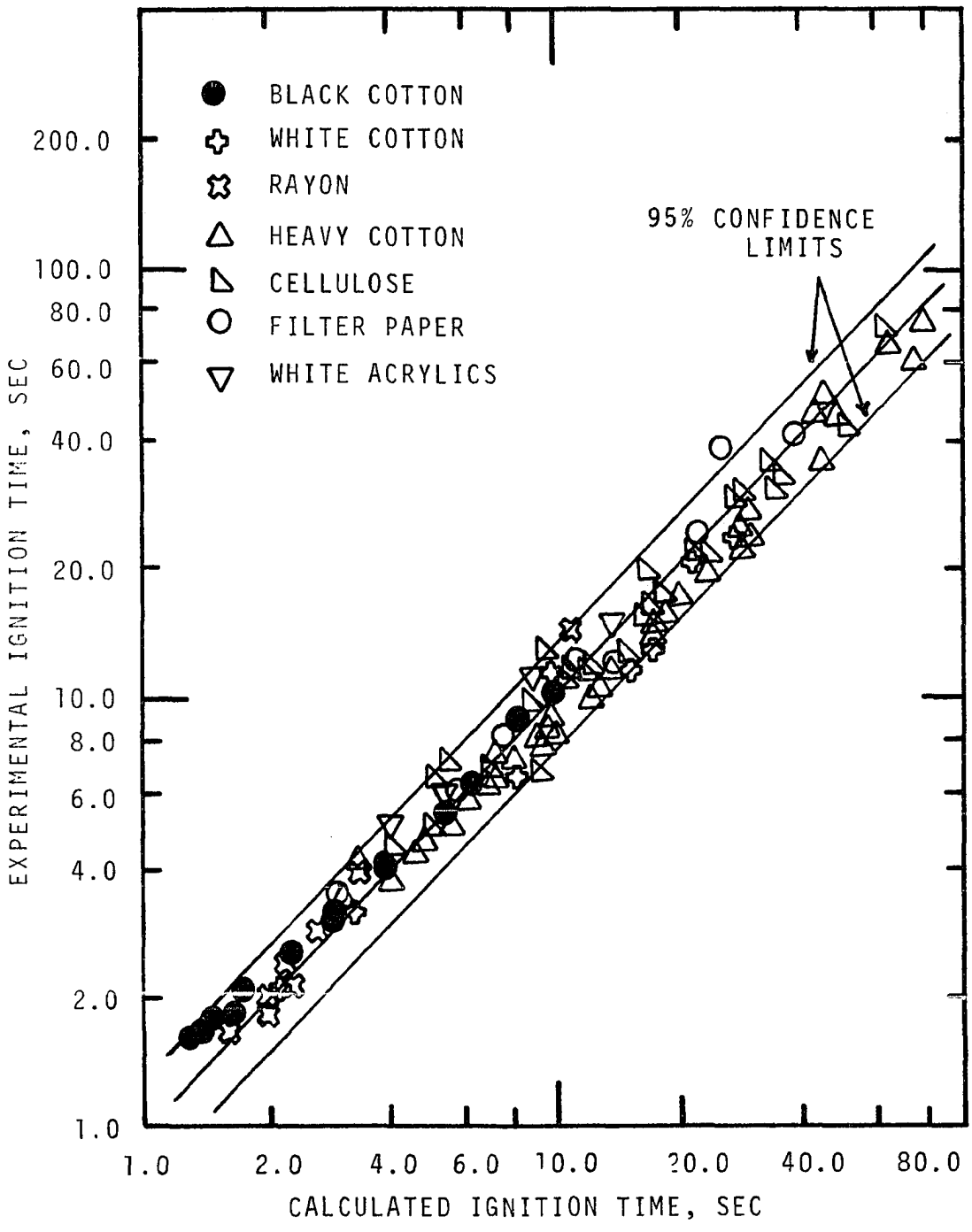

Figure IV-19. The Deviation of Calculated Ignition Time from Experimental Ignition Time.

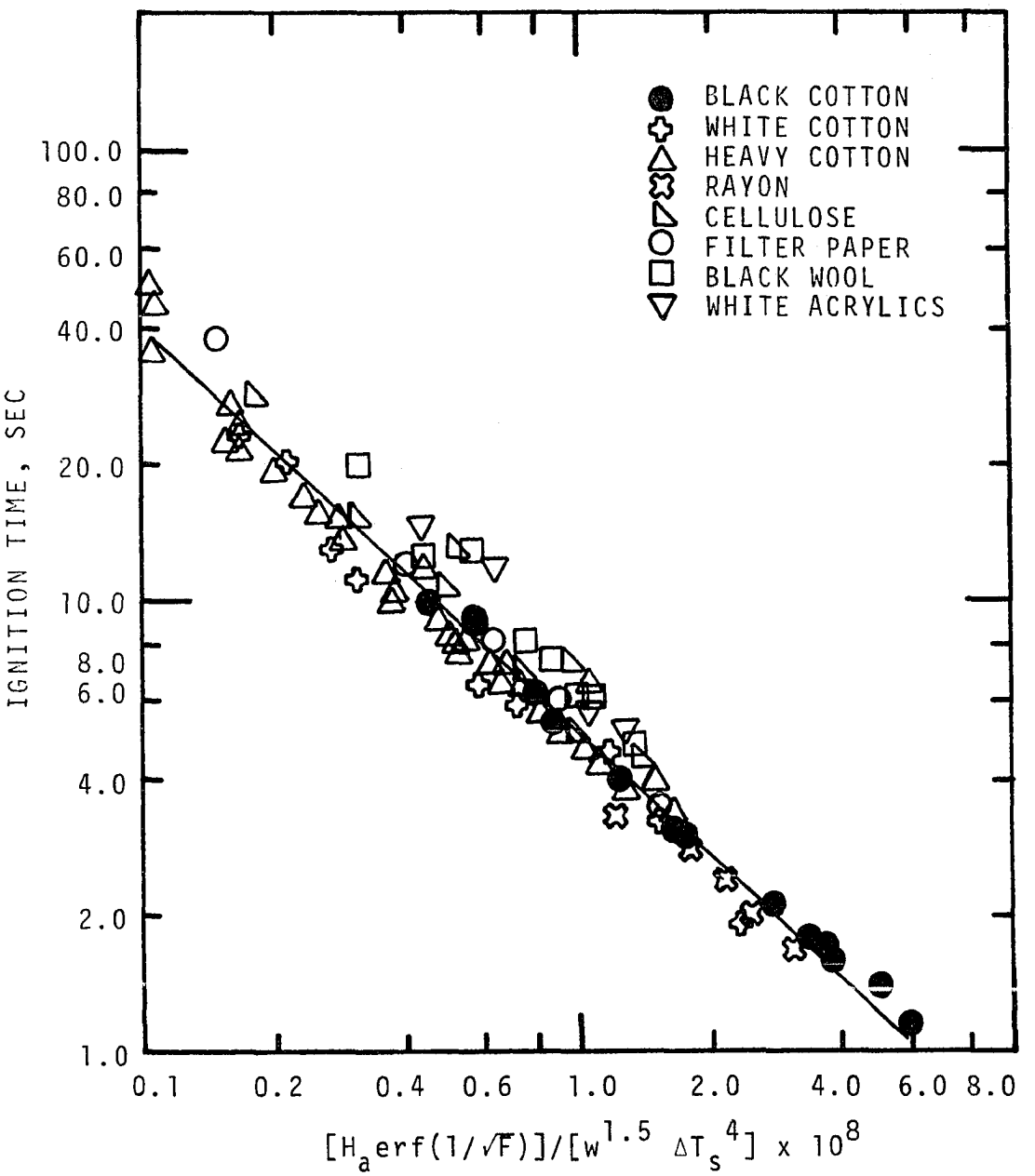

Figure IV-20. Correlation of Ignition Data Using Initially Absorbed Irradiance Corrected for Weight, Ignition Temperature and Thickness Effects.

CHAPTER V

CONCLUSIONS

In this investigation the piloted ignition characteristics of thin materials like cotton, rayon, α-cellulose, acrylics and wool were studied. The ignition data were obtained using benzene flames and 1000-watt tungsten lamps as radiant heat sources. From the analysis of the data the following conclusions have been arrived at.

1. A plot of incident irradiance versus reciprocal of ignition time gives a straight line. By extrapolating the line to Y-axis where $1/t = 0$ (i.e., $t = \infty$) the minimum incident irradiance below which ignition will not occur can be found.
2. For fabrics of the same density, the ignition time increases for a particular incident irradiance as fabric weight per unit area increases. The ignition time can be correlated as a function of incident irradiance and fabric weight per unit area.
3. The ignition time depends on the spectral distribution of the incident radiant energy. The ignition data obtained by flame radiation and tungsten lamp radiation can

be reduced to a single correlation by plotting absorbed irradiance versus ignition time instead of incident irradiance. The absorbed irradiance is given by Equation II-31.

4. A comparison of the present data with the ignition models available in literature reveal that those models do not provide for very good correlation of the data.
5. A dimensional analysis of one dimensional model for an opaque and inert material reveals that the groups controlling the ignition phenomena in the case of thin materials are irradiance modulus $H_a L/\Delta T_s K$ and Fourier Modulus $\alpha t/L^2$. The data can be correlated by these groups.
6. The ignition data can be correlated through the use of a model based on an inert, opaque solid with constant and uniform properties. The data can be correlated by the expression

$$t_{ig} = 1.11 \times 10^{-8} \frac{w^{1.42} \Delta T_s^{4.2}}{H_a [\text{erf}(1/\sqrt{F})]^{0.92}} \qquad \text{(IV-35)}$$

Equation IV-35 reveals the following:

a. The piloted ignition time is inversely proportional to the absorbed irradiance.
b. The effect of sample thickness is accounted for by the error function of the Fourier Modulus. The ignition time is approximately inversely proportional to the error function term.

c. The ignition time is proportional to the fourth power of the temperature difference term. The reason for such a high exponent may be because of the fact that the ignition temperatures of the materials are close together.

d. The ignition time is proportional to the 1.5 power of the weight per unit area term.

BIBLIOGRAPHY

1. Akita, K. "Studies on the Mechanism of Ignition of Wood." Fire Research Abs. and Rev., 4, 109 (1962.)

2. Alvares, N. J. "Measurement of the Temperature of the Thermally Irradiated Surface of Alpha Cellulose." USNRDL-TR-735 (1964).

3. Alvares, N. J.; Blackshear, P. L.; and Kanury, A. M. "The Influence of Free Convection on the Ignition of Vertical Cellulosic Panels by Thermal Radiation." Comb. Sci. and Tech., 1, 407 (1970).

4. Andersen, W. H.; Carpenter, G. E.; Garfinkle, D. R.; and Brown, R. D. "Evaluation Techniques for Flame and Incendiary Agents." Report No. SHI-6005-5 (1968).

5. Bamford, C. H.; Crank, J.; and Malan, D. H. "The Combustion of Wood--Part I." Proc. of Cambridge Philos. Soc., 42, 166 (1946).

6. Brown, C. R. "Determination of the Ignition Temperatures of Solid Materials." Fuel, 14, 14 (1935).

7. Brown, L. E. "An Experimental and Analytical Study of Wood Pyrolysis." Unpublished Ph.D. dissertation. University of Oklahoma, Norman, Oklahoma, 1972.

8. Buschmann, A. J., Jr. "Ignition of Some Woods Exposed to Low Level Thermal Radiation." NBS Project No. 1002-11-10427, July 26, 1961.

9. Butler, C. P.; Martin, S. B.; and Lai, W. "Thermal Radiation Damage to Cellulosic Materials--Part II. Ignition of Alpha Cellulose by Square Wave Exposure." USNRDL Tech. Report-135, NS 081-001, AFSWP-906 (1956).

10. Carslaw, H. S., and Jaeger, J. C. Conduction of Heat in Solids. 2nd ed. London: Oxford University Press, 1959.

11. Deverall, L. I., and Lai, W. "A Criterion for Thermal Ignition of Cellulosic Materials." Comb. and Flame, 13, 8 (1969).

12. Goldsmith, A.; Waterman, T. E.; and Hirschorn, H. J. Handbook of Thermophysical Properties of Solid Materials. Armour Research Foundation. New York: Macmillan Co., 1961.

13. Hallman, J. R. "Ignition Characteristics of Plastics and Rubber." Unpublished Ph.D. dissertation. University of Oklahoma, Norman, Oklahoma, 1971.

14. Havens, J. A. "Thermal Decomposition of Wood." Unpublished Ph.D. dissertation. University of Oklahoma, Norman, Oklahoma, 1969.

15. Kanury, A. M. "Ignition of Cellulosic Solids--A Review." Tech. Report, FMRC Serial No. 19721-7, November 1971.

16. Koohyar, A. N. "Ignition of Wood by Flame Radiation." Unpublished Ph.D. dissertation. University of Oklahoma, Norman, Oklahoma, 1967.

17. Lawson, D. I., and Simms, D. L. "The Ignition of Wood by Radiation." Brit. J. Appl. Phys., 3, 288 (1952).

18. Lee, B. T., and Alvares, J. J. "The Effect of Irradiance on the Ignition and the Rate of Fire Spread Along Composite Cellulosic Materials." Spring meeting, Western States Section, The Combustion Institute, La Jolla, California, April 1967.

19. Lipska, A. E., and Parker, W. J. "Kinetics and Pyrolysis of Cellulose over the Temperature Range 250-300°C." USNRDL, Report No. WSCI-66-22 (1966).

20. MacHattie, L. E. "Temperature Measurement of Textile Fabrics under Intense Thermal Irradiation." Brit. J. Appl. Phys., 14, 267 (1963).

21. Martin, S. "Diffusion Controlled Ignition of Cellulosic Materials by Intense Radiant Energy." Tenth Symposium (International) on Combustion, 877 (1965).

22. Martin, S. B. "The Mechanism of Ignition of Cellulosic Materials by Intense Thermal Radiation." USNRDL-TR-102 NS 081-001, AFSWP-779 (1956).

23. Martin, S. "Simple Radiant Heating Method for Determining the Thermal Diffusivity of Cellulosic Materials." J. Appl. Phys., 31, 1101 (1960).

24. Monahan, T. I.; deLhery, G. R.; and Derksen, W. "Research Report on the Spectral Reflectance and Transmittance of Standard Fabrics for Thermal Radiation Effects Studies." Lab Proj. 5046-3, Part 91, Final Report NS 081-001, AW-9, AFSWP 957, Naval Materials Lab (1956).

25. Muir, W. E. "Studies of Fire Spread Between Buildings." Unpublished Ph.D. dissertation. University of Saskatchwan (1967).

26. Murty, K. A., and Blackshear, P. L. "An X-Ray Photographic Study of the Reaction Kinetics of Alpha Cellulose Decomposition." Pyrodynamics, 4, 285 (1966).

27. Perry, J. H. Chemical Engineers' Handbook. 4th ed. New York: McGraw-Hill Book Company, 1963.

28. Ryan, L. R.; Penzias, G. J.; and Tourin, R. H. "An Atlas of Infrared Spectra of Flames. Part I. Infrared Spectra of Hydrocarbon Flames in the 1-5μ Region." Scientific Report No. 1, Contract AF 19(604)-6106, July 1961.

29. Sauer, F. M. "The Charring of Wood During Exposure to Thermal Radiation." AFSWP-868 (1956).

30. Simms, D. L. "Damage to Cellulosic Solids by Thermal Radiation." Comb. and Flame, 6, 303 (1962).

31. Simms, D. L. "The Correlation of Ignition Time with the Physical Properties of Materials." Fire Research Note No. 319 (1958).

32. Simms, D. L. "On the Piloted Ignition of Wood by Radiation." Comb. and Flame, 7, 253 (1963).

33. Simms, D. L. "Ignition of Cellulosic Materials by Radiation." Comb. and Flame, 4, 293 (1960).

34. Smith, W. K. "Ignition of Materials by Radiant Heat." Naval Weapons Center Tech. Note 40604-8 (1968).

35. Smith, W. K., and Schilberg, L. E. "Surface Temperature History of Materials During Radiant Heating to Ignition." Technical Note 40604-9, Naval Weapons Center (1969).

36. Tang, W. K., and Neill, W. K. "Effect of Flame Retardants on Pyrolysis and Combustion of Alpha Cellulose." Jour. of Polymer Science, C, 65 (1964).

37. Varma, A., and Steward, F. R. "Spontaneous Ignition of High Voidage Cellulosic Materials." J. Fire and Flammability, 1, 154 (1970).

38. Welker, J. R. "The Pyrolysis and Ignition of Cellulosic Materials: A Literature Review." J. Fire and Flammability, 1, 12 (1970).

39. Welker, J. R.; Wesson, H. R.; and Sliepcevich, C. M. "Ignition of Alpha-Cellulose and Cotton Fabric by Flame Radiation." Fire Technology, 5, 59 (1969).

40. Wesson, H. R. "The Piloted Ignition of Wood by Radiant Heat." Unpublished Ph.D. dissertation. University of Oklahoma, Norman, Oklahoma, 1970.

APPENDICES

APPENDIX A

SUMMARY OF IGNITION DATA

A summary of the ignition data for the materials tested in the present work is given in Table A-1. The weight and thickness of samples tested are also given.

TABLE A-1

SUMMARY OF IGNITION DATA

Material	Benzene Flame H_i cal/cm^2-sec	Benzene Flame t sec	Tungsten Lamps H_i cal/cm^2-sec	Tungsten Lamps t sec
Black cotton	0.625	10	0.68	9
Weight =	0.825	6.2	0.82	5.4
0.01328 gm/cm^2	1.1	4.0	1.175	3.1
Thickness =	1.33	3.0	1.63	1.85
0.01524 cm	1.5	2.5	2.0	1.65
	1.81	2.1	2.375	1.40
	2.02	1.8		
	2.15	1.7		
	2.84	1.15		
White cotton	0.66	23.4	0.95	*
Weight =	0.82	11.4	1.28	20.5
0.01328 gm/cm^2	1.16	6.5	1.45	13
Thickness =	2.16	3.2	1.74	9.9
0.01524 cm	2.64	1.9	2.33	5.9
			3.3	4.45
Black wool	0.62	*	0.92	*
Weight =	1.01	*	1.28	15
0.0252 gm/cm^2	1.41	12.0	1.74	13
Thickness =	2.0	8.0	2.27	6.8
0.0361 cm	2.44	6.2	2.52	6.45
	3.04	4.85	3.52	4.7

*No ignition.

TABLE A-1--Continued

Material	Benzene Flame H_i cal/cm^2-sec	Benzene Flame t sec	Tungsten Lamps H_i cal/cm^2-sec	Tungsten Lamps t sec
Black Rayon	0.68	*	0.82	*
Weight	0.9	*	1.4	*
= 0.00678 gm/cm^2	1.3	*	1.8	8.25
Thickness	1.5	3.3	2.52	4.0
= 0.0056 cm	2.24	2.4	3.26	2.2
	3.33	2.0	3.7	1.0
	2.08	2.9		
White acrylics	0.76	*	0.9	*
Weight	1.18	*	1.22	46
= 0.0253 gm/cm^2	1.57	14.75	1.74	22
Thickness	2.04	12.0	2.94	13.3
= 0.036 cm	2.5	5.9	3.3	9.0
	3.28	5.1		
White rayon	0.86	*	0.87	*
Weight	1.1	14.5	1.41	*
= 0.00573 gm/cm^2	1.7	2.5	1.7	16.25
Thickness	2.21	2.15	2.12	8
= 0.0051 cm	2.38	1.85	2.55	4.6
	2.72	1.7	3.11	3.4
Heavy cotton	0.5625	23	0.38	*
Thread count 48 x 60	0.9	10	0.65	*
Weight	1.3	6	0.8	46
= 0.0193 gm/cm^2	1.75	4.4	0.91	27
Thickness	2.325	3.4	1.2	15
= 0.03455 cm			1.65	8.4
			1.9	7.25
			2.375	5.05
Heavy cotton	0.5625	22	0.675	*
Thread count 48 x 56	0.925	12.5	0.88	33
Weight	1.4	5.9	0.8	56
= 0.02027 gm/cm^2	1.7	4.2	1.15	17.5
Thickness	2.15	3.9	1.475	11.8
= 0.0358 cm	2.65	3.5	1.98	7.25
			2.34	6.5

*No ignition.

TABLE A-1--Continued

Material	Benzene Flame H_i cal/cm^2-sec	Benzene Flame t sec	Tungsten Lamps H_i cal/cm^2-sec	Tungsten Lamps t sec
Heavy cotton	0.425	41	0.675	71
Thread count 48 x 50	0.7375	18.5	0.71	51.5
Weight	1.2125	8.5	0.825	47
= 0.02165 gm/cm^2	1.6875	4.8	1.06	20.75
Thickness	2.15	4.0	1.375	12.6
= 0.0394 cm	2.85	3.3	1.7	9.8
			2.05	7.45
			2.375	6.0
Heavy cotton	0.5625	50	0.63	*
Thread count 48 x 44	0.825	13.5	0.7	66
Weight	1.2125	8.5	0.775	45
0.024 gm/cm^2	1.925	4.7	1.0	23.9
Thickness	1.525	7.4	1.275	15.5
= 0 0432 cm	2.65	4.05	1.6	10.55
			1.9	9.05
			2.3	6.55
Heavy cotton	0.525	37	0.65	84
Thread count 48 x 40	0.825	17.5	0.75	52.5
Weight	1.1625	9.8	0.8375	45
= 0.0257 gm/cm^2	1.75	5.4	1.025	25.5
Thickness	2.35	4.3	1.3	15.8
= 0.04575 cm			1.6	10.8
			1.95	8.3
			2.375	6.2
Heavy cotton	0.425	58	0.61	*
Thread count 48 x 34	0.975	13.25	0.675	78
Weight	1.35	9.3	0.84	38.5
= 0.02875 gm/cm^2	1.75	5.7	1.15	19
Thickness = 0.0559 cm	2.375	4.25	1.575	12.6
			1.975	8.75
			2.325	7.75
Heavy cotton	0.425	60	0.585	*
Thread count 48 x 28	0.85	19.5	0.7	73
Weight	1.225	11.5	0.9	35.5
= 0.0352 gm/cm^2	1.575	8.0	1.125	23.25
Thickness	2.15	5.8	1.48	17
= 0.0655 cm	3.025	3.8	1.96	10
			2.48	7.8

*No ignition.

TABLE A-1--Continued

Material	Benzene Flame H_i cal/cm^2-sec	Benzene Flame t sec	Tungsten Lamps H_i cal/cm^2-sec	Tungsten Lamps t sec
Cellulose, Grade-440	0.6	68	0.675	*
Weight	1.06	13	0.75	171
= 0.02415 gm/cm^2	1.575	7.2	1.025	46.5
Thickness	1.725	6.75	1.38	19
= 0.0874 cm	2.0	4.5	1.75	12.4
			2.44	8.4
Cellulose, Grade-450	0.65	77	0.75	*
Weight	0.95	15.5	0.8	173
= 0.02825 gm/cm^2	1.225	11.8	1.175	29
Thickness	1.35	11.0	1.61	19.8
= 0.0704 cm	1.72	6.8	1.98	11.5
	2.15	5.0	2.4	9.85
Cellulose, Grade-300	0.725	94	0.83	136
Weight	0.85	35.5	0.9	102
= 0.03675 gm/cm^2	1.17	23.8	1.225	33
Thickness	1.46	12.6	1.55	21.4
= 0.0817 cm	1.725	8.45	1.925	15.2
	2.1	5.65	2.46	10.35
Cellulose, Grade-317	0.75	50	0.75	190
Weight	0.95	30.5	0.95	72
= 0.03766 gm/cm^2	1.17	17.6	1.25	31
Thickness	1.58	11.5	1.65	20.8
= 0.0838 cm	1.76	6.7	2.025	12.7
			2.46	10.8
Filter paper, Grade-1	0.475	*	0.925	*
Weight	0.55	*	1.125	55
= 0.00865 gm/cm^2	0.85	14.75	1.375	25
Thickness	1.185	4.4	1.675	12
= 0.01675 cm	1.45	3.3	1.875	11.4
	2.09	2.2	2.4	5.15
Filter paper, Grade-3	0.6	*	0.88	78
Weight	0.725	38	1.0	64
= 0.0187 gm/cm^2	0.975	12	1.25	24
Thickness	1.3	8.2	1.575	15.4
= 0.0381 cm	1.61	6.1	1.875	11.2
	2.35	3.35	2.425	7.0

*No ignition.

TABLE A-1--Continued

Material	Benzene Flame H_i cal/cm^2-sec	Benzene Flame t sec	Tungsten Lamps H_i cal/cm^2-sec	Tungsten Lamps t sec
Filter paper, Grade-6	0.725	52.5	0.74	*
Weight	1.025	8.5	1.06	100
= 0.00962 gm/cm^2	1.5	4.1	1.29	24.5
Thickness	2.225	2.2	1.74	11.2
= 0.0178 cm			1.96	9.7
			2.38	7.0
Filter paper, Grade-4	0.725	54.4	0.48	*
Weight	1.05	9.75	0.9	162
= 0.00939 gm/cm^2	1.35	4.6	1.16	47
Thickness	1.58	3.25	1.37	24
= 0.01904 cm	2.075	2.3	1.56	19.4
	0.925	11.9	1.91	13.3
			2.3	5.85
Filter paper, Grade-40	0.78	*	0.74	*
Weight	1.025	*	1.02	*
= 0.00915 gm/cm^2	1.2	6.75	1.17	79
Thickness	1.3	6.6	1.31	45.5
= 0.0188 cm	1.675	3.5	1.6	23.5
	1.975	3.05	1.81	18
	2.225	2.55	2.26	6.0
Filter paper, Grade-54	0.725	*	0.6	*
Weight	0.91	14.25	0.995	*
= 0.00874 gm/cm^2	1.435	3.55	1.21	113
Thickness	1.1	6.4	1.37	28.3
= 0.01625 cm	1.675	3.05	1.64	20.5
	2.075	2.1	2.16	7.9
Filter paper, Grade-115	0.825	*	0.78	*
Weight	1.01	11.75	1.06	*
= 0.00735 gm/cm^2	1.2	5.9	1.19	67.5
Thickness	1.43	4.35	1.41	40
= 0.0094 cm	1.7	2.85	1.74	14.2
	2.3	2.1	2.05	7.9
			2.28	6.55

*No ignition.

APPENDIX B

PHYSICAL PROPERTIES OF THE MATERIALS

The values of the physical properties of the materials used in the present dissertation are listed in Table B-1. Those properties that were obtained from literature sources are not for the particular sample materials used in this work, but they were chosen as those that were most representative of the general class of materials that could be found.

TABLE B-1

PHYSICAL PROPERTIES OF MATERIALS

Material	Density gm/cm^3	Thermal Conductivity cal/cm^2-sec-°C/cm	Specific Heat cal/gm-°C	Thermal Diffusivity cm^2/sec	Average Absorptance (40) Lamps	Flames
Black cotton	0.87	1.8×10^{-4} (31)	0.34 (31)	1.06×10^{-3} (23)	0.818	0.747
White cotton	0.87	1.8×10^{-4} (31)	0.34 (31)	1.06×10^{-3} (23)	0.457	0.721
Black rayon	1.21	1.8×10^{-4} (31)	0.34 (31)	1.06×10^{-3} (23)	0.818	0.747
White rayon	1.21	1.8×10^{-4} (31)	0.34 (31)	1.06×10^{-3} (23)	0.457	0.721
White acrylics	0.703	3.6×10^{-4} (12)	0.40 (12)	1.28×10^{-3}	0.457	0.721
Black wool	0.70	1.32×10^{-4} (27)	0.157 (27)	1.201×10^{-3}	0.818	0.747
Heavy cotton	0.55-0.57	1.8×10^{-4} (31)	0.34 (31)	1.06×10^{-3} (23)	0.457	0.721
α-cellulose	0.28-0.45	1.7×10^{-4} (31)	0.34 (31)	1.06×10^{-3} (23)	0.457	0.721
Filter paper	0.49-0.54	1.7×10^{-4} (31)	0.34 (31)	1.06×10^{-3} (23)	0.457	0.721

APPENDIX C

A TECHNIQUE FOR THE PREDICTION OF TEMPERATURE OF FABRICS SUBJECTED TO IRRADIATION

Since the fabrics are thin, the spatial gradients may be neglected and the system can be described by the following differential equations.

$$wc \frac{dT}{dt} = H_a - 2\varepsilon\sigma T^4 - 2h(T-T_o) + Q \frac{dw}{dt} \qquad (C-1)$$

$$\frac{dw}{dt} = - f(w - w_c) \exp(-E/RT) \qquad (C-2)$$

In order to solve Equations C-1 and C-2, the values of Q, w_c, E and f of the fabrics must be known. These values are obtained from the thermogravimetric analysis (TGA), differential thermogravimetric analysis (DTG) and differential scanning calorimeter (DSC) data. Figure C-1 is a typical TGA plot for heavy cotton. The corresponding DTG plot is given by Figure IV-13. The TGA and DTG plots were obtained for a heating rate of 160°C/min (highest available). Though the heating rate of the sample is much higher in the ignition tests, it is assumed that the heating rate of 160°C/min will be sufficient. The kinetics data from the TGA and DTG curves of the fabrics are verified for first order reactions by plotting k, the reaction

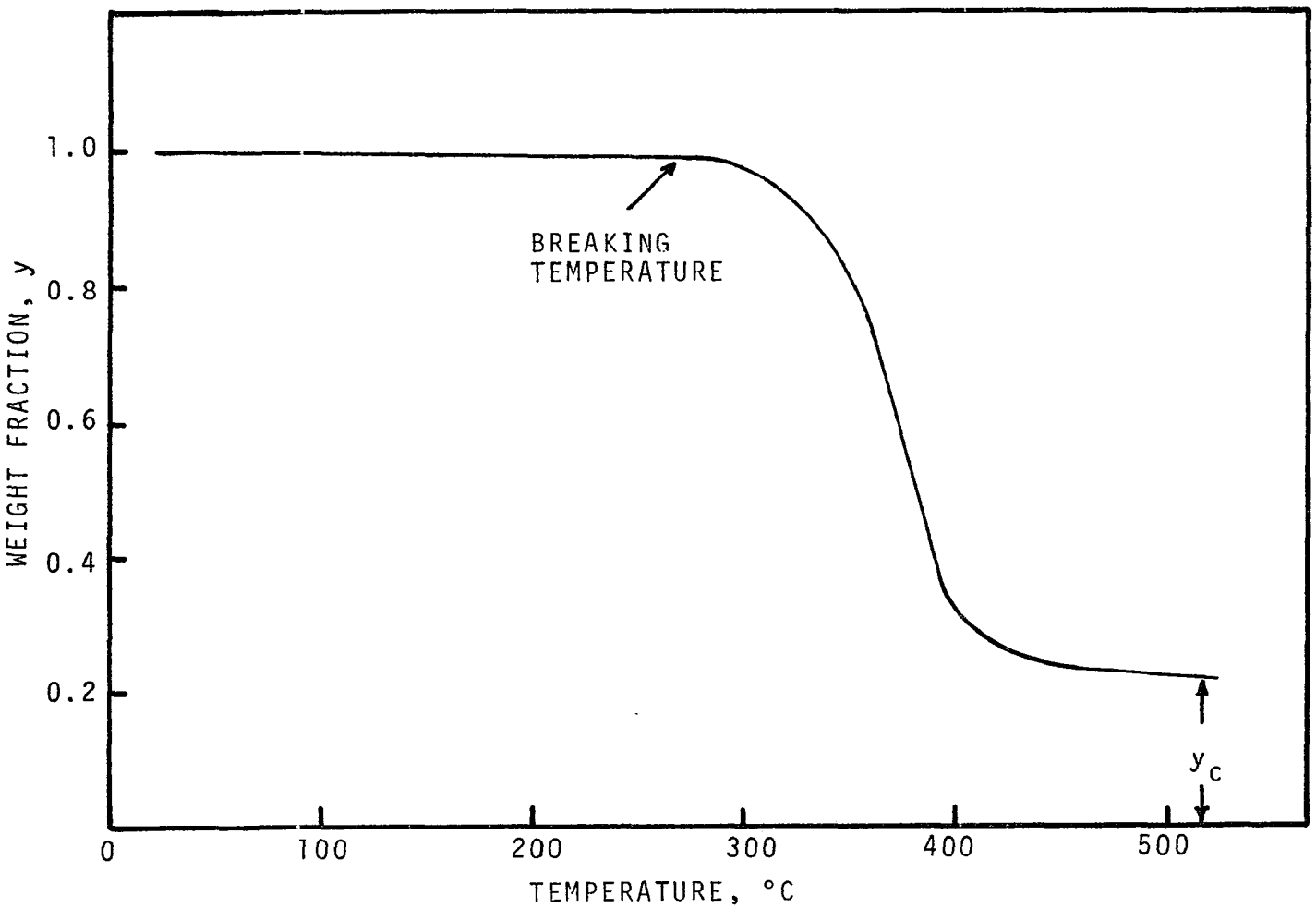

Figure C-1. Typical TGA Curve for Heavy Cotton.

rate constant, against 1/T. For a first order reaction the k versus 1/T plot should be a straight line. The weight remaining, w, is given by the TGA curve and the rate, dw/dt, is given by the DTG curve. The plot of k versus 1/T for heavy cotton is shown in Figure C-2. The slope of the line is -E/R and hence E can be evaluated. The frequency factor f is determined from the following equation.

$$k = f \exp(-E/RT) \tag{C-3}$$

The heat of pyrolysis, Q, is calculated from the DSC data (7, 14). Table C-1 presents the kinetics data of some of the fabrics.

Assuming w_o to be the initial weight of the sample and y to be the weight fraction, w/w_o, Equations C-1 and C-2 can be rewritten as

$$w_o c y \frac{dT}{dt} = H_a - 2\varepsilon\sigma T^4 - 2h(T-T_o) + Qw_o \frac{dy}{dt} \tag{C-4}$$

$$\frac{dy}{dt} = - f (y - y_c) \exp(-E/RT) \tag{C-5}$$

Equation C-4 can be rewritten as follows, assuming y to be dependent on temperature alone.

$$w_o c y \frac{dT}{dt} = H_a - 2\varepsilon\sigma T^4 - 2h(T-T_o) + Qw_o \frac{dy}{dT}\frac{dT}{dt} \tag{C-6}$$

$$w_o \frac{dT}{dt}\left[cy - Q\frac{dy}{dT}\right] = H_a - 2\varepsilon\sigma T^4 - 2h(T-T_o) \tag{C-7}$$

$$\frac{dT}{dt} = \frac{H_a - 2\varepsilon\sigma T^4 - 2h(T-T_o)}{w_o\,(cy - Q\,dy/dT)} \tag{C-8}$$

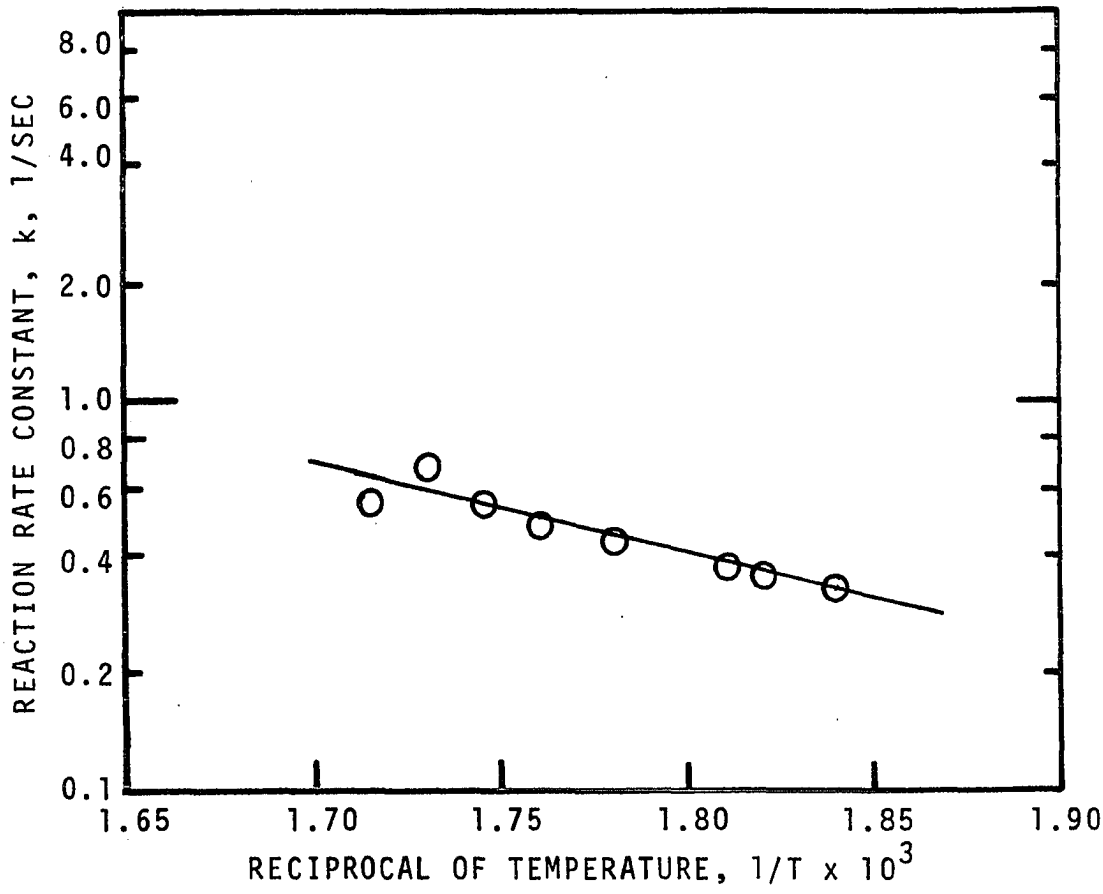

Figure C-2. The Variation of the Reaction Rate Constant with Temperature.

TABLE C-1

KINETICS DATA OF FABRICS

Material	Breaking Temperature °C	Activation Energy cals/gm mole	Frequency Factor 1/sec	Heat of Pyrolysis cals/gm
Black cotton	250	30,500	1.97×10^9	39.38
White cotton	305	19,470	2.29×10^6	85.12
Heavy cotton	260	10,500	5.45×10^3	24.6
Black rayon	250	10,380	1760	13.59*
White acrylics	320	16,015	2.1×10^5	7.5*

*Exothermic heat of pyrolysis.

Equations C-5 and C-8 are simultaneously solved to get temperature T and weight fraction y. Now the breaking temperature is defined as the temperature at which pyrolysis starts. It is shown in Figure C-1. From the TGA curve it is seen that up to the breaking temperature, y versus T is a straight line parallel to the x-axis. Therefore, up to the breaking temperature, $dy/dT = 0$ and y is approximately equal to 1. Hence the equation up to the breaking temperature is

$$\frac{dT}{dt} = \frac{H_a - 2\varepsilon\sigma T^4 - 2h(T-T_o)}{w_o c} \qquad (C-9)$$

Equation C-9 was solved up to the breaking temperature by the Runge-Kutta method, and after that, Equations C-5 and C-8 were solved simultaneously by the Predictor-Corrector method. Figures C-3 and C-4 present the calculated temperature-time

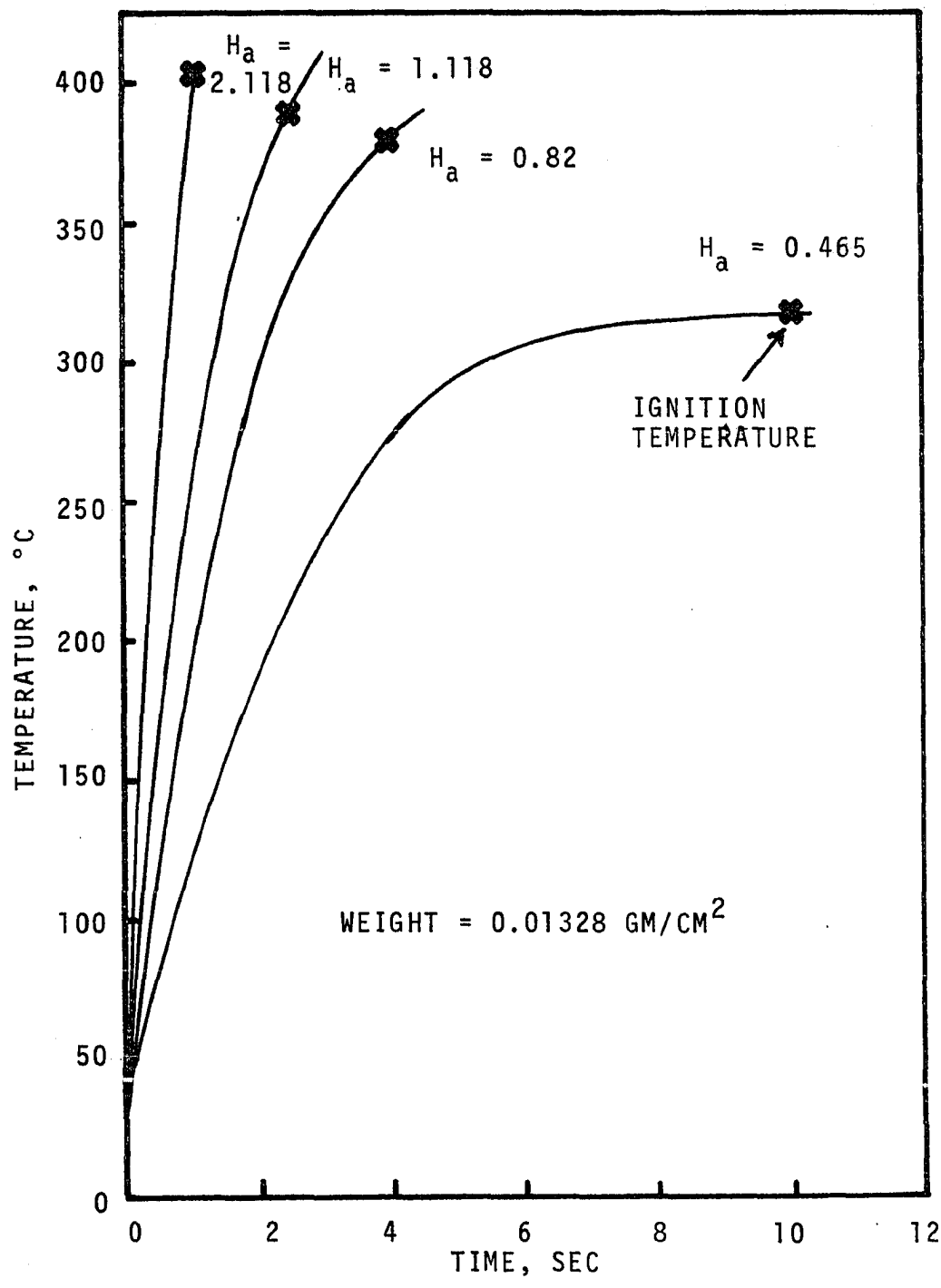

Figure C-3. The Calculated Temperature Curves for Black Cotton Subject to Irradiation.

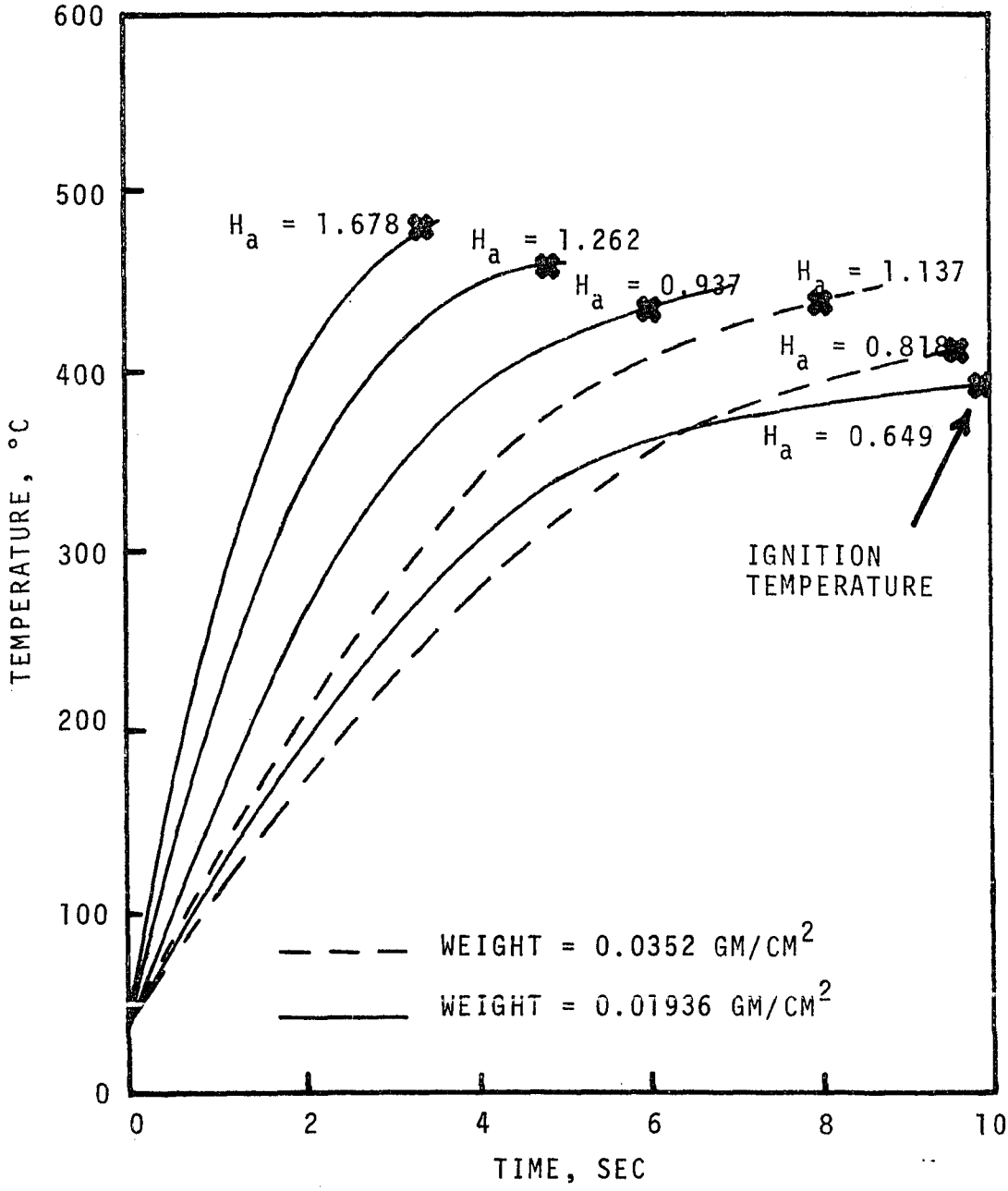

Figure C-4. The Calculated Temperature Curves for Heavy Cotton Subjected to Irradiation.

curves for black cotton and heavy cotton respectively. Corresponding to the ignition time the ignition temperature can be obtained from the calculated temperature-time curves. Figure C-5 is a plot of ignition temperature versus absorbed irradiance. From Figure C-5 it can be seen that the calculated ignition temperature increases as absorbed irradiance increases.

The average rate of evolution of volatile gases was found in the following manner. The ignition temperature for any absorbed irradiance could be found from Figure C-5. From the corresponding TGA curve the fraction of weight remaining, y, was found. The weight per unit area of volatiles evolved is $(w_o)(1-y)$. The average rate of evolution of volatile gases is given by the following equation.

$$m = \frac{w_o(1 - y)}{t_{ig}} \qquad \text{(C-10)}$$

Figure C-6 is a plot of average rate of evolution of volatile gases against absorbed irradiance. From the figure it can be seen that m increases perceptibly as absorbed irradiance increases.

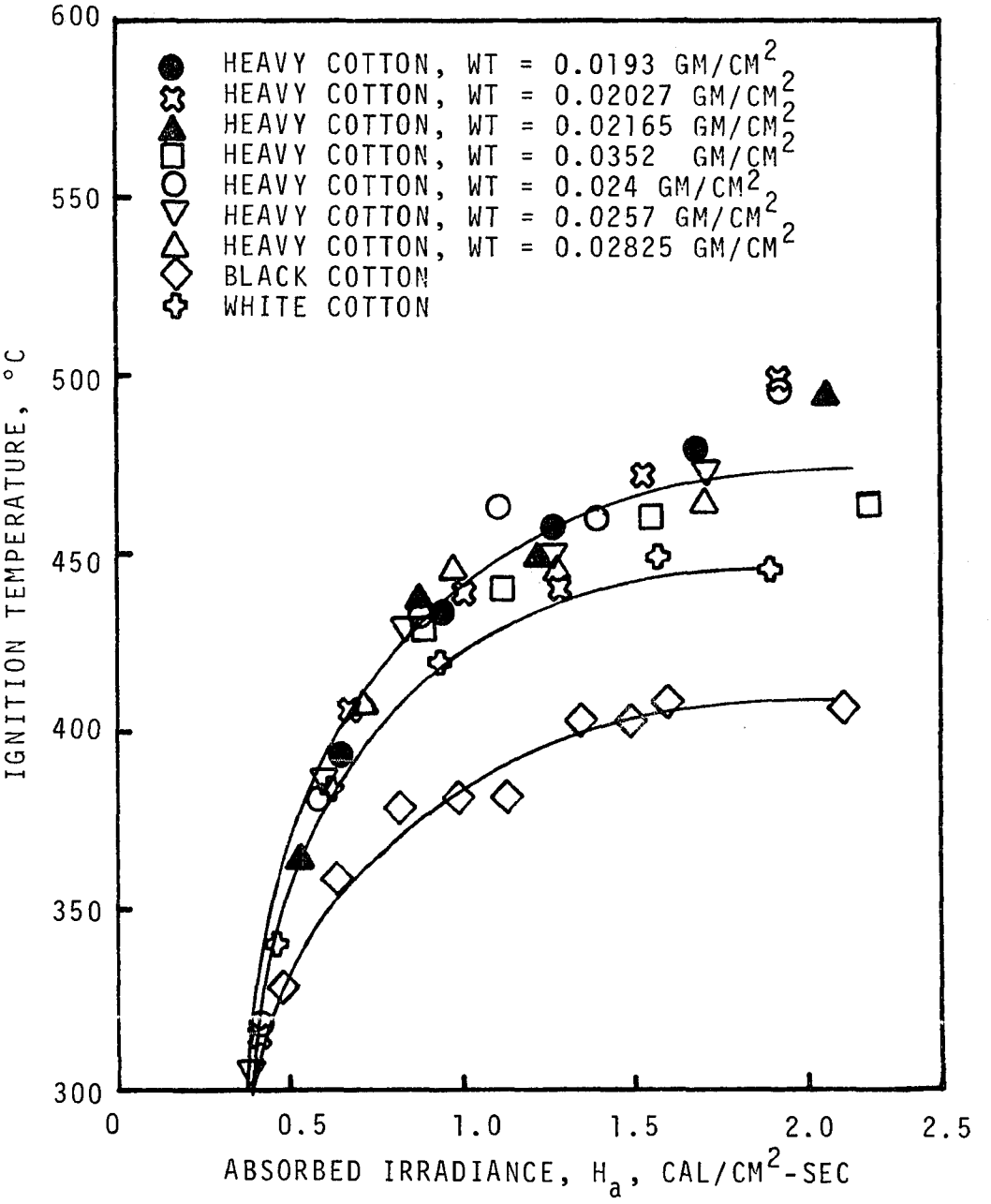

Figure C-5. The Variation of Calculated Ignition Temperature on Absorbed Irradiance.

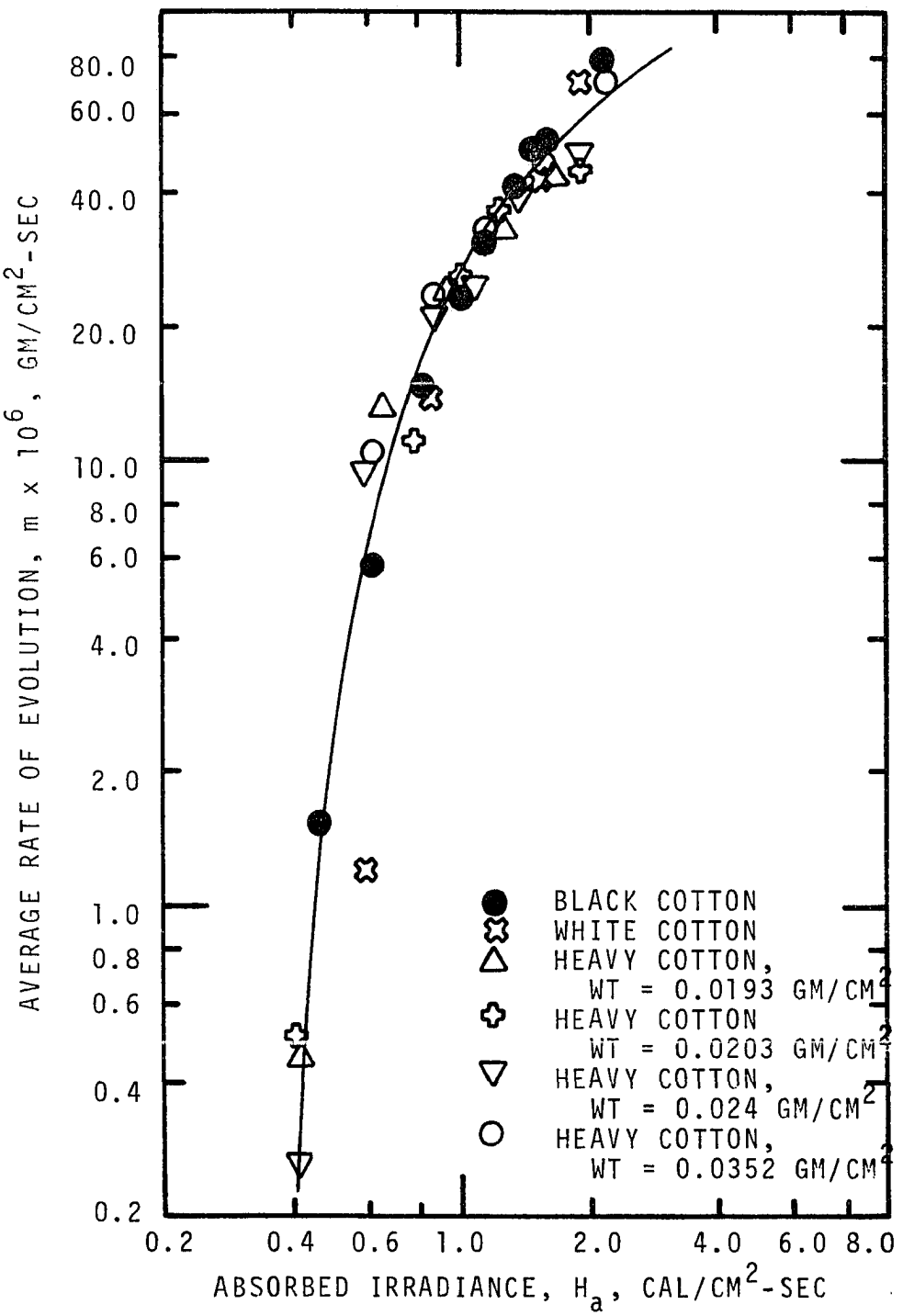

Figure C-6. The Variation of Average Rate of Evolution of Volatile Gases on Absorbed Irradiance.

APPENDIX D

NOMENCLATURE

a,b,b'	constants	
c	heat capacity of the solid	cal/gm-°C
C_g	average heat capacity of volatile products	cal/gm-°C
d	char depth	cm
E	activation energy	cal/gm mole
e	emissive power of radiation	watts/cm^2-cm
f	frequency factor	sec^{-1}
F	Fourier modulus, $\alpha t/L^2$	dimensionless
g	constant	
h	convective heat transfer coefficient	cal/cm^2-sec-°C
H, H_i	incident irradiance	cal/cm^2-sec
H_a	absorbed irradiance	cal/cm^2-sec
H_p'	peak flux	cal/cm^2-sec
k	reaction rate constant	sec^{-1}
K	thermal conductivity	cal/cm^2-sec-°C/cm
L	thickness	cm
m	rate of mass flow of gases per unit area	gm/cm^2-sec
n	order of reaction	
Q	overall heat of decomposition reaction	cal/gm

R	gas constant	cal/gm mole-°K
t	time	sec
t_{ig}	ignition time	sec
t_r	reaction time	sec
$\bar{t}$	dimensionless time, ft	
T	temperature	°K, °C
T_p	pyrolysis temperature	°K, °C
T_s	surface temperature	°K, °C
T_m	mean temperature	°K, °C
T_o, T_∞	initial temperature	°K, °C
ΔT	temperature rise, $T - T_o$	°C
ΔT_s	surface temperature rise, $T_s - T_o$	°C
ΔT_m	mean temperature rise, $T_m - T_o$	°C
$\bar{T}$	dimensionless temperature, RT/E	
w_c	weight of char	gm/cm^2
w_o	initial weight	gm/cm^2
w	weight	gm/cm^2
x	distance	cm
$\bar{x}$	dimensionless distance, x/L	
y	weight fraction	dimensionless

Greek:

α	thermal diffusivity, $K/\rho c$	cm^2/sec
α_{av}	average absorptance	dimensionless
α_λ	monochromatic surface absorptance	dimensionless
γ	Lambert's law attenuation factor	cm^{-1}

ε	emittance	dimensionless
λ	wavelength	cm
ρ	density	gm/cm^3
ρ_c	char density	gm/cm^3
σ	Stefan-Boltzmann constant $= 1.356 \times 10^{-2}$	$cal/cm^2\text{-}sec\text{-}°K^4$
ω	weight loss	gm/cm^3
$\bar{\omega}$	dimensionless weight, ω/ω_o	
Φ	function of	